The Inferior Colliculus: A Target for Deep Brain Stimulation for Tinnitus Suppression

A DISSERTATION
SUBMITTED TO THE FACULTY OF
UNIVERSITY OF MINNESOTA
BY

Sarah Jean Offutt

IN PARTIAL FULFILLMENT OF THE REQUIREMENTS
FOR THE DEGREE OF
DOCTOR OF PHILOSOPHY

Dr. Hubert H. Lim, Advisor

August 2015

ACKNOWLEDGEMENTS

With graduate school coming to an end, I reflect on where I was at the beginning and where I am now and realize I have numerous people to thank for aiding in this growth.

I would like to start by thanking my mentor through all this, Hugh. Your enthusiasm for science and research and your drive to create provided immeasurable motivation through the ups and the downs of graduate school. You taught me how to do good science, approach problems, question results, and find my own appreciation and excitement for research. I am a better scientist because of your guidance.

To my committee members past and present, including Matt Johnson, Chris Honda, Teresa Nick, Christophe Micheyl, and especially Tay Netoff, for guiding my research and challenging me to stretch each project one step further. I appreciate all the help you have provided through this process.

I next thank all the undergraduate students who completed the histological reconstructions for the projects presented in this thesis, including Kellie Ryan, Jessica Rose, Tien Tang, David Edge, Megan Harris, Babak Tabesh, Alex Konop, and Robby Hughes. I would also like to express my gratitude for the patience you all showed and the friendship and support you extended beyond our lab work. I am proud to have had the opportunity to teach and to learn from all of you.

This process would not have been the same without the kinship shared with my fellow SONIC lab graduate students: Margo Straka, Craig Markovitz, Cory Gloeckner, Ben Smith, Hongsun Guo, and Mark Hamilton. I would especially like to thank Margo and Craig, who have been there since the beginning. I would not have made nearly as much progress in my work without learning with you and from you. You have provided support both scientifically and personally that both kept me sane and allowed me to grow. I thank you both for your friendship and hope are paths continue to cross.

Beyond the SONIC Lab, I am thankful for all the BME graduate students I have the pleasure of befriending during my time in Minnesota. Our one hour lunch filled with animal facts, political rants, and absurd science was a much needed break from the tedium of graduate school. You are all fantastic scientists and even better friends; I am excited to see where the future takes you all.

Finally, I cannot thank my family enough for constantly believing in me. Mumsy, Poppy, and Alyssa, you have provided all the love, encouragement, and support anyone could ask for and all that I needed. It doesn't matter how old I get, a call home is the cure for everything. And to Tim, your support, patience, and love has brought me so much joy and made all the difference.

ABSTRACT

Tinnitus is a neurological condition that manifests as a phantom auditory perception in the absence of an external sound source. Tinnitus is often caused by hearing loss associated with noise exposure or aging and as such, the prevalence is only expected to rise in the coming years. Currently there is no cure for tinnitus and available treatment options have only shown limited success, thus there is an ever present need for continued research into new treatments. In this thesis we propose a new approach to treating tinnitus that uses deep brain stimulation to target the inferior colliculus (**IC**) with the goal of altering tinnitus-related neural activity, such as hyperactivity and increased neural synchrony, to suppress the tinnitus percept. We hypothesize that stimulation of the outer cortices of the inferior colliculus will modulate the tinnitus-affected neurons in the central region of the inferior colliculus (**ICC**) and in turn, these neural changes will be carried throughout the central auditory system by the extensive projection network originating in the IC, and will induce modulation in other tinnitus-affected auditory nuclei. The research of this thesis is aimed at determining the feasibility of this tinnitus treatment by assessing the IC as a potential neuromodulation target and identifying optimal stimulation locations and stimulation strategies for achieving maximal suppression. The first study was completed to better understand the auditory coding properties of the IC and to create a three dimensional reconstruction of these functional properties across the entire IC. These results narrowed down the stimulation target to the dorsal cortex of the inferior colliculus (**ICD**) and produced a tool that could be used to consistently place stimulating and recording electrodes in correct regions in the IC. The second and third studies focused on assessing the best stimulation locations and stimulation paradigms within the ICD, respectively, by stimulating throughout and measuring changes in neural activity in the ICC. These results show that maximal suppression is achieved by stimulation of the rostral-medial region of the ICD using either electrical stimulation only or electrical stimulation paired with acoustic stimulation with an 18 ms delay. These results will guide implementation in human patients. There are already deaf patients who suffer from tinnitus that are being implanted with a deep brain stimulator for hearing restoration called the auditory midbrain implant. Hardware modifications to the auditory midbrain implant have been completed that will allow us to stimulate the ICD and evaluate the effects on the tinnitus percept directly in patients.

TABLE OF CONTENTS

LIST OF TABLES

LIST OF FIGURES

ABBREVIATIONS

ABI – auditory brainstem implant

AMI – auditory midbrain implant

A1 – primary auditory cortex

A2 – secondary auditory cortex

AS-only – acoustic stimulation alone

BBN – broadband noise

BF – best frequency

C - caudal

CAS – central auditory system

CF – characteristic frequency

CI – cochlear implant

CN – cochlear nucleus

Control – paradigm with no stimulation

D - dorsal

DBS – deep brain stimulation

Di-I – 1, 1-dioctadecyl-3,3,3',3'-tetramethylindocarbocyanine perchlorate

DCN – dorsal cochlear nucleus

DLPN – dorsolateral pontine nucleus

ES-only – electrical stimulation alone

FSL – first spike latency

FRM – frequency response map

GP – guinea pig

IC – inferior colliculus

ICC – central nucleus of the inferior colliculus

ICD – dorsal cortex of the inferior colliculus

ICO – outer cortices of the inferior colliculus

ICX – external nucleus of the inferior colliculus

Immediate – modulation that occurs during the stimulation paradigm

L – lateral

L# – Lamina with # designating which lamina

M – medial

MGB – medial geniculate body of thalamus

MSE – mean square error

NF2 – neurofibromatosis type II

NLL – nuclei of the lateral lemniscus

PAES_n$_{delay}$ – paired stimulation with a n ms delay (-7, -2, 3, 8, 18, 23)

PC# – Planar cut with # designating from which lamina it was derived

PHA-L – Phaseolus vulgaris-leucoagglutinin

PSTH – post stimulus time histogram

Residual – modulation that occurs after the stimulation paradigm

SC – superior colliculus

SOC – superior olivary complex

Spread – percent of ICC sites significantly modulated

Strength – amount of change that occurred

T$_0$ – assessment time point immediately after stimulation paradigm

T$_{30}$ – assessment time point thirty minutes after stimulation paradigm

VCN – ventral cochlear nucleus

θ – gradient angle

2-AFC – two alternative forced choice

CHAPTER 1: INTRODUCTION

TINNITUS

Tinnitus, known as "ringing in the ears" is a neurological condition that is estimated to affect 10-15% of the population, with 20 million people afflicted in the United States alone (Heller, 2003; Eggermont and Roberts, 2004; ATA, 2013). For about two million of those tinnitus sufferers, this condition is so disturbing and debilitating that it impedes the patient's ability to perform daily tasks, and can lead to anxiety, sleep loss, headaches, and thoughts of suicide (ATA, 2013). Tinnitus is characterized as a phantom auditory sensation in the absence of any external source that is typically a result of hearing loss, though other etiologies exist (Coles, 2000; Sindhusake et al., 2003; Hoffman and Reed, 2004; Henry et al., 2014). As it is related to hearing loss, the number of tinnitus sufferers is expected to rise with increasing environmental noise and an aging population (Passchier-Vermeer and Passchier, 2000; Ortman et al., 2014). Additionally, there is a growing population of veterans experiencing tinnitus attributed to hearing loss as a result of the environmental hazards they are exposed to during war (i.e., explosions, high noise levels; Lew et al., 2007; Theodoroff et al., 2015).

Hearing loss leading to tinnitus is often a result of damage to the peripheral auditory system due to noise exposure or aging (Axelsson and Ringdahl, 1989; Nicolas-Puel et al., 2002; Eggermont and Roberts, 2004; Sindhusake et al., 2004; Henry et al., 2014). Loss of hearing results in altered auditory information being introduced into the central auditory system (**CAS**), often as lower levels of neural activity related to the frequencies associated with the hearing loss (Popelár et al., 1987; Qiu et al., 2000). In

response to the altered information, the central auditory system attempts to adapt to and/or restore the lost auditory information generating new, irregular firing patterns of auditory neurons that are perceived as a constant auditory sensation (Eggermont and Roberts, 2004; Roberts et al., 2010; Noreña, 2011; Henry et al., 2014). As such, the true origin of tinnitus is believed to be in the CAS, where aberrant plasticity emerges as a consequence of gain increases for particular frequencies or even across a broad frequency range (Lockwood et al., 1998; Qiu et al., 2000; Schaette and Kempter, 2006; Møller, 2011a; Eggermont and Tass, 2015).

Animal and human studies have shown tinnitus-related plasticity leads to hyperactivity and increased neural synchrony (reviewed in (Roberts et al., 2010; Kaltenbach, 2011; Henry et al., 2014). These neural correlates of tinnitus are found throughout the auditory system including the dorsal and ventral cochlear nucleus (**DCN** and **VCN**, respectively; Brozoski et al., 2002; Kaltenbach, 2006; Bledsoe et al., 2009; Vogler et al., 2011), the inferior colliculus (**IC**; Chen and Jastreboff, 1995; Ma et al., 2006; Melcher et al., 2009; Manzoor et al., 2012; Vogler et al., 2014) and the primary and secondary auditory cortices (**A1** and **A2**, respectively; Eggermont and Kenmochi, 1998; Noreña and Eggermont, 2003; Seki and Eggermont, 2003). Onset of these neural correlations varies in the auditory nuclei and is highly dependent on the induction and measurement protocols used. For example following noise exposure, hyperactivity in the DCN has emerged two to five days following noise exposure, while hyperactivity in the IC can be found seven to eleven days later (Kaltenbach et al., 2000; Manzoor et al., 2013). This suggests that changes in activity patterns in DCN may in part drive the CAS

2

to a tinnitus state, though other mechanisms are likely involved. However once in the tinnitus state, the percept is dependent on the network of auditory nuclei involved, as tinnitus persists after the removal of the DCN (Brozoski and Bauer, 2005).

In spite of its prevalence, a cure for tinnitus remains elusive though many treatment options have been tested. Many of these treatments aim to either restore normal firing patterns or completely inhibit firing associated with tinnitus through activation at different levels of the auditory system (Møller, 2011b; Vanneste and De Ridder, 2012). Treatment in humans has targeted the auditory nerve, the cochlear nucleus, and the auditory cortex in attempts to fix the trigger, generator, and perception points of tinnitus, respectively. Corrections to errant incoming auditory information entering the CAS at the level of the auditory nerve have been attempted with the use of cochlear implants (**CIs**) (Osaki et al., 2005; Baguley and Atlas, 2007; Quaranta et al., 2008; Van de Heyning et al., 2008; Kleinjung et al., 2009; Zeng et al., 2011). This stimulation has reduced or suppressed the tinnitus percept in a majority of patients, but has not yet been extended beyond CI users. The auditory brainstem implant (**ABI**) has also been employed for tinnitus treatment by invasively stimulating the DCN, where tinnitus-related activity may originate. A survey of ABI patients shows that reduction, but not complete elimination of the tinnitus percept is possible with daily use of the ABI (Soussi and Otto, 1994). Non-invasive methods to treat tinnitus at the level of the DCN are currently being tested, with outcomes still pending. This treatment pairs acoustic and somatosensory stimulation in attempts to retrain activity in the DCN where these two pathways merge (Dehmel et al., 2012). As perception occurs in the auditory cortex, the cortex has been most extensively

targeted with both invasive and non-invasive methods. Cortical stimulation has been implemented in both the A1 and the A2 using intradural or extradural electrodes (De Ridder et al., 2006; Friedland et al., 2007; De Ridder et al., 2011; Engelhardt et al., 2014). Reduction in the tinnitus percept was seen in most patients, but a majority of those patients only achieved partial suppression of the percept, with results highly dependent on the type of tinnitus and pattern of stimulation. Non-invasive methods assessed include transcranial direct current stimulation (Song et al., 2012; Shekhawat et al., 2015) and transcranial magnetic stimulation (Kleinjung et al., 2011; Hoekstra et al., 2013; Piccirillo et al., 2013). Again there was high individual variance in the results and long term efficacy would need to be evaluated to determine an optimal treatment schedule to see lasting effects. Lastly, more holistic approaches using cognitive-behavioral therapy (Cima et al., 2014) and sound therapy approaches that mask the tinnitus have been attempted with varied levels of success (Davis et al., 2007; Davis et al., 2008; Trotter and Donaldson, 2008; Moffat et al., 2009; Roberts and Bosnyak, 2011).

Further research into new tinnitus treatments is warranted by the growing number of tinnitus sufferers and the inconsistent results of current treatments. For this thesis work, we have investigated a new approach to treating tinnitus by using deep brain stimulation (**DBS**) to target the IC. The potential of the IC to suppress tinnitus has not previously been evaluated, but we believe there is great promise for success for three main reasons. First, the IC is the convergence center for auditory information with the potential to induce changes in all other auditory nuclei. Unlike the DNC, which is at the beginning of the auditory pathway receiving mainly ipsilateral input or the cortex which

is at the end receiving processed information, the IC is a central hub that can interact with other auditory nuclei through ascending and descending connections (Casseday et al., 2002). Second, anatomical studies suggest that secondary regions of the IC may be able to modulate the primary region of IC which may correct the errant firing patterns before transmission throughout the auditory system including to the auditory cortex, possibly suppressing the tinnitus percept. Third, there are deaf patients who suffer from tinnitus due to hearing loss that are already being implanted in the IC with a DBS array for hearing restoration known as the auditory midbrain implant (**AMI**). Thus we have the potential to directly test this method in patients. Therefore, the motivation of this thesis is to determine the feasibility of this tinnitus treatment by assessing the IC as a potential neuromodulation target and identifying optimal stimulation locations and strategies within the IC. The following sections will detail the motivation for this new treatment, our hypotheses, and the project aims.

INFERIOR COLLICULUS

The IC is an important integration hub within the central auditory system with converging descending, ascending, and bilateral inputs. Ascending inputs arise directly from all auditory regions in the brainstem including: the cochlear nucleus (**CN**), the superior olivary complex (**SOC**), and the nuclei of the lateral lemniscus (**NLL**) (Aitkin and Phillips, 1984a; Coleman and Clerici, 1987; Saint Marie and Baker, 1990; Schofield and Cant, 1996, 1997; Alibardi, 2000; Casseday et al., 2002). Descending inputs from the medial geniculate body of the thalamus (**MGB**) and the auditory cortex also synapse

throughout the IC (Saldana et al., 1996; Winer et al., 1998; Kuwabara and Zook, 2000; Winer et al., 2002; Malmierca and Ryugo, 2011). For every region that synapses in the IC, there are reciprocal projections back to that region, apart from the auditory cortex (Calford and Aitkin, 1983; Caicedo and Herbert, 1993; Malmierca et al., 1996; Schofield and Cant, 1999). Additionally, there are projections into non-auditory regions including the superior colliculus (**SC**) and motor areas (Aitkin and Boyd, 1978; Edwards et al., 1979; Huffman and Henson, 1990; Caicedo and Herbert, 1993; King et al., 1998). The IC can be subdivided into three regions, the central nucleus (**ICC**), the dorsal cortex (**ICD**), and the external nucleus (**ICX**; Fig. 1*A*), each with different projections networks. Additionally, each of these regions has a distinctive organization, different physiological responses, and thus serve diverse functions in the auditory system (Roth et al., 1978; Faye-Lund and Osen, 1985; Coleman and Clerici, 1987; Casseday et al., 2002; Oliver, 2005; Cant and Benson, 2006; Loftus et al., 2010).

The ICC is part of the lemniscal auditory system and is the core processing center in the midbrain for all ascending auditory information, with litte descending innervation (Adams, 1979; Brunso-Bechtold et al., 1981; Shneiderman et al., 1988; Saint Marie and Baker, 1990; Oliver et al., 1995; Schofield and Cant, 1996; Winer et al., 1998; Malmierca and Ryugo, 2011). The ICC is composed of disc-shaped cells arranged in fibrodentric lamina (Morest and Oliver, 1984; Oliver and Morest, 1984; Faye-Lund and Osen, 1985; Meininger et al., 1986; Malmierca et al., 1993). Neurons within a single lamina fire maximally to a charcteristic frequency (**CF**) and together all laminae form a tonotopic gradient within the ICC (Merzenich and Reid, 1974; Malmierca et al., 1995; Snyder et

al., 2004). The tonotopic gradient is arranged from low to high frequencies in the dorsolateral to ventromedial direction (Fig. 1*B*). Individually, neurons in the ICC are narrowly tuned with strong frequency selectivity, low thresholds, and sustained firing (Aitkin et al., 1994; Syka et al., 2000; Egorova et al., 2001; Palmer et al., 2013). Projections out of the ICC are the most extensive of any IC region, synapsing in every auditory nuclei except the auditory cortex (Winer and Schreiner, 2005).
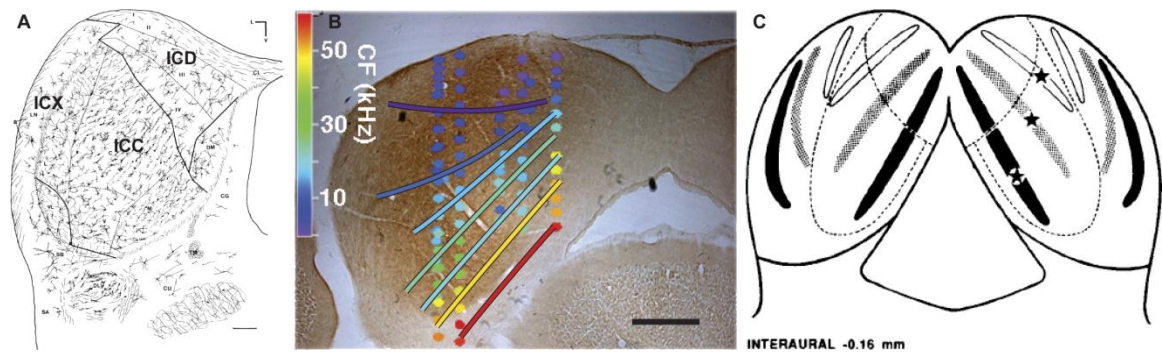
Figure 1. Subdivisions, tonotopicity, and connectivity in the IC. *A*, Anatomical subdivisions of the IC in cat were determined using Golgi methods (scale = 0.5 mm). Individual cells have been labeled and redrawn. Each region has been divided based on the cell distribution (Morest and Oliver, 1984). *B*, The tonotopic map of a mouse IC is superimposed over a cytochrome oxidase-stained slice (scale = 0.5 mm). Electrode penetrations were made perpendicular to the surface of the IC with recordings made at different depths, indicated by circles. Laminae were fit to the CFs measured at each location (Portfors et al., 2011). *C*, A representation of the connectivity of IC is shown. Injections of Phaseolus vulgaris-leucoagglutinin are indicated by the stars. Each location labels four laminar plexuses: one in the ipsilateral CF lamina, one in the contralateral CF lamina, one in the ipsilateral ICX, and one in the contralateral ICX. The same patterning can be found when injections are made in the ICD (Saldaña and Merchán, 1992). Images were reprinted with permission from John Wiley and Sons and Elsevier.

The ICX and the ICD belong to the non-lemniscal system, assisting but not primarily responsible for ascending auditory processing (Lee and Sherman, 2010). The

ICX is organized in three layers: a fibrous outer layer, a small-celled middle layer, and a mixed third layer, with both small and large cells (Morest and Oliver, 1984; Faye-Lund and Osen, 1985; Oliver, 2005). The ICX shows frequency selectivity, but can be distinguished from the ICC by a frequency reversal at their border (Stiebler and Ehret, 1985). Unique to the ICX are the somatosensory projections that synapse throughout allowing for multi-sensory integration (Aitkin et al., 1981; Morest and Oliver, 1984; Binns et al., 1992). With projections from the ICX synapsing on the SC and various motor areas, the ICX is part of circuitry that controls sound localization and head orienting (Huffman and Henson, 1990). The ICD is organized into four layers. The first two are similar to the ICX with an outer fibrous layer and a second, small-celled layer (Morest and Oliver, 1984). The third contains commissural fibers in route to the contralateral IC, and the fourth layer contains larger cells where it meets the ICC (Oliver et al., 1991). The border between the ICD and the ICC is hard to characterize with CF alone, and relies on cell morphology and organization as well as neural response properties for division. Notably, the ICD has layered innervation, predominately receiving projections from the ascending system in the shallow layers and from the descending system in the deeper layers (Oliver, 1984; Shneiderman et al., 1988; Winer et al., 1998; Oliver, 2005). Projections leaving the ICD enter the MGB and to a lesser extent the DCN (Calford and Aitkin, 1983; Schofield, 2001; Thompson, 2005). Studies have not yet probed the function of the ICD in hearing, including the purpose of the differential innervation. However its possible role in auditory processing is the focus of Chapters 3 and 4. Response properties of the ICD and the ICX appear to be similar based on

previous studies and are more broadly tuned, have longer latencies on average, higher thresholds, and more variable response shapes compared to neurons in the ICC (Aitkin et al., 1975; Willott and Urban, 1978; Aitkin et al., 1994; Syka et al., 2000). Our findings in Chapter 2 further explore these differences in subregions and reveal an underappreciated spatial organization of responses across these two regions which offer new insights into their role in auditory processing.

CONNECTIVITY AND MODULATION WITHIN THE INFERIOR COLLICULUS

Intrinsic and commissural projections throughout the IC are extensive and have been well documented anatomically using tracers injected into each of the three main IC subregions. Injection of the anterograde tracer Phaseolus vulgaris-leucoagglutinin (**PHA-L**) into the ICC labeled four laminar plexuses, two contralateral and two ipsilateral to the site of injection (Fig. 1*C*). The same patterning exists on each side with one plexus along the isofrequency lamina extending into ICD and one parallel to the IC surface that lies within the ICX (Saldaña and Merchán, 1992; Malmierca et al., 1995; Saldana and Merchan, 2005). Injections of PHA-L in the ICD mirrored the patterning of the ICC with two laminar plexuses in both ICs (Saldaña and Merchán, 1992; Saldana and Merchan, 2005). The ICX does not appear to have the same contribution to the internal network, though results are dependent on the tracer used. Using PHA-L, projections from the ICX remain within the outer cortices, with a heavier labeling of the hemisphere ipsilateral to the injection (Saldaña and Merchán, 1992; Saldana and Merchan, 2005). However, injection of the retrograde tracer horseradish peroxidase into the ICC revealed extensive

labeling in the ipsilateral and the contralateral ICX (Willard and Martin, 1983; Coleman and Clerici, 1987; Frisina et al., 1998). Despite disparities of the ICX projection patterns, which may be attributed to stain methodology, it is apparent that there is a widespread intracollicular network.

The functional purpose of intracollicular network is less understood and evidence suggests that it is part of the descending modulation network. Corticofugal projections provide necessary modulation to shape the way ascending auditory information is processed in route to perception in the auditory cortex (Yan and Ehret, 2002; Winer, 2005; Suga, 2008; Xiong et al., 2009; McLachlan and Wilson, 2010; Markovitz et al., 2015). Excitatory and inhibitory modulation of the ICC via corticofugal projections has been demonstrated in numerous experiments by stimulating or inactivating the A1 to suppress firing, reshape the frequency tuning, and shift threshold and latency in the ICC (Massopust and Ordy, 1962; Mitani et al., 1983; Syka and Popelar, 1984; Sun et al., 1989; Torterolo et al., 1998; Zhang and Suga, 2000; Zhou and Jen, 2000; Bajo and King, 2012; Suga, 2012). Considering that projections from the A1 to the IC, including directly to the ICC, are predominately glutamatergic and presumed to be excitatory, the required inhibition must come from sources other than the A1 (Rockel and Jones, 1973; Feliciano and Potashner, 1995; Saint Marie, 1996; Saldana et al., 1996). This inhibition may be provided by multi-synaptic pathways to the ICC via intrinsic IC projections from the ICX and the ICD. This has been previously shown for the ICX, where direct and indirect stimulation of the ICX (i.e., through stimulation of the A1 to excite the ICX) suppressed neural activity in the ICC (Jen et al., 2001; Jen et al., 2002). However, no study to our

knowledge prior to the ones included in this thesis (Chapters 3 and 4) has examined the type and extent of modulation possible by the ICD. As projections from the A1 synapse throughout the outer cortex, we hypothesized that inhibition could also be accomplished via the ICD (Faye-Lund, 1985; Huffman and Henson, 1990; Herbert et al., 1991; Winer et al., 1998). We further hypothesized that based on sources of innervation, the ICD may have an even greater ability to modulate the ICC than the ICX. The ICX processes not only auditory information, but also integrates multi-sensory information (Aitkin et al., 1978; Aitkin et al., 1981; Binns et al., 1992; Knudsen, 2002; Gruters and Groh, 2012). By comparison, a majority of all projections to the ICD are auditory and thus the ICD may have a strong modulatory effect on auditory processing (Coleman and Clerici, 1987; Winer et al., 1998).

AUDITORY MIDBRAIN IMPLANT

The auditory midbrain implant was originally designed to restore hearing in neurofibromatosis type II (**NF2**) patients, as an alternative to the ABI. NF2 is a genetic disorder that often manifests as bilateral acoustic neuromas (Lenarz et al., 2006; Schwartz et al., 2008; Colletti et al., 2009b; Lim et al., 2009b). During tumor resection, ABIs or AMIs can be implanted with minimal added surgical risk and supply auditory cues that would be otherwise lost (Samii et al., 2007; Lim et al., 2009a). Current ABI performance has yet to attain the success of the CI, with patients receiving mainly limited open-set speech perception compared to the high levels of hearing possible by CI patients (Otto et al., 2002; Adams et al., 2004; Behr et al., 2007; Colletti et al., 2009a). Limited ABI

performance in NF2 patients may be attributed to damage to the brainstem incurred during tumor growth or tumor removal surgery. This hypothesis is corroborated by the improved performance in non-tumor ABI patients (e.g., deafness due to being born without an auditory nerve or head trauma) using the same implant technology and stimulation strategies (Colletti and Shannon, 2005; Colletti et al., 2009a). To avoid tumor and surgical effects within the brainstem area, the AMI was developed for implantation in the IC (Lenarz et al., 2006; Lim et al., 2009b). The AMI was originally designed as a single shank array with twenty electrode contacts to be placed along the tonotopic gradient within the ICC, which allowed for stimulation strategies similar to the CI (Fig. 2*A,B*; Lenarz et al., 2006; Lim and Anderson, 2006).
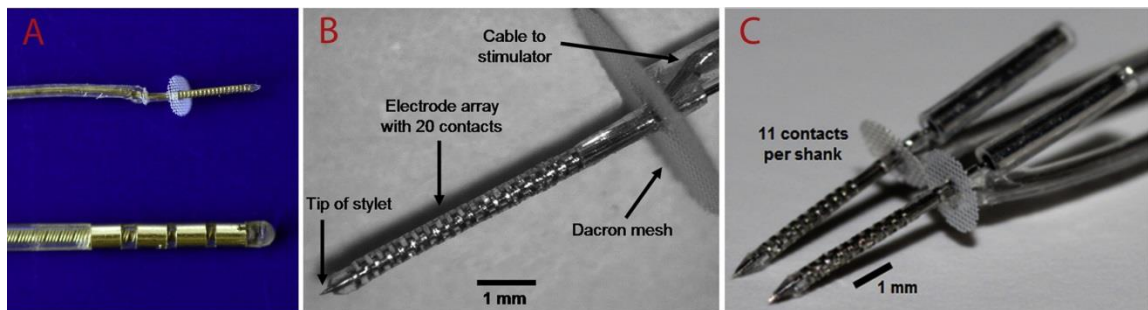
Figure 2. First and second generation AMIs. *A*, The first generation AMI (top - Cochlear Limited, Australia) compared to a typical array used for DBS for Parkinson's (bottom - Medtronic, Ireland) has a smaller overall size, smaller contacts, and a greater number of contacts . *B*, The first generation AMI has 20 contacts (200 μm spacing, 200 μm thickness, 400 μm diameter), a Dacron mesh to prevent over-insertion, and a cable tethering it into the brain. *C*, The second generation AMI has two separate shanks with the same Dacron mesh and cable. Each shank has 11 contacts, (300 μm spacing, apart from one site close to the Dacron mesh that is used for tinnitus treatment as described in the text). This new generation AMI will be used in the upcoming clinical trial. Images were taken from Lenarz et al., 2006; Samii et al., 2007; Lim and Lenarz, 2015 and reprinted with permission from Lippincott Williams & Wilkins and Elsevier.

Unfortunately, the first AMI clinical trial was not able to achieve the same success as CI users in speech understanding due to implant location and temporal coding limitations (Shannon et al., 1995; Lim et al., 2008b; McKay et al., 2013). However, based on the enhanced lip-reading abilities, increased environmental awareness of the initial patients, and indications of more optimal stimulation locations, a second clinical trial is now underway (Lim et al., 2008a; Straka et al., 2014; Lim and Lenarz, 2015). This clinical trial will use the new, two-shank design (Fig. 2*C*) which is expected to greatly overcome the limited temporal coding capabilities observed in the first AMI clinical trial (Calixto et al., 2012; Straka et al., 2013; Lim and Shannon, 2014; Lim and Lenarz, 2015).

In this upcoming clinical trial we would like to treat a second need of these AMI patients: tinnitus. Many NF2 patients experience hearing loss and some develop tinnitus due to their hearing loss. Therefore, we would like to leverage the AMI technology and the IC implant location to also treat tinnitus. We hypothesize that by stimulating the outer cortices that are presumed to be modulatory, particularly the ICD, we may be able to achieve the suppression necessary to reduce the hyperactivity and neural synchrony associated with tinnitus within the ICC. We further hypothesize that suppressing activity within the ICC could affect other nuclei that are part of the abnormal tinnitus network via the massive projection network originating in the ICC and extending throughout the CAS. To achieve this treatment, one site along each shank was purposely positioned near the Dacron mesh that can stimulate the outer cortices of the IC in order to induce modulatory effects across the auditory system to potentially treat tinnitus (Fig. 2*C*).

RESEARCH AIMS

Prior to assessing AMI stimulation for treating tinnitus directly in patients, we need to understand how DBS of the IC can be utilized to alter neural activity which will guide novel stimulation strategies in upcoming AMI patients. This treatment will be initially limited to NF2 patients who are completely deaf since these individuals are already being implanted with the AMI and the effects of IC stimulation on tinnitus perception can be explored in these patients with minimal added risk. However, we hope that early success in these AMI patients would enable implantation of the AMI into patients solely for treating tinnitus who still have residual or near-normal hearing. These patients would be those who experience debilitating tinnitus enough to justify the DBS surgery.

In order to determine the feasibility of this tinnitus treatment and to guide stimulation strategies in upcoming AMI patients, I performed three studies for my thesis research in a guinea pig animal model. The guinea pig was selected for the animal model because it exhibits an anatomical and functional organization of the IC similar to other mammalian species, including in humans (Oliver, 2005), and its frequency hearing range is similar to that of humans (Harper, 1976; Rode et al., 2013). In these three studies we sought to assess the IC as a potential neuromodulation target, to identify optimal stimulation locations, and to determine stimulation strategies that may lead to tinnitus suppression.

The aim of the first study was to better understand the auditory coding properties across the different subregions of the IC and to create a three-dimensional brain

reconstruction of the whole guinea pig IC to aid in target selection and electrode placement. Although numerous studies have characterized the coding properties across the ICC and have identified various topographic maps within the ICC, no study to our knowledge has mapped the functional properties across the outer IC regions, including the ICD and the ICX. Additionally, as described above, though there is much speculation that the ICD likely serves a stronger modulatory role in auditory information processing compared to the ICX, few functional studies have provided evidence to support this prediction. In Chapter 2, we provide data further suggesting the ICD's modulatory role in auditory processing and indicating the ICD may be a better target for tinnitus treatment with the AMI. Importantly, we created the first detailed three-dimensional reconstruction of the whole IC in the guinea pig, with accurate visualization of the ICD and the ICC regions that assisted in placement of stimulation and recording sites for the proceeding studies described in Chapters 3 and 4.

Once we were able to identify where to consistently place the electrode sites into the ICC and the ICD, we proceeded with the second study described in Chapter 3. The aim of the second study was to investigate the effects of electrically stimulating many different locations of the ICD on neural activity across different locations of the ICC. This study was proof-of-concept to determine if any modulation of the ICC was possible using ICD stimulation paired with and without acoustic stimulation, as previous studies had only examined effects of directly stimulation the ICX on ICC activity. For this study, only a few stimulation paradigms were explored in order to focus on determining effective stimulation locations across the ICD. From the results, we identified a certain

stimulation parameter and specific locations within the ICD that exhibited strong suppressive effects that may be relevant for reducing tinnitus-related activity.

The results presented in Chapter 3 were encouraging for tinnitus treatment; however, there were limitations to the protocol used for the study, in which we attempted to stimulate many different locations with several different paradigms. To accommodate all of these conditions, each paradigm was presented in a set order without any recovery of modulation, and thus cumulative effects likely contributed to confounding results. The aim of the third study described in Chapter 4 was to repeat the experiments in Chapter 3, but this time targeting one specific region of the ICD that exhibited the strongest suppressive effects in the study in Chapter 3 and exploring several different paradigms in each animal with a randomized order across animals. Moreover, by limiting the experiments to one stimulation site per animal, there was sufficient time in the protocol to allow for at least thirty minutes of recovery of modulation back to baseline activity. The findings in Chapter 4 revealed new and optimal ICD stimulation paradigms that were masked in the experiments in Chapter 3. Furthermore, it revealed that both ICD stimulation alone and ICD stimulation paired with acoustic stimulation at a specific delay could potentially treat tinnitus, and thus would be relevant for both proposed tinnitus populations, those with and without hearing.

Although outside of the scope of this thesis research, the Appendix includes an additional study that was performed in a chronic animal model for exploring plasticity effects in the ICC. This study was the original focus of my thesis research but due to challenges in its setup and the encouraging findings presented in Chapters 2 and 3, I

changed the focus of my thesis research towards developing a new DBS stimulator in the IC for tinnitus treatment. The Appendix provides the work that went into developing a chronic electrode implant setup in guinea pigs and the initial EEG and plasticity studies, which are now being used by others in the lab for other hearing and tinnitus studies.

CHAPTER 2: ACOUSTIC RESPONSE MAPS SPAN THE WHOLE INFERIOR COLLICULUS AND REVEAL THE FASTEST NEURONS WITHIN THE NON-LEMNISCAL PATHWAY

Neural responses to acoustic stimulation have long been studied throughout the auditory system to understand how auditory information is coded for perception. Within the IC, a central hub in the auditory system, a majority of the effort has been toward characterizing response of the ICC, as it is part of the lemniscal system mainly responsible for perception. In comparison, the responses of the outer cortices (ICO) have largely been unexplored, though they also function in perception tasks, such as in sound localization. Therefore we sought to expand on previous work by completing a three dimensional functional mapping study of the whole IC. We analyzed responses to pure tone and broadband noise stimulation across all IC subregions and correlated those responses with recording location to create spatial maps. Our study revealed there are well organized trends for temporal response properties that extend throughout the whole IC with little distinction between IC subregions. Interesting, these maps show two populations of neurons in the ICO: one with the fastest and most precise neurons, faster even than ICC responses, and one with the slowest and least precise responses. Relevant for the functional role of the IC, these fast ICO responses may be necessary for executing accurate head orienting responses or other sensorimotor reflex actions. The slow ICO responses may be involved with auditory modulation of the ICC related to attention and learning. Both of these functions are supported by anatomical projections to the different regions in the ICO.

INTRODUCTION

The IC is an essential hub in the central auditory system, integrating numerous converging pathways from the brainstem in route to the thalamus and cortex (Aitkin and Phillips, 1984a; Casseday et al., 2002). The roles of the IC are varied, including auditory processing leading to speech understanding, multisensory integration, and sound localization (Aitkin, 1979; Huffman and Henson, 1990; Knudsen, 2002). As such, the IC

has been studied extensively to understand how auditory information is coded into neural responses that contribute to sound perception (Ehret, 1997; Portfors and Sinex, 2005; Rode et al., 2013).

There is already a large body of research focused on coding properties within the ICC as it is the main auditory or lemniscal pathway within the midbrain (Roth et al., 1978; Irvine, 1992). The ICC has a well-defined tonotopic organization composed of fibrodentric laminae of cells that preferentially code from low to high best frequencies (**BFs**) in the dorsal-lateral to ventral-medial direction (Merzenich and Reid, 1974; Snyder et al., 2004; Oliver, 2005; Malmierca et al., 2008). Multiple topographic maps of the ICC have been identified along the BF laminae for first spike latencies (**FSLs**), thresholds, Q-values, periodicity and frequency modulation coding, and binaurality (Semple and Aitkin, 1979; Wenstrup et al., 1985; Stiebler, 1986; Schreiner and Langner, 1988; O'Neill et al., 1989; Hattori and Suga, 1997; Langner et al., 2002; Hage and Ehret, 2003). These studies suggest a major conversion of coding properties into spatial representations occurs at the level of the midbrain.

Compared to the ICC, there have only been a few studies characterizing the functional properties within the outer region of the IC (**ICO**), which includes the ICD and the ICX. These studies have generally shown slower latencies, more variable response durations, lower spontaneous firing rates, higher thresholds, broader frequency tuning, and a weak or non-existent tonotopy in the ICO compared to the ICC (Aitkin et al., 1994; Syka et al., 2000; Lumani and Zhang, 2010). Additionally, studies have shown greater adaptive effects and greater duration selectivity within the ICO versus the ICC (Pérez-

González et al., 2005; Pérez-González et al., 2006). However, to our knowledge, no studies have yet systematically mapped different coding properties fully across the ICO in mammals. Only a few studies have recorded across specific portions of the ICO (e.g., ICX) for maps of sound localization (Knudsen and Knudsen, 1983; Binns et al., 1992; Knudsen, 2002).

Due to the scarcity of functional data spanning different subregions of the ICO, we sought to map response properties fully across the IC using a robust method for three-dimensional reconstruction of recording sites (Markovitz et al., 2012). The original intention of this study was to construct functional maps across the IC for several response properties in the same preparation in order to more accurately compare response trends and to begin building up a database of IC responses across different species. Unexpectedly, we discovered topographic maps of temporal response features systematically varied across the entire IC without any clear distinction between traditionally defined subregions of the IC. Furthermore, we identified a region within the rostral-lateral portion of the ICO that exhibited fast, temporally precise responses including the fastest responses to acoustic stimulation for the entire IC. These responses were faster than what was observed in the ICC, which is typically viewed as the main and robust pathway for ascending auditory information to higher perceptual centers. Conversely, the caudal-medial portion of the ICO exhibited slower, less precise responses than typically found in the ICC. These findings raise new insights and questions as to the functional role of the ICO in auditory processing.

MATERIALS AND METHODS

Surgery and Experimental Setup

Experiments were performed on three Hartley guinea pigs (mass: 578.6 g, 610.2 g, 595.0 g, Elm Hill, Chelmsford, MA) in accordance with the standards set forth by University of Minnesota Institutional Animal Care and Use Committee. Basic surgical and electrophysiological methods used in these experiments have been detailed in previous work and are only summarized here (Lim and Anderson, 2007a; Markovitz et al., 2013; Offutt et al., 2014). Animals were anesthetized with an intramuscular injection of ketamine (40 mg/kg) and xylazine (10 mg/kg) and kept in an areflexive state with additional doses. Temperature, blood oxygenation, and heart rate were continually monitored and atropine sulfate (0.05 mg/kg) was administered periodically to reduce mucous secretions.

Experiments were performed in an electrically and acoustically isolated sound chamber. Stimulation delivery and data collection was controlled by TDT hardware (Tucker-Davis Technologies, Alachua, FL) and custom software written in MATLAB (MathWorks, Natick, MA). Animals were positioned into a stereotaxic frame (David Kopf Instruments, Tujunga, CA) and a craniotomy was performed to expose the right occipital lobe. Acoustic stimulation was delivered through a speaker coupled to the left hollow ear bar at a sampling frequency of 195 kHz. The speaker and ear bar were calibrated using a 0.25-in condenser microphone (ACO Pacific, Belmont, CA). Neural signals were recorded using a monopolar configuration with the return needle positioned

in the neck muscle. The recorded neural signals were passed through analog DC-blocking and anti-aliasing filters from 1.6 Hz to 7.5 kHz and sampled at 25 kHz.

Electrode Array Placement and Acoustic Stimulation

A four shank multi-site silicon substrate electrode array (NeuroNexus, Ann Arbor, MI) was used in these experiments. Eight sites ($403 \mu m^2$ site area; 0.4-0.9 MΩ at 1 kHz) were linearly spaced along each shank with a 100 μm separation and the distance between shanks was 500 μm. The electrode array was inserted into the IC using micromanipulators (Kopf Instruments, Tujunga, CA) at a 45° angle to the sagittal plane in order to align each shank parallel to the tonotopic axis of the IC (Malmierca et al., 1995; Snyder et al., 2004). The IC was initially located by delivering broadband noise (**BBN**) stimulation (50 ms duration, 0.5 ms rise/fall time, 6 octave bandwidth from 0.625 to 40 kHz, 70 dB-SPL) during insertion until consistent acoustic-driven responses were elicited. Once located, the electrode array was stained with red fluorescent dye (**Di-I**: 1, 1-dioctadecyl-3,3,3',3'-tetramethylindocarbocyanine perchlorate; Sigma-Aldrich, St Louis, MO) so that the electrode array trajectories could be identified during the histological procedure. In order to sample the entire IC, multiple electrode array placements were made in a grid-like pattern and multiple depths were recorded at each placement. The grid-like pattern was achieved by first varying the medial to lateral location by 1 mm per placement along the same rostral to caudal axis, then moving to a new rostral to caudal axis and repeating the medial to lateral movement. Two rostral to caudal axes were required to assess the full extent of the IC. Across animals the initial

placement and movement direction of each proceeding placement was varied to avoid bias and is further depicted in *Results: Spectral Parameters Show No Systematic Spatial Trends*.

There were a total of 51 electrode array placements across all three animals. For each placement, recordings were done at two or three depths, resulting in a total of 115 recording positions in the IC. At each position, we recorded BBN-driven, pure tone-driven, and spontaneous activity. BBN stimulation consisted of 100 trials each of 30, 50, and 70 dB-SPL (50 ms duration, 0.5 ms rise/fall time, 6 octave bandwidth from 0.625 to 40 kHz). BBN stimulation was interleaved with 100 trials of spontaneous activity (with no stimulation), presented in a random order at 2/s. Pure tone stimulation was used to create frequency response maps (**FRMs**; 1-40 kHz with 8 tones/octave, 0-70 dB-SPL in 10 dB steps, all presented in a random order at 2/s).

Histology

The histological method used in these experiments was developed in our lab and detailed in a previous paper (Markovitz et al., 2012). Important points and additional steps are highlighted here. Upon completion of each experiment, animals were given an intracardiac overdose of pentobarbital and decapitated. The head was placed in a 3.7% paraformaldehyde solution. Over the next 10 days, the brain was fixed, blocked, and cryo-sliced to 60 μm thick slices. The slices were imaged and imported into Rhinoceros, a CAD software (Seattle, WA) to create 3D reconstructions of the IC. In this protocol, anatomical landmarks from the midbrain were used to consistently align slices and allow

for normalization and comparison of the IC across animals (Markovitz et al., 2012). For each IC, the red marks left by the Di-I were aligned across the slices to reproduce the location of the electrode array tracks.

Once the electrode array tracks were identified, the location of each site along those tracks was determined by calculating the depth from the IC border. The border of the IC was resolved during the experiment using BBN-driven responses at each electrode array placement. The electrode array was inserted to a depth where some but not all sites on each shank showed acoustic-driven responses. The IC border of each shank was deemed to be halfway between a deeper site with consistent responses to BBN and the subsequent, shallower site with weak or imperceptible responses (Markovitz et al., 2012). From this, the insertion depth of each recording position along a given placement was known in relation to its IC border depth. Next, we corrected the site location depths for changes in dimensions due to the fixation process. The change in dimension was calculated for each brain as the percent difference of the average, measured distance between adjacent shanks in the reconstruction compared to the expected, fixed distance of 500 μm. The resulting changes due to fixation were <10% for each brain. Within the reconstruction, the recording site locations were populated along the shank trajectories based on their corrected depths from the border. The accuracy of this method requires the assumption that anatomical and functional borders are coincident such that locations which do not respond to BBN lie outside the IC. In a recent report by Ito *et al.* (2014), acoustic-driven responses were recorded from layer 1 of the ICD using in vivo calcium imaging. Based on the focal depth, the acoustic-driven responses in that study were found

within 40 μm from the surface. This depth is within the error we can expect from our border technique where the actual border can be anywhere between the two adjacent sites (i.e., 100 μm, where we set the border at 50 μm between the adjacent sites). Therefore we can conclude that in using this assumption, there may be a small depth error but not enough to offset our overall trends.

Finally, the three brains were normalized to each other, and all the best fit lines and electrode array sites were imported to a single midbrain reconstruction. There were a total of 172 shanks and 2935 electrode array sites (number of sites per guinea pig: $n_{GP1}=995$, $n_{GP2}=949$, $n_{GP3}=991$). Thirty-two additional shanks were excluded from the reconstruction because none of their sites exhibited consistent acoustic-driven responses at any position along that placement and therefore were considered to be outside of the IC.

Data Analysis

The goal of this study was to determine how response parameters differ across the entire IC and if systematic trends exist. Analysis was done first to compute the different response parameter values for each recording site. Sites were then separated into appropriate subregions (i.e., ICC, ICO, and SC; based on functional responses) and planar cuts were made along ICC laminae in order to investigate location trends across each lamina. Finally, comparisons were made between response parameters values found within subregions and within different laminae to assess functional differences.

*Response Parameters.*For this functional study, we assessed temporal parameters with BBN stimulation, spontaneous firing activity with no-stimulation trials, and spectral parameters with pure tone stimulation. Post stimulus time histograms (**PSTHs**) were used to analyze BBN-driven and spontaneous responses for four parameters: FSL, FSL jitter, response duration, and spontaneous firing rate. Each of the temporal parameters was analyzed at fixed levels of 30, 50, and 70 dB-SPL for each site. Analysis was done at fixed sound levels to better estimate how sound is processed by neurons. It seemed more realistic to use set sound levels to characterize responses versus using levels dependent on the thresholds of each neuron as perception occurs from sounds of varying levels independent of neural threshold. FSL and FSL jitter were determined by calculating the mean and standard deviation of time from onset of acoustic stimulation to the first spike over 100 trials. For each trial, the time to first spike was measured between a window that started after a 4 ms lockout period and ended at the offset of acoustic stimulation. This lockout period represents the shortest latency previously reported in the IC (Schreiner and Langner, 1988; Syka et al., 2000). Response duration was calculated by determining the window of spiking activity that significantly exceeded the spontaneous activity according to the signal detection theory value of d'>1 (Green and Swets, 1966; Lim and Anderson, 2007a). The response durations were normalized by the length of BBN stimulation (i.e., 50ms) to provide ratio values in which one indicated the response lasted the entire duration of the stimulus. Lastly, spontaneous firing rates were calculated over a 50 ms window, corresponding to the time window when the stimulus was presented in the other

BBN conditions. The spontaneous firing rates were calculated over the 100 no-stimulation trials.

Responses to pure tones were examined for the four additional response parameters: threshold, BF, Q-value at 10 dB above threshold, and Q-value at 60 dB-SPL. Response parameters were evaluated from the FRM of each site utilizing custom written MATLAB software used in Rode *et al*. (2013). The threshold was visually determined and the BF was calculated as the centroid of the bandwidth of activity 10 dB above threshold (Lim and Anderson, 2006). The Q-values were calculated by dividing the center frequency by the bandwidth of activity at either 10 dB above threshold or at 60 dB-SPL. Of these response parameters, only threshold and Q-values were evaluated for spatial trends, while BF was used to categorize sites into midbrain subregions.

Midbrain Subregions. Sites were divided into different subregions depending on their tuning properties and/or location. ICC sites were characterized as those that displayed a tonotopic gradient, where consecutive sites along a shank showed a change from high to low frequencies across deeper to shallower sites (Snyder et al., 2004). If a reversal of frequencies occurred at the low frequency border, sites following the reversal were not included in the ICC. SC sites were identified by their reconstructed location within the SC portion of the midbrain. These sites had predominantly narrow, high frequency tuning with an average BF of 16 kHz and occasionally had broader tuning centered around 7 kHz (Wise and Irvine, 1983; Hirsch et al., 1985; Carlile and Pettigrew, 1987). In addition, no tonotopic gradient was identified across SC sites. All remaining

sites were considered to be within the ICO, comprised of sites in the ICD and in the ICX. The FRMs of these ICO sites included several varieties: narrowly tuned sites that showed a BF reversal, double peaked FRMs, broad tuning with no gradient changes along the shank, and no clear frequency selectivity. The locations of sites within the three subregions can be seen in 3D (Fig. 3*A*) and in 2D (Fig.3*B*). Based on these divisions, there were 1075 ICC sites, 450 SC sites, and 1410 ICO sites.
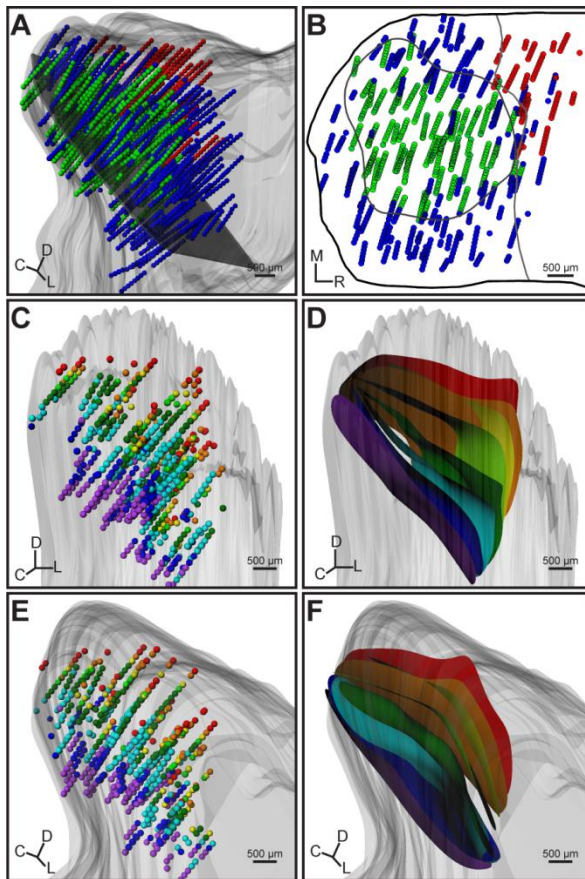
Figure 3. Histological reconstructions of all recording locations. *A*, Sites were separated into subregions that included ICC (n=1075, green), ICO (n=1410, blue), and SC (n=450, red) depending on the tuning properties and midbrain location. *B*, For visualization and analysis purposes, planar cuts were used to create 2D maps, in which *B* corresponds to the view along the gray planar cut shown in *A*. The 2D maps include estimated borders delineating the subregions. *C,E*, The ICC sites were further separated into BF laminae. See *Methods: Midbrain Subregions* for lamina BFs, bandwidths, and number of sites. *D,F*, Three-dimensional planes were fit to the ICC laminae. BF sites and lamina planes are shown at two different angles to better view their shapes and location within the IC.

After dividing sites into appropriate subregions within the midbrain, the BFs were used to further separate the ICC sites into eight different isofrequency laminae. These laminae were selected such that individually, each lamina spanned one critical bandwidth of 0.34 (Schreiner and Langner, 1997; Egorova et al., 2006). The resulting laminae as shown in Figure 3*D,F* are as follows: Lamina 1, 1.5-1.9 kHz (**L1**, n=43, red); Lamina 2, 2.0-2.5 kHz (**L2**, n=43, orange); Lamina 3, 3.0-3.8 kHz (**L3**, n=47, yellow); Lamina 4, 4.0-5.1 kHz (**L4**, n=37, green); Lamina 5, 6.0-7.6 kHz (**L5**, n=114, dark green); Lamina 6, 8.0-10.1 kHz (**L6**, n=169, cyan); Lamina 7, 12.0-15.2 kHz, (**L7**, n=93, blue); Lamina 8, 16.0-20.3 kHz (**L8**, n=123, purple). Sites within each lamina in the ICC (Fig. 3*C,E*) have been fitted with 3D planes to depict the size, shape, and directionality of the best frequency laminae inside the whole IC (Fig. 3*D,F*).

Based on the location of the sites in each lamina defined in Figure 3*C-F*, planar cuts (i.e., sites within a similar area projected onto a given plane) were created that encompassed not only all of the ICC sites sorted to a specific lamina but also the ICO and the SC sites that fell in the same plane as those ICC sites. To create each planar cut, a mean plane was first calculated from all of the ICC sites designated to be within a single ICC lamina, as previously defined in Figure 3*C-F*. Next, we calculated borders to serve as the limits for each planar cut in order to avoid outliers and reduce the amount of overlap. The borders were created as planes parallel to the mean plane and placed at an interval above and below the mean plane, which varied for each lamina. That interval was calculated by finding the distance from each ICC point in the lamina to the mean plane and averaging. The planar cut was then comprised of all sites, regardless of the BF

subregion, that lay between these two border planes. In other words, each planar cut could consist of sites that are technically from different BF laminae that were originally defined in Figure 3 because the planes are flat whereas the laminae are curved. This type of analysis was necessary to be able to easily view the data in two dimensions and to identify spatial trends across these laminae. The result was eight planar cuts derived from the eight previously defined laminae from Figure 3*C-F*. As an example, the mean plane calculated for Lamina 6 can be seen in Figure 3*A* and the corresponding planar cut with the sites within the outer border planes projected onto that cut can be seen in Figure 3*B*. Although the planes are tilted in a roughly 45° angle, since we are projecting the sites onto a 2D plane, it is possible to simplify the terminology by using just medial-lateral and rostral-caudal coordinates for viewing purposes and for describing trends along each plane. It is clear from our reconstruction in Figure 3*D,F* and previous anatomical work that laminae vary in shape and curvature (Malmierca et al., 1995). However, an approximation of a flat plane with projected sites onto that plane is adequate for our purposes, as will be later demonstrated in *Results*. The absolute distance between sites may be slightly skewed due to this projection process, but the relative locations of the sites with each other are preserved, and thus we can still estimate trends along each plane. For visualization purposes only (but not the actual analysis), the sites were slightly skewed in the figures in the medial-lateral direction to be able to view all of the sites in each 2D map since many sites were exactly on top of each other. Additionally, borders were between the IC and the SC based on anatomical landmarks viewed from the dorsal surface and encircling a majority of the ICC sites in the planar cut were drawn (Fig. 3*B).*

30

These borders are unique to each planar cut dependent on where the plane intersected the IC/SC border and on the location of ICC sites in the plane. Within the *Results,* lamina refers to only ICC sites from a specific frequency range and is denoted by lamina number with frequency range as necessary (e.g. L6 or L6: 8.0-10.1 kHz). Planar cut refers to all midbrain sites within a defined area and is denoted by the lamina number from which it was derived and the mean BF of the ICC and the ICO sites within the planar cut when necessary (e.g. PC6 or PC6: 9.1 kHz).

Location Effects and Lamina Comparisons. All SC sites were excluded from these analyses since we only sampled a subset of the SC which may not be representative of the acoustic responses expected from the entire SC. SC sites are still included in the visualization of the trends in the figures. Sites that lacked significant acoustic-driven activity at each level were further excluded from the location analyses for that level. Significant acoustic-driven activity was determined using signal detection theory, as described in Green and Swets (1966) and Lim and Anderson (2007a). Spike count distributions from 50 ms of acoustic-driven activity and 50 ms of spontaneous activity were compared and sites were included if the two distributions were significantly different from each other ($d'>1$). Due to threshold differences, the number of sites in the IC that showed sufficient evoked activity varied across level with 2055 sites included for 30 dB-SPL, 2439 sites included for 50 dB-SPL, and 2477 sites included for 70 dB-SPL.

Two-dimensional multiple linear regression was used to examine the existence of linear gradients along a given 2D planar cut by determining if measured response

31

parameters could be predicted by location along each planar cut. For each response parameter that yielded a significant trend, the gradient angle (θ) and the R^2 statistic are reported in *Results*. The θ gave the direction along the planar cut where the greatest change in values was found, with $\theta=0°$ indicating a change in the caudal to rostral direction and $\theta=-90°$ indicating a change in the medial to lateral direction. The R^2 value was a measure of the strength of the correlation along the gradient angle. Concentric and clustering analyses were employed for response parameters that did not show a linear gradient. However, these analyses did not yield any significant results and thus are not further discussed.

Statistical analysis was performed to identify any differences in response properties between the ICC and the ICO, between different ICC laminae, and between different stimulation levels. All comparisons were performed using a two-tailed, unequal variance, ranked t-test (Ruxton, 2006b). Lamina and level comparisons were performed with a Bonferroni correction. Significance was determined at $p<0.05$. For subregion comparisons, the exact p-values are provided. For lamina and level comparisons, only the largest significant p-value found is provided for simplicity since lamina comparisons resulted in twenty-eight unique values and level comparison resulted in three unique values.

RESULTS

Temporal Parameters Show Systematic Spatial Trends across the Whole IC

A consistent organization across the IC was found only for temporal parameters and spontaneous activity, but not for spectral parameters. For FSL, FSL jitter, response duration, and spontaneous firing rate, there was a clear distinction between neural activity exhibited in the caudal-medial versus rostral-lateral areas of the IC. In response to BBN, rostral-lateral sites had shorter latencies, smaller jitter, sustained response durations, and higher spontaneous firing rates. The direction of change for each trend was the same, but the trend strength varied, which was evident when comparing response parameter maps in Figure 4. These maps plot the response parameter values that correspond to each recording site. The maps and trends shown in Figure 4 and discussed here were a result of BBN at 70 dB-SPL; however, similar trends were observed at 30 and 50 dB-SPL and are later discussed in *Results: Spatial Trends and Response Differences Are Not Dependent on Stimulation Level.*

Trends for FSL and FSL jitter showed a clear gradient from caudal-medial to rostral-lateral areas of the IC, which is apparent in the full 3D maps and 2D planar cut maps (Fig. 4*A-D*). FSL responses varied from long to short latencies across a gradient angle equal to -41.3° for PC4, -43.8° for PC6, -45.7° for PC7, from the caudal-medial corner (R^2=0.55, 0.54, 0.52, respectively). Similarly, FSL jitter responses varied from large to small jitter, (i.e., increased precision) from the caudal-medial to rostral-lateral areas (PC4, θ=-33.2°, R^2=0.48; PC6, θ=-38.3°, R^2=0.48; PC7, θ=-38.6°, R^2=0.46). Due to placement of sites in the ICC and the ICO, it was not possible to calculate separate

33

Figure 4. Functional maps reveal temporal response parameter trends from the caudal-medial to rostral-lateral area of the IC in response to 70 dB-SPL stimulation. For each response parameter, a full 3D map of all the sites and 2D plots of three individual planar cuts are provided. *A,C,E,G* For the 3D maps, a total of 2918 sites were included (n_{ICC}=1072, n_{ICO}=1405, n_{SC}=441) for (*A*) FSL, (*C*) FSL jitter, (*E*) response duration, and (*G*) spontaneous firing rate. *B,D,F,H*, Only PC4, PC6, and PC7 are shown here of the eight planar that were analyzed. Trends found for these planar cuts were representative of what was found in all planar cuts. *B,D*, FSL and FSL jitter showed a clear gradient from the caudal-medial to rostral-lateral area of the IC, with similar gradient angles (PC4: θ_{FSL}=-41.3°, θ_{Jitter}=-33.2; PC6: θ_{FSL}=-43.8°, θ_{Jitter}=-38.3°; PC7: θ_{FSL}=-45.7°, θ_{Jitter}=-38.6°). *F*, For response duration, there was a clear division between the rostral-lateral versus caudal-medial portion of the IC, with the former having sustained response durations with

34

ratios near one and the latter displaying different response durations with ratios typically exceeding one. *H*, Spontaneous firing rate showed a weak gradient with higher spontaneous firing rates more often in the rostral-lateral and lateral areas of the IC.

gradient angles for each subregions without bias. However, it was clear that no division can be made between the two subregions as the gradient extended over the whole IC. This result was surprising since it was originally expected that clear differences in acoustic response properties would be found between the ICC and the ICO, considering that previous studies have proposed different roles for these two subregions (Aitkin, 1979; Huffman and Henson, 1990; Knudsen, 2002). The ICC is part of the lemniscal pathway, which corresponds to the main ascending pathway for robustly transmitting sound information to higher perceptual centers; thus, it would be expected that the shortest and most precisely-timed latencies would occur within the ICC instead of the ICO. Instead, there is a general rostral-lateral region of the IC (compared to the caudal-medial IC) with the fastest and most precisely timed responses that includes neurons in the non-lemniscal pathway.

The trend for response duration was different than the gradients seen for FSL and FSL jitter. In contrast to those smooth gradients, a clear division could be drawn in the IC that separates two distinct populations of responses. One population contained sites with response durations that were sustained during acoustic stimulation (i.e., with normalized response duration ratios near 1), represented by the yellow-orange color in Figures 4*E,F*. This population contained 66.5% of the ICC sites and 65.8% of the ICO sites with a mean response duration equal to 1.12 ± 0.22. The second population consisted of sites with response durations that exceeded the duration of the stimulus, with a mean response ratio

equal to 1.49 ± 0.46. This population comprised 33.5% of the ICC sites and 34.2% of the ICO sites. This trend revealed that the sustained population resided in the rostral-lateral area of the IC and the other population resided in the caudal-medial area. As with FSL and FSL jitter, there were no clear differences observed in the spatial trend for response duration ratio between the ICC and the ICO.

Spontaneous activity showed a weak gradient with sites exhibiting high spontaneous firing rates in the rostral-lateral and lateral portions of the ICC and the ICO (PC4, θ=-65.7°; PC6, θ=-72.3°; PC7, θ=-75.3°). The calculated strength (PC4, R^2=0.11; PC6, R^2=0.13; PC7, R^2=0.10) indicated the gradient does not account for a majority of the sites but rather verified that there was an area of higher firing rates (Fig. 4*G,H*). Again, there were no clear differences observed for spontaneous activity between the ICC and the ICO spatial trends.

A comparison of the overall distributions of values found in each subregion or lamina was made for each response parameter in Figure 5 There was a significant difference between the two subregions for FSL (ICC mean ± std: 8.1 ± 2.8 ms; ICO: 8.1 ± 4.5 ms; p=0.026 two-tailed, unequal variance, ranked t-test), FSL jitter (ICC: 2.1 ± 2.3 ms; ICO: 3.1 ± 3.3 ms; p=4.9E-6), response duration (ICC: 1.3 ± 0.4; ICO: 1.2 ± 0.4; p=5.0E-9), and had spontaneous activity (ICC: 46.3 ± 16.2 spikes/s; ICO: 42.5 ± 19.1 spikes/s; p=3.8E-12). The ICC on average had shorter latencies, was more precise, had shorter response durations, and higher spontaneous firing rates than the ICO. This statistical result is expected when viewing Figure 4 since the ICO contains response property values at the extreme edges of each trend (i.e., the most caudal-medial and the
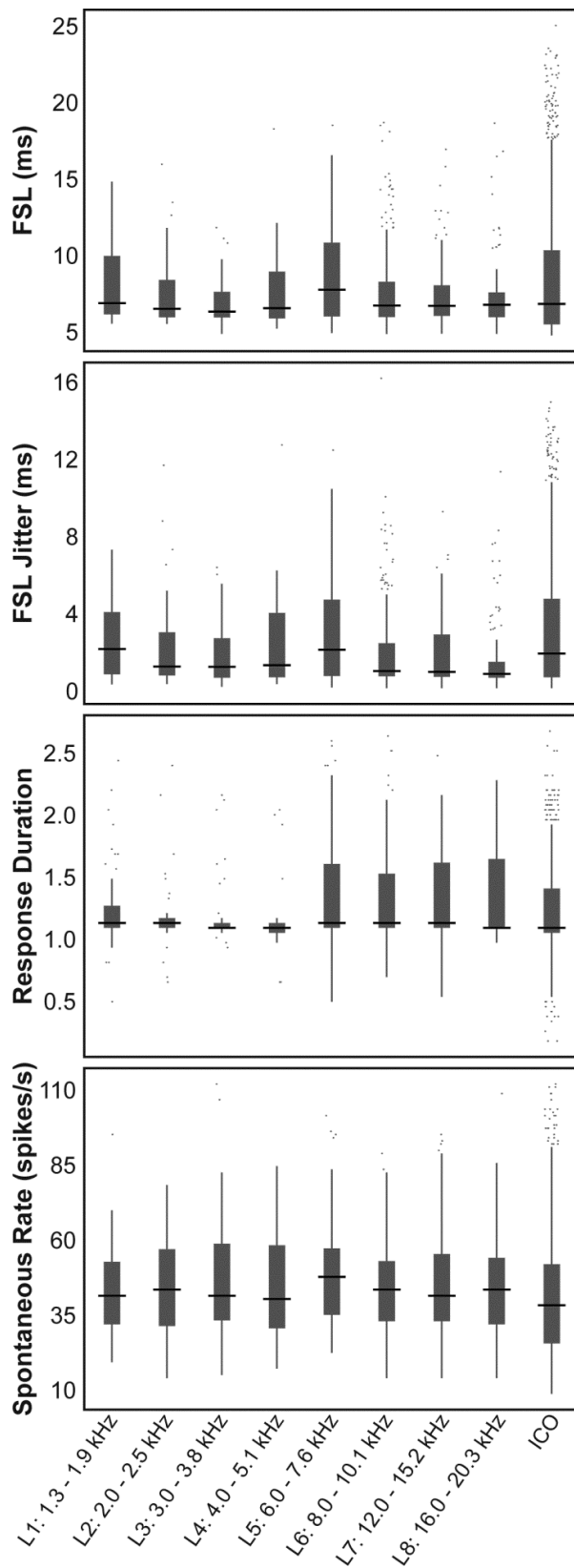
most rostral-lateral areas). Comparisons between the different ICC laminae revealed that there were no systematic differences across different BFs, though some laminae were significantly different from others (Fig. 5). The details of those significant differences are provided in Table 1.

Figure 5. No systematic difference exists between BF laminae for temporal response parameters. Distributions are plotted for all eight ICC lamina and for ICO for the BBN noise and no-stimulation parameters. For each lamina and the ICO, plots provide the median, 1st and 3rd quartiles, and outlier values. Similar FSL, FSL jitter, and spontaneous firing rates were found across all laminae. Response duration showed the greatest number of differences between laminae, with shorter responses and a smaller distribution of values found in laminae with BFs less than 5.1 kHz. Significant differences in response parameters are summarized in Table 1.

Spatial Trends and Response Differences Are Not Dependent on Stimulation Level

In addition to 70 dB-SPL stimulation, temporal parameters were also analyzed at 30 and 50 dB-SPL. At lower stimulation levels, the general spatial trends remained the same as at 70 dB-SPL, but the range of response values varied. As an example of this result, 2D maps of FSLs for each stimulation level can be seen in Figure 6. Each map showed a clear gradient from the caudal-medial and rostral-lateral areas of the IC, though the direction of each gradient varied slightly, represented by the arrow in each map (Fig. 6). The apparent difference found in each of these 2D maps was the range of values measured, with faster latencies occurring with 70 dB-SPL acoustic stimulation. This conclusion is evident when comparing distributions per ICC lamina (Fig. 7). The median and range was inversely correlated with stimulation level. For FSL, each lamina had a larger median and range of values at 30 dB-SPL with smaller median FSLs and reduced ranges of values at higher levels (p<0.003).
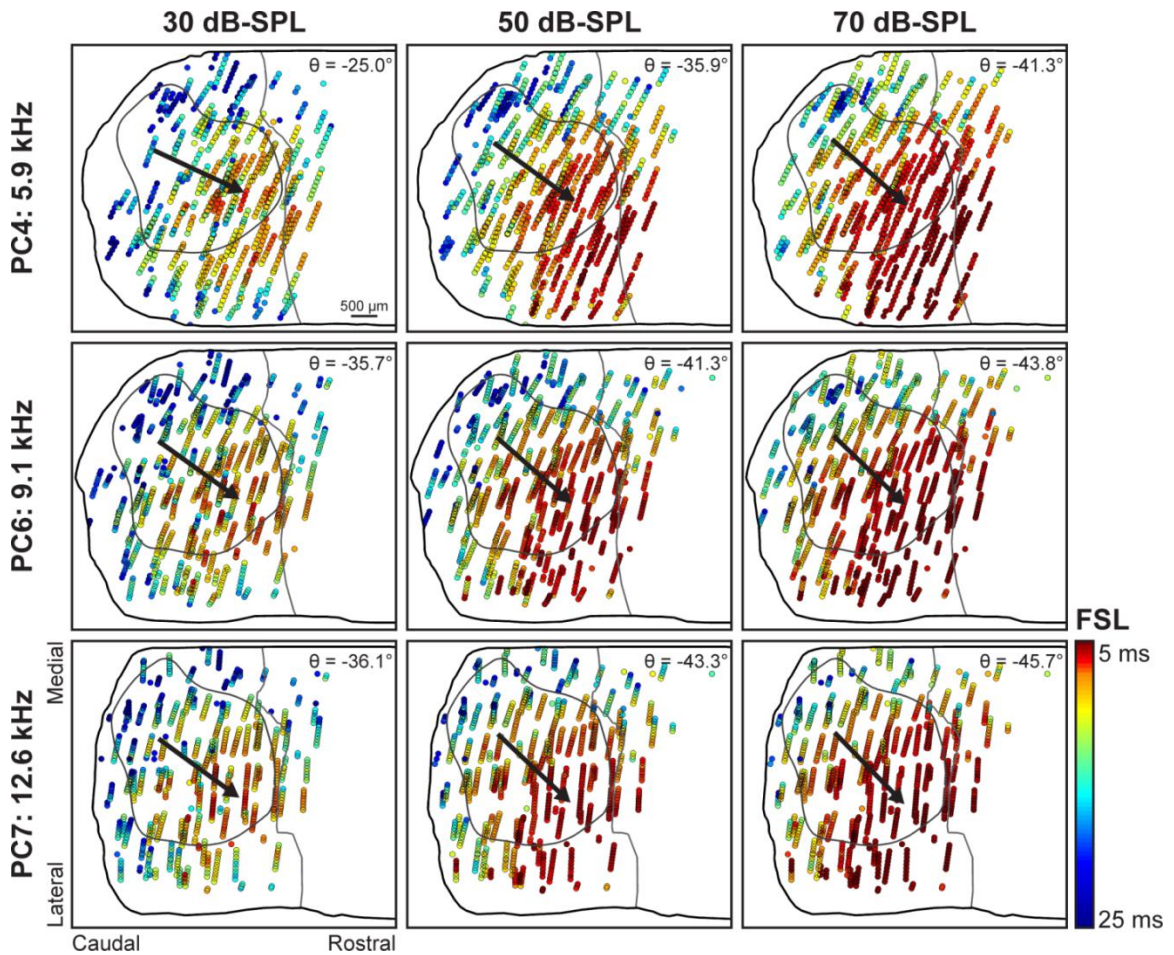
Figure 6. FSL spatial maps for the three BBN stimulation levels show that the general direction of the trends is similar across levels, though the gradient angles vary slightly. Arrows point in the direction of the shortest latencies at the specified gradient angle. This angle was calculated from the caudal-medial corner of the 2D maps. All maps show a clear gradient from the caudal-medial to the rostral-lateral area of the IC, without any clear transition between the ICC and the ICO.

Similar to FSL, the location trends do not differ across stimulation level for FSL jitter and response duration (maps not shown), but the median and range do. FSL jitter was larger at 30 dB-SPL than 70 dB-SPL, and on average the range of measured values diminished with higher stimulation levels ($p<0.002$). In contrast, there was no systematic variation in response duration across stimulation levels. Taken as a whole, the temporal

parameters measured at lower acoustic stimulation levels reflect the same spatial trends shown in Figure 4 for 70 dB-SPL, but with different maximum and minimum values dependent on the level.
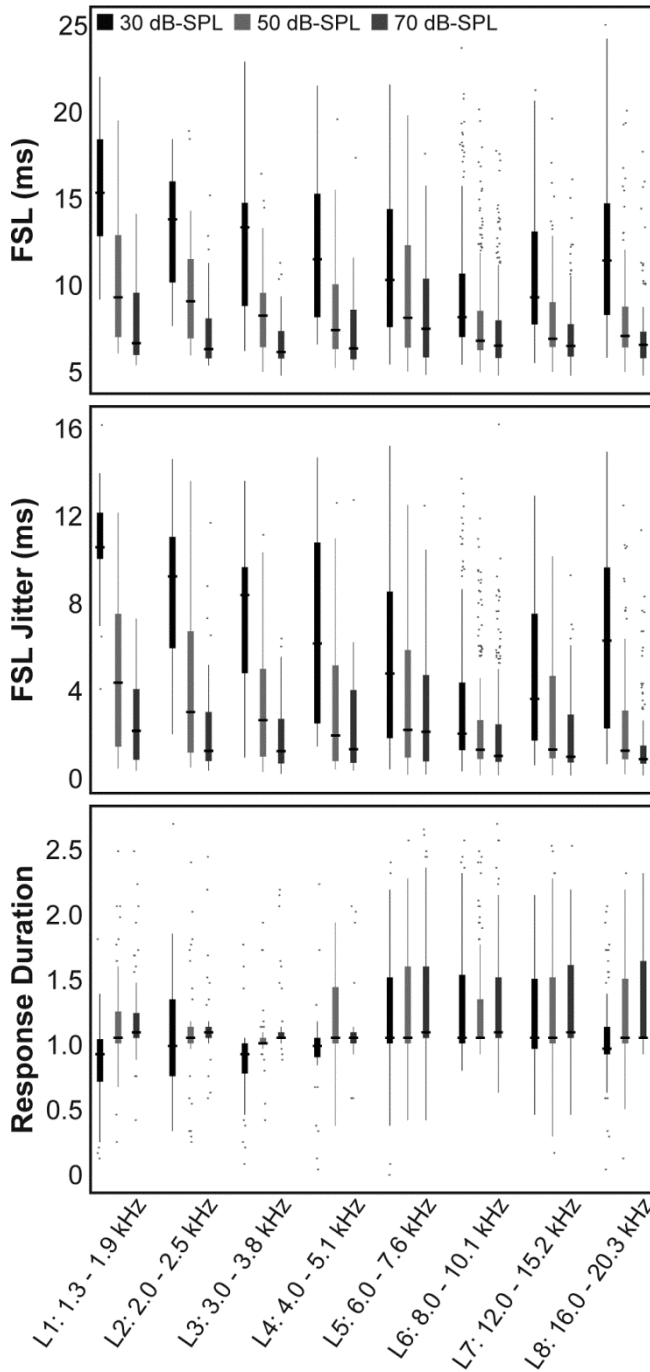
Figure 7. Response ranges for temporal parameters are dependent on stimulation level. As stimulation levels increased, latency decreased, reflected by a larger median and range of values at 30 dB-SPL and smaller median FSL values with reduced ranges at louder stimulation levels (p<0.003 two-tailed, unequal variance, ranked t-test with Bonferroni correction). FSL jitter medians and ranges of measured values decreased with higher stimulation levels (p<0.002). No systematic differences were found for response duration across different levels.

Fastest Neurons Located External to the Lemniscal Auditory Pathway

As shown in Figure 4, the sites with the shortest FSL and smallest FSL jitter values were located in the rostral-lateral area of the IC. In comparing the subregion of fastest 5% of sites and the most precise 5% of sites, most of these sites were outside of the ICC and within what we have defined as the ICO (Fig. 8). The ICO contained the absolute fastest sites, while the ICC contained the absolute most precise sites, but overall there were a greater majority of ICO sites that make up both populations (FSL – ICO: 79.5%, ICC: 13.0%, SC: 7.5%; FSL Jitter – ICO: 69.2%, ICC: 28.1%, SC: 2.7%). It is not certain based on our methods if all sites categorized as ICO are part of what is traditionally defined as the non-lemniscal auditory pathway since some sites may extend beyond what anatomical studies have marked as the non-lemniscal region of the auditory midbrain. However, it is clear from our data that the fastest and most precisely timed neurons exist outside of the ICC, which is part of the lemniscal auditory pathway.
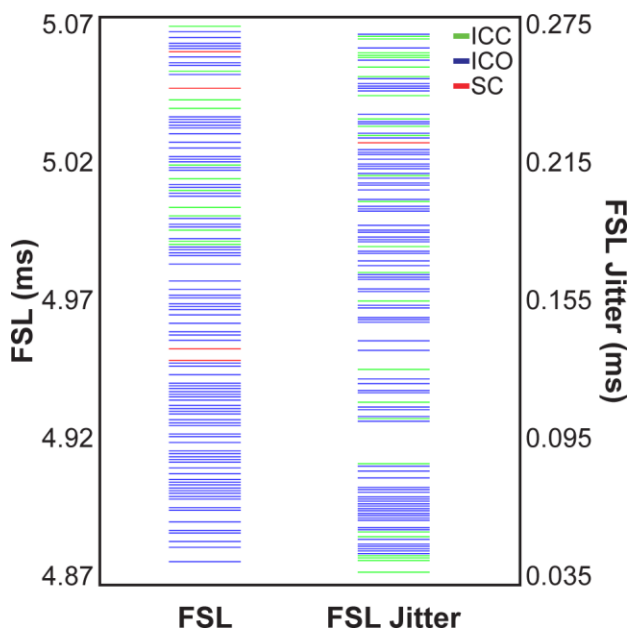
Figure 8. The fastest neurons are located in the ICO. The fastest 5% of sites and most precise 5% of sites across the midbrain are provided. The absolute fastest neurons were located in the ICO and ICO sites accounted for 79.5% of the fastest overall sites (ICC: 13.0%, SC: 7.5%). The most precise neuron resided in the ICC, however a majority of the overall most precise neurons were from the ICO compared to the other subregions (ICO: 69.2%, ICC: 28.1%, SC: 2.7%).

Spectral Parameters Show No Systematic Spatial Trends

Unlike temporal parameters, no consistent trends could be found across the IC for spectral parameters, which include BF threshold, Q-value at 10 dB above threshold, and Q-value at 60 dB-SPL. Though no apparent gradients or concentric spatial trends existed, these response parameters did show systematic differences when comparing between IC subregions and between ICC laminae.

Inspection of the 3D map for threshold reveals that low and high thresholds were scattered throughout the IC subregions and could not be characterized by a spatial trend (Fig. 9*A*). On average across all animals, sites in the ICC had significantly lower thresholds than sites in the ICO (ICC: 19.5 ± 11.7 dB-SPL; ICO: 22.2 ± 11.6 dB-SPL; p=7.2E-7). As shown in Figure 9*B*, we did not observe any obvious differences or trends across animals. In each animal, we purposefully varied the initial placements and the direction of subsequent placements per animal (e.g., GP1's initial placements was in the rostral-medial corner of the IC and subsequent placements were made in a clockwise direction, indicated by the circle and arrows for GP1 in Figure 9*B*, which is different from GP2 and GP3). This step reveals no indication of thresholds shifting due to time-specific adaptation or potential damage caused by subsequent placements in each animal that might have washed out any spatial trends for threshold.

Compiling all of the recordings sites across animals, we analyzed threshold trends across different BF laminae (Fig. 9*C*). L5 (p<1.4E-9) and L6 (p<1.1E-16) had significantly lower thresholds than all the other laminae. The two flanking BF laminae (L4 and L7), had significantly higher thresholds than L5 and L6 (p<1.4E-9), but

significantly lower thresholds than the remaining laminae (p<1.1E-5). With lowest thresholds at 6.0-10.1 kHz, our results match audiograms showing lowest thresholds at around 8 kHz for the guinea pig (Heffner et al., 1971; Prosen et al., 1978; Gourévitch et al., 2009).
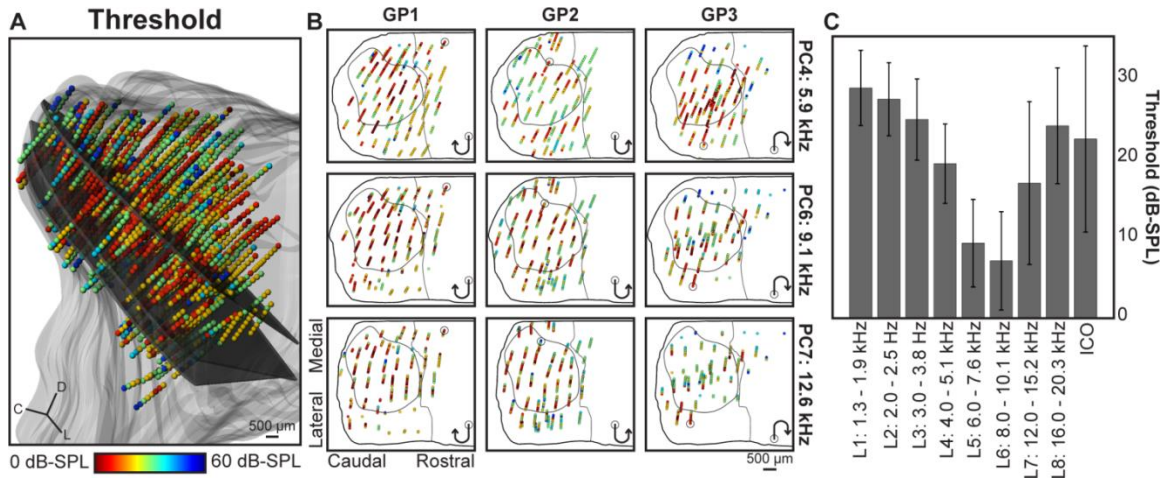
Figure 9. No spatial trends are apparent for threshold, but there are significant differences between laminae. *A,B*, Spatial trends were not evident in either the full 3D reconstruction (*A*) or the 2D visualizations of planar cuts separated for each animal (*B*). The arrow indicates the order of electrode array placements made during the experiment with a circle signifying the initial position for each animal. The initial recording placements were made in the rostral-medial corner, caudal-medial corner, and caudal-lateral corner for GP1, GP2, and GP3, respectively. Lowest thresholds were found within the ICC, but no spatial trend within the ICC was found. *C*, Between the laminae, L5 and L6 had significantly lower thresholds than all of the other laminae (p<0.01).

Similar to thresholds, no spatial trends were identified for Q-value at 10 dB above threshold or at 60 dB-SPL (Fig. 10*A-D*) and significant differences were detected when comparing between subregions and between laminae. ICC sites were more sharply tuned resulting in larger Q-values (10 dB: 2.1 ± 1.3; 60 dB-SPL: 1.3 ± 0.7) compared to those in the ICO, which on average were more broadly tuned (10 dB: 1.7 ± 1.5, p<1.4E-36; 60

dB-SPL: 0.7 ± 0.8, p<7.6E-24), signifying greater frequency selectivity in the ICC. This difference was evident when examining the 2D maps (Fig. 10*B,D*); sites with larger Q-values lie within the ICC border. Further analysis was completed to determine if the sites within the ICC were organized concentrically, but no systematic organization was
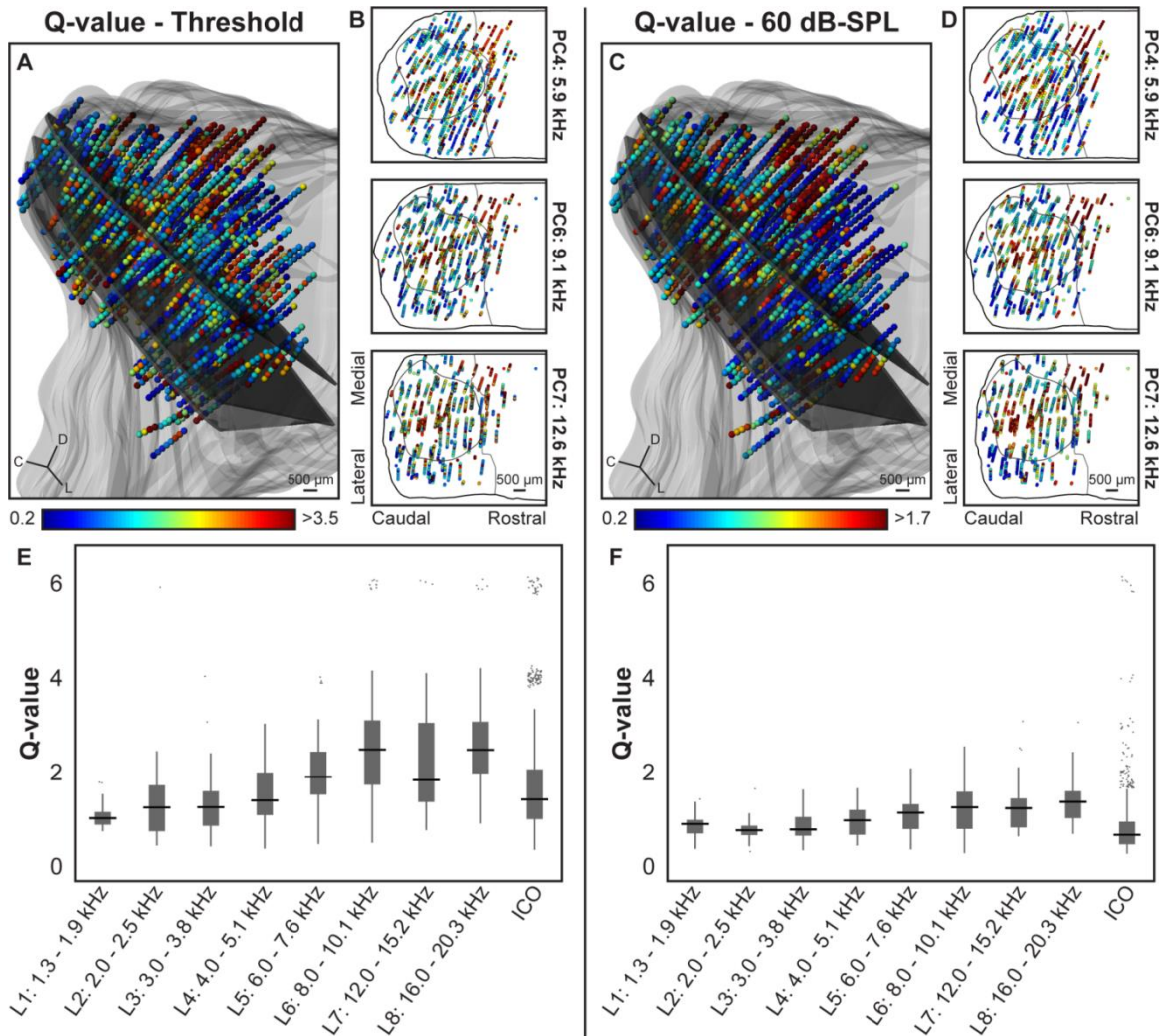
Figure 10. Spatial trends along each planar cut are not apparent for Q-value, but there are significant differences between laminae. *A-D*, Neither the full 3D reconstruction (*A*,*C*) nor the 2D visualizations per planar cut (*B*,*D*) showed a spatial trend; however there was narrower tuning found in the ICC compared to the ICO. *E*,*F*, Tuning width decreased with increasing BFs, with the narrowest tuning occurring at L8 for both 10 dB above threshold (*E*) and at 60 dB-SPL (*F*).

revealed. Significant differences were found for Q-values dependent on frequency (Fig. 10*E*,*F*). As BF increased, tuning width decreased (i.e., Q-values increased) with the narrowest tuned sites found in L8. Laminae with BFs greater than 8 kHz had significantly higher Q-values at 10 dB above threshold and at 60 dB-SPL than laminae with BFs lower than 3.8 kHz (p=1.2e-19). All of the lamina results for every parameter are summarized in Table 1.

Table 1. Significant difference for response parameters between laminae.

	Lamina 1	Lamina 2	Lamina 3	Lamina 4	Lamina 5	Lamina 6	Lamina 7
Lamina 8	‡ ● ■ ♦	■ ♦	■ ♦	§ ■ ♦	‡ ● ■ ♦	§ ●	§ ●
Lamina 7	● ■ ♦	● ■ ♦	● ■ ♦		●	●	
Lamina 6	● ■ ♦	● ■ ♦	● ■ ♦	● ■	■		
Lamina 5	● ■	● ♦	●	●			
Lamina 4	●	§ ●	●				
Lamina 3							
Lamina 2							

A summary of significant differences for response parameters across different laminae are provided in the table (p<0.0016, the largest p-value found that was still significant with Bonferroni correction). Comparison of the temporal parameters is shown for responses at 70 dB-SPL. Each symbol represents a different response parameter: FSL (†), FSL jitter (‡), response duration (§), spontaneous firing rate (▲), threshold (●), Q-value at 10 dB at threshold (■), and Q-value at 60 dB-SPL (♦).

Response Parameter Model Fits

Simple equations were used to model FSL and FSL jitter as their spatial trends followed linear gradients along the caudal-medial to rostral-lateral axis. To create the model equations, all locations were first normalized between zero and one using the

smallest cube possible that encapsulated all the IC recording sites in the reconstruction. The origin point was set at the most rostral, medial, and ventral location and the variables in the equations give the normalized distance to the most lateral (***L***), caudal (***C***), and dorsal (***D***) position. The final models were fit with parametric equations such that the location of each recording site (i.e., all three Cartesian coordinates) was represented by a single parametric value. The models were evaluated for high goodness of fit (R^2) and similarly to experimental values (low mean square error, **MSE**). The final equations were exponential describing the expected response as a function of location in the IC (*FSL =* *7.88e$^{1.43t}$ where t = 0.54L – 0.60C + 0.60V – 0.25; FSL Jitter = 1.44e$^{4.06t}$ where t = 0.48L* *– 0.50C + 0.72V – 0.39).* The upper panels in Figure 11 show the measured values from these two parameters. Using those same locations within the IC, the lower panels show the expected responses calculated from the provided equations (Fig. 11). The resulting equations render a much smoother gradient than was actually measured, but the equations can successfully predict the parameter values as a function of location. It should be noted that these are not the smallest MSEs achievable, but that there is tradeoff between best fit and ease of implementation. Multiple linear regression fits with second and third order terms could achieve lower MSEs and higher R^2 values, but at the cost of having over ten terms for each equation. In the end, we opted for equations that were feasible to implement, and simply demonstrate that FSL and FSL jitter can be systematically quantified as a function of location across the IC.
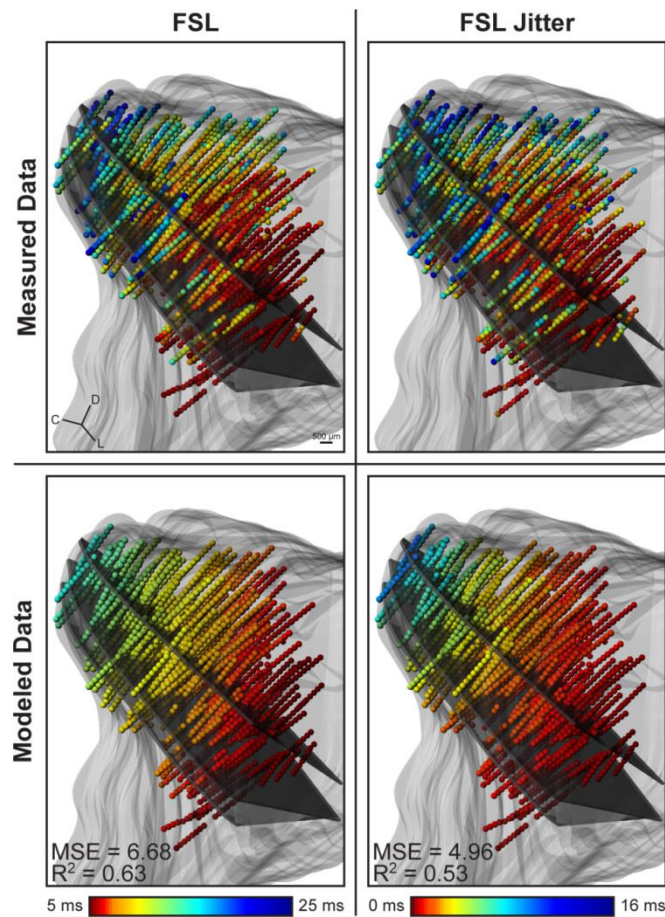
Figure 11. Simple equations could be used to model FSL and FSL jitter values as a function of location throughout the whole IC. Measured values are shown in the upper panels and expected responses calculated from the modeled equations as a function of locations are shown in the bottom panels. The measures of goodness of fit (R^2) and similarity of the modeled to measured values (MSE) are provided in the plots.

DISCUSSION

In mapping acoustic responses throughout the entire IC, we have compiled the most complete set of response parameter values available in the field, thus allowing us to assess the functional topography found in the IC and compare patterns across subregions. Our results indicate that clear spatial trends can be found for temporal response

parameters and spontaneous activity across the whole IC and clear distinctions can be made between subregions and laminae for spectral response parameters. The spatial trends for temporal responses revealed two unexpected results. First, no clear distinction can be made between the subregions, with trends extending into the ICO. The rostral-lateral IC, regardless of subregion, shows faster FSLs, greater precision, sustained response durations, and higher spontaneous firing rates compared to the caudal-medial IC. Second, as part of the lemniscal system, we expected responses from the ICC to be faster and more robust than sites in non-lemniscal regions. However, while slow, imprecise responses were found in parts of the ICO, a majority of the fastest and most precise sites were also located in the ICO. Examination of the functional roles of these different regions in the ICO provides context for differences in responses found.

Comparison of Functional Maps, Level and Lamina Trends to Previous Studies

To our knowledge, no functional mapping study has been completed that includes sites outside of the ICC or in response to BBN. Therefore, all the comparisons for our data are made with previous studies using pure tones and only in the ICC. Apart from spatial trends for spectral parameters, our results for spatial trends for temporal parameters and comparisons of the subregions, levels, and between laminae are consistent with previously found results.

The caudal-medial to rostral-lateral trend for FSL, FSL jitter, and response duration match those found in a previous study completed by our lab that focused on only two specific frequency laminae in the ICC . Our results show shortest FSL values in the

rostral-lateral area, while earlier work found shorter latencies mainly in lateral areas (Schreiner and Langner, 1988; Langner et al., 2002). Unlike previous studies that found concentric organizations with lower thresholds and narrower tuning in the center of the ICC (Stiebler, 1986; Ehret et al., 2003; Hage and Ehret, 2003), we found no concentric spatial trends. Instead, our results indicate locations with low thresholds and narrow tuning are dispersed throughout the ICC, similar to more recent studies (Portfors et al., 2011).

Our results agree with previous studies showing that on average the ICC contains sites with shorter latencies, smaller jitter values, more sustained response durations, higher spontaneous firing rates, lower thresholds, and narrower tuning compared to ICO (Aitkin et al., 1994; Syka et al., 2000; Lumani and Zhang, 2010). Comparing results across levels, we found that latencies, FSL jitter, and Q-values were inversely proportional to stimulus level, wherein values decreased with increasing stimulus levels, which is also consistent with previous studies (Hind et al., 1963; Egorova et al., 2001; Tan et al., 2008). We did not see non-monotonic jitter relationships that have been found in the ICC previously (Tan et al., 2008). Finally in comparing trends across lamina, our results agree with others that found Q-values increase with BFs (Ramachandran et al., 1999; Syka et al., 2000; Egorova et al., 2001; Egorova and Ehret, 2008) and that found no trend for latencies (Hind et al., 1963; Tan et al., 2008). We have not found literature on changes in jitter, response duration, or spontaneous firing rate as a function of BF, and therefore cannot make further comparisons.

Some of the inconsistencies, specifically for spectral trends, may be accounted for by the use of ketamine-xylazine anesthesia and multi-unit versus single unit recordings. Ketamine-xylazine anesthesia has been shown to have little or no effect on auditory coding in the IC for temporal properties, but can increase spontaneous firing rates and decrease inhibitory areas in FRMs (Astl et al., 1996a; Alkhatib et al., 2006; Ter-Mikaelian et al., 2007). In regard to multi-unit activity, if a trend was not observed, it may still occur on the single-unit level but was masked or obscured by multi-unit activity. However, it is unlikely a spatial trend would be completely eliminated due to multi-unit recording since neurons with similar properties would be clustered together, and thus general trends should still be observed. We did not observe any spatial spectral trends, at least under anesthesia. Results will need to be verified in awake preparations

Function of Temporally Precise and Imprecise Neurons in the ICO

Based on previous studies, we expected responses in the ICO to be slower and less precise than responses in the ICC, as the lemniscal system is mainly responsible for efficient, reliable transmission of auditory information necessary for perception. In the caudal-medial area of the ICO we found temporally imprecise neurons as expected. However a surprising result was that a majority of the fastest and most precise neurons reside in the rostral-medial ICO. Examining the anatomical projections to and from these regions of the ICO provide necessary context to determine the use of both types of information in auditory processing and in the functions of those regions.

The spatial trends found in the ICC may be aligned with and a result of the differential innervation by brainstem sources (Brunso-Bechtold et al., 1981; Aitkin and Schuck, 1985; Cant and Benson, 2006; Loftus et al., 2010). As the spatial trends extend out to the ICO in our functional data, it is possible that the same differential innervation that occurs in the ICC also extends out to the ICO. Since most ascending projections from the brainstem nuclei end in the ICC with some projections to the ICX, but with little innervation of the ICD, it is likely that the regions with fast, precise neurons in our studies correspond to the ICX (Ehret, 1997). This claim is supported by previous studies have observed fast, precise responses in the ICX (Aitkin et al., 1994; Syka et al., 2000). These studies however did not indicate the location of these fast, precise responses within the ICX, as we have provided in our results. For the ICD, in addition to the minor contribution from the ascending system, there are dense projections from the descending system, perhaps accounting for the slower, less precise responses found in our ICO data (Winer et al., 1998; Bajo and Moore, 2005; Malmierca and Ryugo, 2011). Based on these anatomical projections and organization, the question becomes what ICX function requires fast, precise responses and what ICD function requires slower information.

Fast, precise responses by the ICX may be necessary for its role in multimodal circuits. Prior evidence shows that the ICX is involved in head orientating actions and sound localization (*reviewed in* Huffman and Henson, 1990), with projections to the SC, the dorsolateral pontine nucleus (**DLPN**), ventrolateral tegmental nucleus, and dorsal cochlear nucleus (Aitkin and Boyd, 1978; Edwards et al., 1979; Caicedo and Herbert, 1993; King et al., 1998). Information received by the ICX is sent directly to the SC and

indirectly to the cerebellum via the DPLN, allowing for initiation of necessary pinna, eye, and head movement to orient and to localize to the sound source (Syka and Straschill, 1970; Hoddevik et al., 1977). These pathways suggest that the information is bypassing the cortical network, acting as a reflex versus relying on auditory perception before motor initiation. Studies confirm this reflex, as cortical inactivation does not affect head orienting (Smith et al., 2004; Nodal et al., 2012). Thus, the simultaneous projection of fast information to the ICX and the ICC allows for parallel processing leading to movement and perception, coordinating accurate, timely interaction with the surrounding environment.

In contrast, slow, imprecise responses in the ICD may allow for the integration of cortical feedback for auditory modulation. Activation and inactivation of the cortex has led to plastic changes throughout the ICC (Bajo and King, 2012; Suga, 2012). One pathway for this modulation is directly from the cortex to the ICC (Bajo and Moore, 2005; Lim and Anderson, 2007b; Markovitz et al., 2013). However, as this pathway is predominantly excitatory, a second inhibitory pathway may exist via the ICD (Offutt et al., 2014). The delayed response of neurons in the ICD may allow for integration of ascending and descending input to correctly modulate the ICC. FSL in the auditory cortex in response to BBN ranges from 10-15 ms (Hackett et al., 2011) and transmission time to the IC from the A1 is 4-10 ms (Markovitz et al., 2013). The FSLs for the caudal-medial ICO, or the ICD, were from 15 to 25 ms, in line with the summation of time for sound to travel up to the cortex and then back to the ICD. This modulation may affect salience of or attention to auditory information that is coded within the ICC, as lesions to the ICD

have resulted in altered attention to an auditory stimulus (Jane et al., 1965). These descending networks to the ICD and the ICC have also been implicated in plasticity and learning (Xiong et al., 2009; Malmierca and Ryugo, 2011). Thus, the ascending information to the ICD and descending signal from the cortex can coordinate modulation of ICC neural activity to better attend to and learn the incoming sound information.

In conclusion and supported by previous anatomical and behavioral studies, our data suggest that different subregions of the auditory midbrain exhibit significant differences in timing properties necessary for supporting varying behavioral roles. For head and body orienting reactions to meaningful or life-threatening sounds, the coordination of the ICX and the ICC for movement and perception requires fast, precise responses in the ICX. For auditory modulation involved with attention or learning, coordination between ascending and descending auditory projections requires slow, imprecise responses in the ICD. These response properties are spatially organized in a distinct and systematic way across the IC, as revealed for the first time through our mapping results.

CHAPTER 3: SUPPRESSION AND FACILITATION OF AUDITORY NEURONS THROUGH COORDINATED ACOUSTIC AND MIDBRAIN STIMULATION

The IC is the primary processing center of auditory information in the midbrain and is one site of tinnitus-related activity. One potential option for suppressing the tinnitus percept is through deep brain stimulation via the AMI, which is designed for hearing restoration and is already being implanted in deaf patients who also have tinnitus. However, to assess the feasibility of AMI stimulation for tinnitus treatment we first need to characterize the functional connectivity within the IC. Previous studies have suggested modulatory projections from the ICD to the ICC, though the functional properties of these projections need to be determined. In this study, we investigated the effects of electrical stimulation of the ICD on acoustic-driven activity within the ICC in ketamine-anesthetized guinea pigs. We observed ICD stimulation induces both suppressive and facilitatory changes across ICC that can occur immediately during stimulation and remain after stimulation. Additionally, ICD stimulation paired with broadband noise stimulation at a specific delay can induce greater suppressive than facilitatory effects, especially when stimulating in more rostral and medial ICD locations. These findings demonstrate that ICD stimulation can induce specific types of plastic changes in ICC activity, which may be relevant for treating tinnitus. By using the AMI with electrode sites positioned within the ICD and ICC, the modulatory effects of ICD stimulation can be tested directly in tinnitus patients.

INTRODUCTION

The IC is a major convergence center of the auditory system located within the midbrain that integrates bilateral ascending and descending inputs. The IC is subdivided into three main regions: the ICC, the ICX, and the ICD, each with a distinct role in auditory processing that can be substantiated by the projections to that region (Roth et al., 1978; Faye-Lund and Osen, 1985; Coleman and Clerici, 1987; Casseday et al., 2002;

Oliver, 2005; Cant and Benson, 2006; Loftus et al., 2010). The ICC is the best characterized of all the IC regions, comprised of disc-shaped cells arranged in fibrodendritic laminae that constitute the tonotopic area of the IC (Morest and Oliver, 1984; Oliver and Morest, 1984; Faye-Lund and Osen, 1985; Meininger et al., 1986; Malmierca et al., 1993). As the core auditory processing center in the IC, a majority of projections into the ICC ascend from lower auditory centers with a smaller percentage of innervation originating from the auditory cortex (Adams, 1979; Brunso-Bechtold et al., 1981; Shneiderman et al., 1988; Saint Marie and Baker, 1990; Oliver et al., 1995; Schofield and Cant, 1996; Winer et al., 1998; Malmierca and Ryugo, 2011). Unlike the ICC, which is mainly an auditory center, the ICX is innervated by auditory, visual, and somatosensory projections and thus has a role in multi-sensory integration (Aitkin et al., 1978; Aitkin et al., 1981; Binns et al., 1992; Knudsen, 2002; Gruters and Groh, 2012). Questions, however, remain about the role of the ICD in auditory processing.

The role of the ICD in auditory processing may be modulatory, suggested by the extensive inputs the ICD receives descending from the auditory cortex (Faye-Lund, 1985; Huffman and Henson, 1990; Herbert et al., 1991; Winer et al., 1998). Corticofugal projections have been shown to modify frequency tuning and tonotopic maps, shift thresholds, and alter sensitivity to sound localization cues within the ICC (Zhang et al., 1997; Yan and Suga, 1998; Yan and Ehret, 2002; Suga and Ma, 2003; Nakamoto et al., 2008; Bajo and King, 2012). Because the descending projections from the A1 targeting the ICD are more abundant than those targeting the ICC, it is possible that this descending modulation is achieved, at least in part, by a multi-synaptic pathway to the

ICC via the ICD. Anatomical studies within the IC have shown a network of intrinsic projections from the ICD to the ICC that supports this multi-synaptic pathway (Saldaña and Merchán, 1992; Malmierca et al., 1995; Saldana and Merchan, 2005). Modulation via ICD is also implicated by the results of inactivation studies, which have demonstrated changes in the ICC coding properties and plasticity effects when inactivating the IC surface, which likely included the ICD (Jen et al., 2001; Ji et al., 2001; Ji and Suga, 2009). However, there are no studies to our knowledge that have directly activated ICD neurons to confirm and characterize their modulatory effects on ICC neurons.

The effects of ICD stimulation on ICC activity are particularly relevant for recent investigations of a new deep brain stimulator for tinnitus treatment. The AMI was initially developed for hearing restoration in patients with NF2, a genetic disease that is typically associated with bilateral acoustic neuromas (Lenarz et al., 2006; Schwartz et al., 2008; Colletti et al., 2009b; Lim et al., 2009b). These patients become bilaterally deaf due to damage of the auditory nerves inflicted by growth and/or surgical removal of these tumors. For these patients, the AMI array consisting of one or two shanks with up to 22 electrode sites can be inserted along the tonotopic axis of the ICC with minimal added risks by using the same surgical opening as tumor removal (Samii et al., 2007; Lim et al., 2009a). Due to the hearing loss associated with the tumors, many of these patients also develop tinnitus, which has been linked to changes in spiking activity and synchrony across the auditory system, including the ICC (Eggermont and Kenmochi, 1998; Zhang and Kaltenbach, 1998; Brozoski et al., 2002; Ma et al., 2006; Bauer et al., 2008; Lanting

et al., 2009; Melcher et al., 2009; Roberts et al., 2010; Møller, 2011b; Wang et al., 2011; Mulders et al., 2014; Vogler et al., 2014).

In the initial AMI clinical trials, three of the five patients had tinnitus. In those three patients, the AMI array was implanted in the ICC, the ICD, and the lateral lemniscus. Stimulation in these patients interfered with the tinnitus percept but did not sufficiently suppress tinnitus (unpublished observations). Considering the proposed modulatory role of ICD, our hypothesis is that appropriate stimulation of ICD may alter auditory neural activity that is effective at suppressing tinnitus. For the one AMI patient implanted in the ICD, complete tinnitus suppression may not have been achieved due to inappropriate placement and stimulation of the electrode sites. Ultimately, we hope the AMI will be able to treat the general tinnitus population and not just deaf individuals undergoing implantation for hearing restoration. For most tinnitus patients who have functional hearing, one exciting opportunity is to combine AMI activation with acoustic stimulation paradigms. There are numerous studies in animals that have demonstrated the immense capability to shift neural coding and induce plasticity within the auditory system by pairing electrical stimulation of modulatory pathways with acoustic stimulation (Weinberger et al., 1993; Gao and Suga, 1998; Kilgard and Merzenich, 1998; Suga and Ma, 2003; Xiong et al., 2009; Engineer et al., 2011). Therefore, we further hypothesize that acoustic stimulation paired with AMI stimulation of different ICD regions could potentially treat tinnitus in humans. Currently, the AMI is designed for stimulating the ICC, but this array can be slightly modified to have electrodes positioned within the ICD

(Lim and Lenarz, 2015). With this modification, we will have the unique opportunity to assess the effects of ICD stimulation on tinnitus perception directly in human patients.

The goal of this study was to investigate the effects of electrical stimulation of the ICD on ascending auditory activity, not only to characterize the modulatory role of the ICD but also to begin assessing the potential for using the AMI for tinnitus treatment. We were primarily interested in determining if differential modulation can be achieved dependent on the ICD stimulation location. In addition, we were interested in the effects of different stimulation paradigms, including electrical stimulation only and electrical stimulation paired with broadband noise stimulation. We initially characterized the changes in acoustic-driven activity within the ICC since anatomical studies have already identified direct connections from the ICD to the ICC. In future studies, we can further assess how ICD stimulation alters neural coding across the auditory system through ascending and descending pathways (Aitkin and Phillips, 1984a; Caicedo and Herbert, 1993; Winer et al., 1998; Malmierca and Ryugo, 2011), especially for properties directly linked to tinnitus. In each animal experiment, we electrically stimulated different regions of the ICD combined with or without broadband noise stimulation. We recorded the corresponding neural changes within different regions of the ICC before, during, and after a given stimulation paradigm to assess immediate and residual effects. Our results reveal that ICD stimulation induces both suppressive and facilitatory changes throughout the ICC that depend on the location of ICD stimulation as well as its relative timing with acoustic stimulation. These results show that modulation can be achieved through ICD

stimulation; whether this modulation is effective in tinnitus treatment can be investigated in future AMI patients.

METHODS

Overview

All experiments were performed in ketamine-anesthetized guinea pigs (Elm Hill Labs, Chelmsford, MA) in accordance with the guidelines of the University of Minnesota Institutional Animal Care and Use Committee. Basic surgical and electrophysiological recording and stimulating methods were detailed in previous works (Lim and Anderson, 2007a; Markovitz et al., 2012; Straka et al., 2013). Multi-site, silicon-substrate electrode arrays (NeuroNexus Technologies, Ann Arbor, MI) were used to electrically stimulate and record neural activity in the IC. To investigate suppression and facilitation in the ICC during stimulation, multi-unit spike data were recorded in the ICC in response to electrical stimulation of the ICD alone as well as paired with acoustic stimulation at specific inter-stimulus intervals. Additionally, responses to acoustic stimulation alone were recorded before and after each ICD stimulation paradigm to evaluate changes in activity remaining in the ICC after stimulation.

Surgery

Experiments were performed on 12 Hartley guinea pigs (393 ± 50g, Elm Hill, Chelmsford, MA). Animals were initially anesthetized with an intramuscular injection of ketamine (40 mg/kg) and xylazine (10 mg/kg). Anesthesia was administered throughout

the experiment to maintain an areflexive state. A warm water blanket was used to maintain a body temperature of $38.0 \pm 0.5°C$, which was monitored with a rectal thermometer. Additionally, atropine sulfate (0.05 mg/kg) was administered periodically to keep the airway clear of mucous secretion. Animals were positioned in a stereotaxic frame (David Kopf Instruments, Tujunga, CA) using hollow ear bars into the ear canals and a bite bar. A craniotomy was performed to expose the right occipital lobe.

Stimulation and data acquisition

Experiments were performed in an electrically and acoustically isolated sound chamber. Stimulation delivery and data collection were controlled by TDT hardware (Tucker-Davis Technologies, Alachua, FL) and custom software written in MATLAB (MathWorks, Natick, MA). Acoustic stimulation was delivered to the left ear by a speaker coupled to the hollow ear bar at a sampling frequency of 195 kHz. The speaker and ear bar were calibrated using a 0.25-in condenser microphone (ACO Pacific, Belmont, CA). Electrical stimulation was delivered through an optically isolated stimulator. A monopolar configuration was used for both electrical stimulation and recording, with the returns through needle electrodes placed directly into the parietal lobe and in the neck muscle, respectively. Neural signals were passed through analog DC-blocking and anti-aliasing filters from 1.6 Hz to 7.5 kHz and sampled at 25 kHz.

Electrode array placement

Upon removing the dura, micromanipulators (Kopf Instruments, Tujunga, CA) were used to insert arrays into the ICC and the ICD. The electrode arrays consisted of two shanks separated by 500 µm with 16 sites linearly spaced along each shank at a separation of 100 µm. The recording electrode array was inserted at a 45° angle to the sagittal plane and through the occipital cortex into the midbrain to a depth that spans the tonotopic axis in the ICC (Malmierca et al., 1995; Snyder et al., 2004). The stimulating electrode array was inserted at a 90° angle to the horizontal plane and through the occipital cortex to a depth corresponding to the ICD. Some lateral locations corresponding to the ICX may have been included in the analysis; however excluding those points would not have changed our main findings (see data in the *Results*).

To identify the IC during placement of the electrode arrays, broadband noise (50 ms duration, 0.5 ms rise/fall time, 6 octave bandwidth from 0.625 to 40 kHz, 70 dB-SPL) was delivered to the left ear to elicit acoustic-driven responses within the IC. FRMs, which indicate tuning properties of neurons, were created by presenting a random sequence of pure tones (1-40 kHz, 8 steps per octave) at varying levels (0-70 dB-SPL, 10 dB-SPL steps) with four trials presented for each stimulus at 2/s. These FRMs were used to differentiate sites within the ICC versus those within the ICD. Sites in the ICC exhibited a tonotopic gradient from high frequencies on the deepest locations to low frequencies on more shallow sites (Merzenich and Reid, 1974; Snyder et al., 2004; Malmierca et al., 2008). The FRMs of sites in the ICD lacked a tonotopic organization and were predominantly double-peaked or broad in shape with no clear frequency

selectivity (see Chapter 2, LeBeau et al., 2001; Palmer et al., 2013). Prior to placement, electrode arrays were stained with Di-I (Sigma-Aldrich, St Louis, MO) in order to enable identification of the array placements across the IC during the histological analysis.

In some experiments (n=5 animals), a single stimulation array placement was made in the ICD and multiple recording array placements were made in the ICC (Fig. 12*A*). In the other experiments (n=7 animals), a single recording array placement was made in the ICC and multiple stimulating array placements were made in the ICD (Fig. 12*B*). Across all 12 experiments, recording placements were made throughout the ICC (Fig. 12*C*), that fully sampled the ICC along the isofrequency dimension. Figure 12*E* shows a comparison of the recording locations across the ICC from this study to recording locations outside of the ICC taken from a separate mapping study (unpublished data from our lab). Sites designated as outside of the ICC were identified by the lack of systematic tonotopic shifts along the recording shank and fully encapsulate our recording locations (Straka et al., 2014). The stimulating array placements from all 12 experiments are shown in the 3D reconstruction (Fig. 12*D*) and along a 2D plane perpendicular to the array shanks (Fig. 12*F*). Most of the ICD was sampled; however it was not possible to sample the most medial portions of the ICD due to obstructive vasculature on the occipital cortex surface. For experiments where one ICD stimulation array placement and multiple ICC recording array placements are made, analysis was done for each of the ICC sites. Across the 12 experiments, where there are different numbers of ICD and ICC sites stimulated and recorded dependent on the experimental design used, modulation of each ICD-ICC site pair was analyzed.
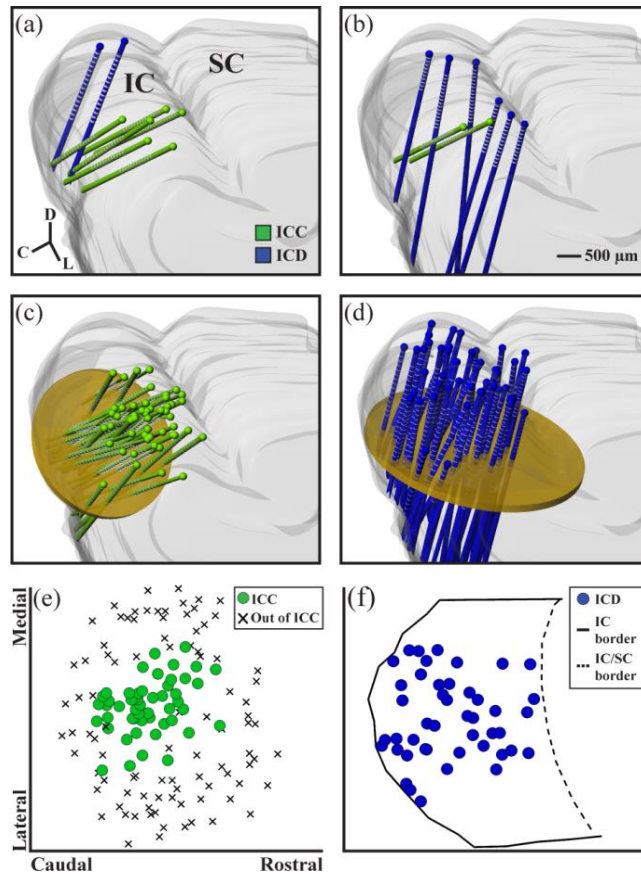
Figure 12. Experimental protocols and array placements. *A*, In five experiments, one stimulation array placement (each array consists of two shanks) was made in the ICD and multiple recording array placements across the ICC. *B*, In seven experiments, one recording array placement was made in the ICC and multiple stimulating array placements in the ICD. *C*, All of the recording array placements (n=51 shanks shown in green) and *D*, all of the stimulating array placements (n=45 shanks shown in blue) were superimposed onto a single 3D reconstruction of the IC. Planar cuts (shown in yellow) were made through the reconstructions orthogonal to the electrode array trajectories. *E*, *F*, Coordinates of the shanks through each plane are plotted as 2D maps. *E*, For the recording locations, each shank location was plotted along what is approximated as an isofrequency lamina that also includes recording locations identified as being outside of the ICC (see Chapter 2) in order to show that we fully spanned the isofrequency dimension of the ICC. *F*, For the stimulation locations, the borders of the IC were included on the horizontal plane in order to show that we fully spanned the rostral-caudal extent of the ICD. We were unable to sample the most medial portion of the ICD due to obstructive vasculature on the occipital cortex surface. The most lateral locations may include some portions of the ICX.

Stimulation parameters

Different acoustic and electrical stimulation paradigms were used to examine both suppression and facilitation of neural activity in the ICC. Acoustic stimulation (**AS-only**) consisted of broadband noise stimulation (90 ms duration, 0.5 ms rise/fall time, 6 octave bandwidth from 0.625 to 40 kHz). The level presented varied based on the hearing threshold of each animal, with a typical level delivered at 10 to 20 dB-SPL above the neural threshold such that at least 50% of the ICC sites showed activity significantly above the spontaneous level (see *Methods: Data analysis* for further details). The acoustic stimulation level ranged from 30-70 dB-SPL with an average level across experiments of 40 dB-SPL.

Electrical stimulation consisted of 100 µA biphasic, charge balanced, cathodic leading pulses (205 µs/phase) presented to the ICD. The largest current level safe for the electrode (Lim and Anderson, 2006) was used to elicit the greatest modulation. Due to the limited time per experiment, additional current levels were not tested, though future studies can investigate varying electrical and acoustic levels. Electrical stimulation paradigms included electrical-only stimulation (**ES-only**) and paired acoustic-electrical stimulation. For the paired acoustic-electrical paradigms, the electrical pulse was delivered 8 ms or 18 ms following the onset of acoustic stimulation. The 8 ms paired acoustic-electrical paradigm (**PAES_8**) allowed electrical stimulation to effect the ICC approximately before or simultaneous with the onset of acoustic activation. Onset latencies for acoustic-driven activity within the IC typically range between 4 and 25 ms with an average found for guinea pigs of about 13 ms (Langner et al., 1987; Schreiner

and Langner, 1988; Syka et al., 2000; Ter-Mikaelian et al., 2007). The 18 ms paired acoustic-electrical paradigm (**PAES_18**) allowed electrical stimulation to effect the ICC approximately after the onset of acoustic activation.

For each ICD array placement, 3-4 stimulating sites were selected from each shank located within the ICD. The following paradigms were completed sequentially for each stimulating site: AS-only, ES-only, AS-only, PAES_18, AS-only, PAES_8, AS-only. Each paradigm consisted of 100 trials presented at 2 trials/s. All 100 trials were presented for each paradigm before starting the subsequent paradigm. For each stimulating site, the AS-only paradigm was interleaved with electrical paradigms in order to assess different modulatory effects. All seven stimulation paradigms were completed for each stimulation site before proceeding to the next stimulation site. For these experiments, there were many parameters that could have been varied, each potentially affecting the results in different ways. Due to the limited time per experiment and in order to systematically track these potential effects across a reasonable number of animals, we initially chose to focus on varying electrode array placements in the ICC and in the ICD to test the effects of location. In doing so, we used the same acoustic and electrical levels, paradigm order, and recovery time across experiments to minimize their confounding influences on the location effects. In part, we chose this protocol because keeping the locations in the ICC and ICD constant across experiments was not readily possible whereas randomizing locations while keeping the other parameters constant was. Furthermore, identifying locations for implanting an array in patients will be critical for

tinnitus treatment. The ramifications of this methodology in interpreting the results will be discussed in *Discussion: Stimulus timing dependent plasticity.*

Data analysis

The neural recordings were bandpass filtered offline from 0.3 to 3 kHz to extract and analyze multi-unit spike activity. For recordings taken during electrical stimulation, the artifact was removed prior to bandpass filtering the signal. Spikes were counted if the amplitude exceeded three standard deviations above the background noise level. Modulation of ICC activity was only analyzed on sites where acoustic-driven activity was significantly greater than spontaneous activity using signal detection theory (Green and Swets, 1966; Lim and Anderson, 2007a), which compared the spike distributions of 90 ms windows of acoustic-driven and spontaneous activity. Sites were excluded if the two distributions of spike counts per trial were not significantly different from each other ($d'<1$), which was deemed as insufficient evoked neural activity.

Immediate and residual modulation. A two-tailed, unequal variance, ranked t-test (Ruxton, 2006a) was used to compare spike count distributions to determine if a recording site underwent immediate or residual modulation, with significance determined at $p<0.01$. **Immediate** modulation occurred when the spike count distribution for a paired acoustic-electrical stimulation paradigm was significantly different than that for the preceding AS-only paradigm. For all immediate comparisons, spike counts were found within a window which began 4 ms after the onset of the electrical artifact (i.e.,

immediately after the electrical artifact removal window) and ended at the offset of acoustic stimulation, giving total window lengths of 68 ms for PAES_18 and 78 ms for PAES_8. **Residual** modulation compared the two AS-only spike count distributions surrounding an electrical paradigm. The window for this analysis started 8 ms after the onset of acoustic stimulation to allow for sound transmission to the ICC and ended at the offset of acoustic stimulation for a total window of 82 ms.

Immediate suppression (facilitation) occurred if the activity to paired acoustic-electrical stimulation was significantly lower (higher) than that of the AS-only response preceding the paired paradigm. Immediate modulation was only assessed in comparison to the activity elicited from the preceding AS-only and not to the activity elicited from the preceding ES-only (e.g., to assess the amount of enhancement beyond the sum of the individual paradigms). This approach was selected because there was a relatively small number of ICD-ICC site pairs that exhibited activity in response to ES-only (513 of 4109 ICD-ICC site pairs), which would have limited our ability to perform a summation analysis. Furthermore, the immediate modulation elicited for this group of ICD-ICC site pairs was distributed, with suppression for 101 site pairs, facilitation for 155 site pairs, and no significant change for 257 site pairs, indicating that the presence of activity to ES-only did not always result in facilitation or enhancement. For these reasons, the immediate modulation analysis only focused on how much ICD stimulation could alter ongoing acoustic-driven activity (i.e., ascending coding properties). Residual suppression (facilitation) occurred if the AS-only response following the electrical paradigm yielded a

significantly lower (higher) spike count than the AS-only response preceding the electrical paradigm.

Modulation spread and strength.   Two metrics were used to quantify the extent of modulation within the ICC caused by ICD stimulation. The first metric was **spread**, which was the percent of sites across the ICC that were significantly suppressed or facilitated for each ICD stimulation location. The second metric was **strength**, which measured the amount of change that occurred on each of the significantly modulated sites. Strength was calculated as a normalized value by dividing the spike count during the electrical paradigm (for immediate) or the following AS-only paradigm (for residual) by the spike count of the preceding AS-only paradigm.

Histology and maps. The histological process and 3D reconstruction were detailed in a previous publication (Markovitz et al., 2012) and are briefly described here. At the end of an experiment, the animal was euthanized with an intracardiac injection of an overdose of pentobarbital. The head was removed and placed in 3.7% paraformaldehyde. The brain was completely removed from the skull within four days following the acute experiment and the right midbrain was sectioned and placed in sucrose within ten days of the acute experiment. After 24 hours in sucrose, the tissue was cryo-sliced into 60 μm thick slices and mounted on slides. The slices were then imaged and digitally processed to create a 3D midbrain reconstruction using Rhinoceros software (Seattle, WA). A brightfield image was taken of each slice to digitally trace its outline

and to align all the slice tracings together into a 3D reconstruction of the midbrain. The positions of the electrode arrays within the 3D midbrain were reconstructed from images taken under a green fluorescent filter, which captured the Di-I stains of the arrays within the brain slices. Once the 3D brain reconstructions were completed for each animal, they were normalized across animals so that all recording and stimulation shanks were superimposed onto one normalized midbrain (Fig. 12).

Additional steps were taken to create 2D maps from the 3D renderings that would be used for assessing location trends across the ICC or the ICD for spread and strength. For the ICC, 2D planes were constructed to approximately align with the isofrequency laminae (i.e., orthogonal to the recording arrays; an example plane is shown in Figure 12*C*). Planes were created at three different depths relative to the IC surface corresponding to specific laminae in guinea pigs (unpublished data from our lab: 1.3 mm for 3-4.5 kHz, 1.6 mm for 6-9.1 kHz, 1.9 mm for 10-15.2 kHz). The frequency ranges of these laminae were based on the BFs of the recorded sites at those corresponding depths. The BF was calculated from the FRM of each site by taking the frequency centroid of activity at 10 dB-SPL above the minimum threshold, as further described in (Lim and Anderson, 2006). We selected these three frequency ranges, that each spanned two critical bandwidths, because there were a sufficient number of sites for assessing locations trends along these ICC laminae (n=86 for 3-4.5 kHz, n=189 for 6-9.1 kHz, n=158 for 10-15.2 kHz). It is important to note that while the different laminae exhibit some variations in shape and curvature relative to the 45° tonotopic orientation (Malmierca et al., 1995), an approximation of each lamina as a flat plane does not

69

compromise the ability to identify location trends. The absolute distance between sites may be skewed by the projection onto a flat plane, but the relative locations of sites to each other are preserved.

For analyzing the ICD location effects, the medial-lateral and caudal-rostral coordinates for all stimulating shanks were compiled onto one normalized midbrain reconstruction and mapped onto a single transverse plane (Fig. 12*D*,*F*). We initially attempted to analyze ICD location effects along the dorsal-to-ventral axis, but further analysis was not pursued as no obvious trend was observed across this dimension. By using a single transverse plane, each shank position only appears as a single point in Figure 12*F* even though there can be up to four stimulation sites corresponding to that location. For analyzing stimulation location trends across this single plane, we slightly staggered the locations of all the sites for each shank location so that they could be visible and included in the analysis (e.g., see Figure 18).

RESULTS

We analyzed and compared the immediate and residual effects across the ICC for stimulation of different ICD sites for PAES_18, PAES_8, and ES-only to examine modulation differences due to recording and stimulation locations as well as stimulation paradigms. Separate maps for the effects elicited during and after each stimulation paradigm were created in the ICC and the ICD. For the ICC, the strength of the modulation was mapped onto each recording site. For the ICD, the spread produced across ICC by each ICD stimulation site was mapped onto each site location. We did not

observe any noticeable location trends across the ICC or the ICD for immediate effects for any of the stimulation paradigms. However, we did observe stimulation location trends across the ICD for residual effects using PAES_18, but not PAES_8 or ES-only. Considering these findings, only the residual data for PAES_18 is presented below. However, a summary of the differences in residual spread resulting from the three stimulation paradigms and a comparison of residual and immediate simulation effects for PAES_18 are included to highlight the unique modulation properties caused by PAES_18.

Residual modulation in the ICC

Neural activity was recorded across the ICC in response to 154 different stimulation sites in the ICD. Stimulation of every ICD site modulated activity in the ICC, though the spread and strength of the suppression or facilitation varied across sites. To obtain a representative measure of spread across the ICC for a stimulated ICD site, we initially analyzed data from experiments in which we mapped multiple shank locations across the ICC (i.e., >34 ICC sites recorded for a given ICD stimulation site). These data correspond to 35 ICD sites from five animals. Figures 13*A,B* present data from a single animal to show how stimulation of two different ICD sites with PAES_18 can result in large suppression spread (Fig. 13*A*, 46.0% of ICC sites suppressed) while stimulation of a second site that was separated by 500 μm resulted in minimal suppression spread (Fig. 13*B*, 11.1%). Differences in spread across ICD sites can also be seen for facilitation, in which stimulation of one ICD site resulted in large facilitation spread (Fig. 14*A*, 23.4%)

while stimulation of another site from the same animal resulted in minimal facilitation spread (Fig. 14*B*, 4.7%). For the 35 stimulated ICD sites, histograms of the suppression spread (Fig. 13*C*) and facilitation spread (Fig. 14*C*) indicate that stimulation of the ICD generally causes greater residual suppression (mean: 18.2%, SD: 9.5%) than facilitation (mean:6.1%, SD: 6.5%). Significance was determined at $p<0.01$ two-tailed, unequal variance, ranked t-test.
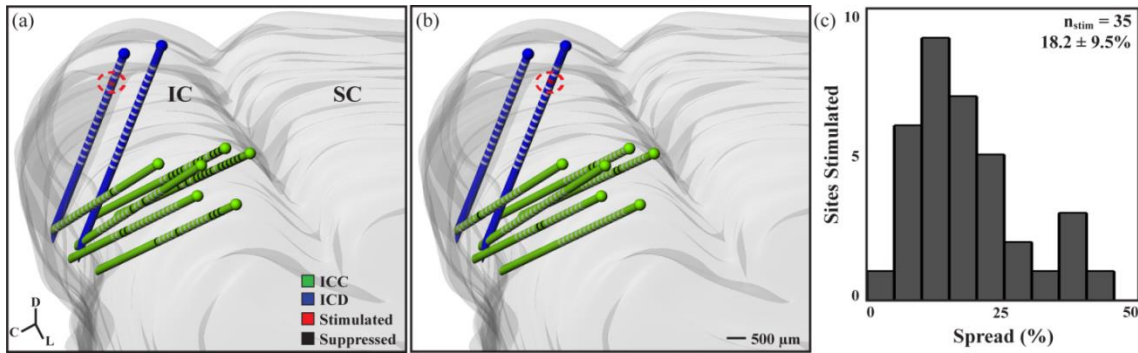
Figure 13. Examples across cases show variability of suppression spread. *A*, A single stimulation site in the ICD (circled in red) resulted in a suppression spread of 46.0% (29 significantly suppressed sites out of 63 ICC sites shown in black, see *Methods: Data Analysis* for statistical methods) compared to *B*, an ICD stimulation site 500 μm away that resulted in a suppression spread of 11.1% (7 of 63 ICC sites). *C*, A histogram of the suppression spread resulting from 35 stimulated ICD sites from five animals is shown with an average of 18.2 ± 9.5% (mean ± SD). A total of 2428 ICC sites were included in this analysis, with 456 ICC sites showing suppression.
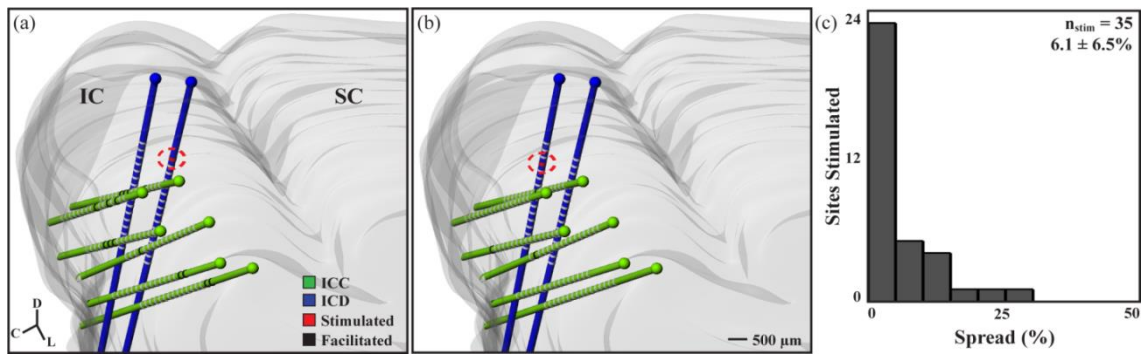
Figure 14. Examples across cases show variability of facilitation spread. *A*, A single stimulation site in the ICD (circled in red) resulted in a facilitation spread of 23.4% (15 significantly facilitated sites out of 64 ICC sites shown in black) while *B*, another ICD site 500 μm away resulted in a facilitation spread of 4.7% (3 of 64 ICC sites). *C*, A histogram of the facilitation spread resulting from 35 stimulated ICD sites from five animals is shown with an average of 6.1 ± 6.5% (mean ± SD). A total of 2428 ICC sites were included in this analysis, with 146 ICC sites showing facilitation.

In addition to spread effects, the strength of modulation varied across different ICC recording sites. PSTHs of AS-only recordings before and after stimulation are plotted for two different ICC recording sites in response to the same stimulated ICD site (Fig. 15*A*). For this example, different suppression strengths were observed for the two ICC sites (decrease of 51.4% versus 13.9%). Figure 15*B* plots the histogram of different suppression strengths across all ICC recording sites in which there was an average decrease of 17.1%. Differences in facilitation strength were also observed across ICC sites. Figure 16*A* shows one example in which different facilitation strengths were observed for two different ICC sites in response to the same stimulated ICD site (increase of 66.5% versus 17.7%). Figure 16*B* plots the histogram of different facilitation strengths across all ICC recordings sites in which there was an average increase of 19.7%. We did not observe any significant differences in the distribution of suppressive and facilitatory

strengths, which is evident when comparing Figures 15*B* and 16*B*. Overall, stimulation of each ICD site resulted in weak and strong modulation of different ICC sites, but there were generally more sites being suppressed than facilitated using PAES_18.
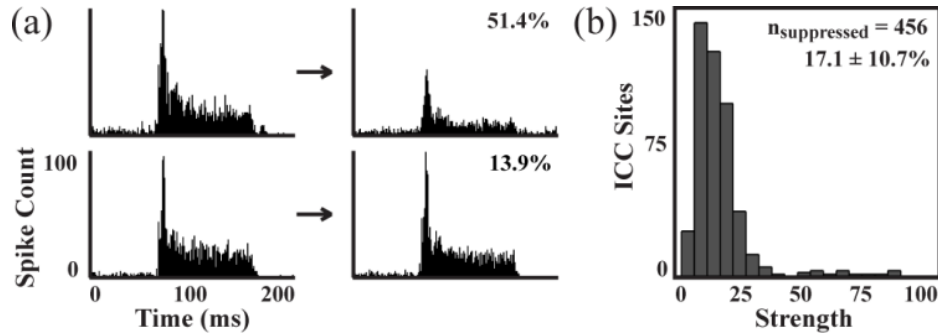
Figure 15. Examples of suppression strength. *A*,*B*, Stimulation of a single ICD site could induce strong suppression (*A* - 51.4% decrease) or weak suppression (*B* - 13.9% decrease) on different ICC sites. *C*, A total of 456 out of 2428 ICC sites were suppressed by the 35 stimulated ICD sites from Fig. 13 and 14 with an average decrease of $17.1 \pm 10.7\%$.
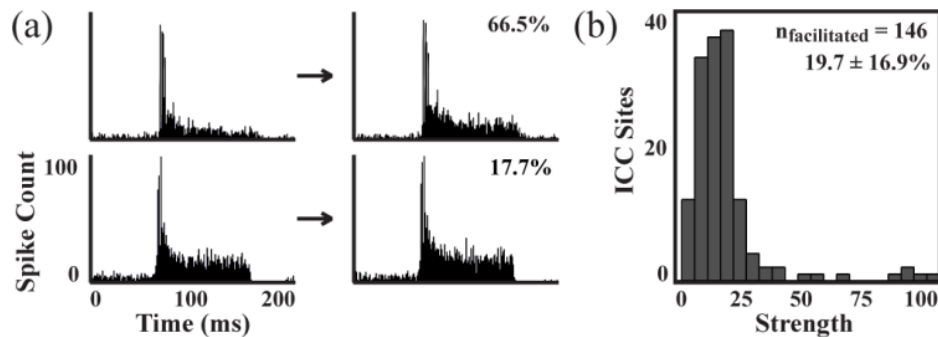
Figure 16. Examples of facilitation strength. *A*,*B*, Stimulation of a single ICD site could induce strong facilitation (*A* - 66.5% decrease) or weak facilitation (*B* - 17.7% decrease) on different ICC sites. *C*, A total of 146 out of 2428 ICC sites were facilitated by the 35 stimulated ICD sites from Fig. 13 and 14 with an average increase of $19.7 \pm 16.9\%$.

Residual modulation trends across the ICC recording locations

To assess if ICD modulation varied for different recording locations across the ICC laminae, we assembled the data into three different isofrequency planes (Fig. 17), as explained in the *Methods: Histology and maps*. Each site represents where the shank intersected with the isofrequency plane (Fig. 17). On some shanks, multiple recording sites had BFs within each frequency range (low frequency, n_{shanks}=29, n_{sites}=86; middle frequency, n_{shanks}=47, n_{sites}=189; high frequency, n_{shanks}= 44, n_{sites}=158). For each shank, a binary analysis was performed to indicate whether or not sites in each frequency range could be significantly modulated by any stimulated ICD site. The filled circles represent locations in ICC that were modulated and unfilled circles represent unmodulated locations. For the low frequency lamina, 58.6% of locations were suppressed and 44.8% were facilitated. For the middle frequency lamina, 91.5% of the locations were suppressed and 68.1% were facilitated. For the high frequency lamina, 75.0% of the locations were suppressed and 52.3% were facilitated. Visual inspection of the binary analysis (Fig. 17) reveals that suppression and facilitation can occur throughout an ICC lamina without any specific regions exhibiting greater modulation. To further evaluate if differential modulation occurred across the ICC, maps of strength were plotted as a function of ICC location (data not shown). No clear location trends were observed across the ICC laminae, consistent with the binary spread plots (Fig. 17).
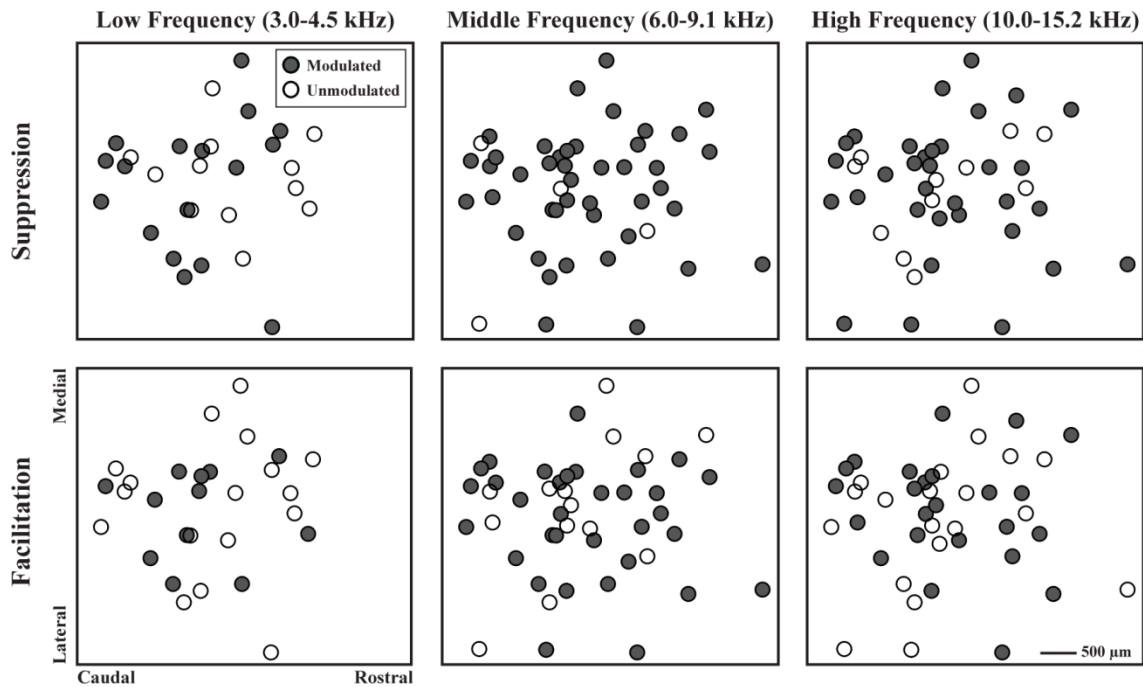
Figure 17. Modulation across an ICC lamina. ICC recording sites from 12 animals and three different frequency ranges (low frequency, n_{shanks}=29, n_{sites}=86; middle frequency, n_{shanks}=47, n_{sites}=189; high frequency, n_{shanks}= 44, n_{sites}=158) were mapped onto their corresponding isofrequency plane. Modulated locations showed significant suppressive or facilitatory residual changes to PAES_18. Modulated and unmodulated locations were distributed throughout an entire ICC lamina.

Residual modulation trends across the ICD stimulation locations

We mapped all of the ICD site locations onto a 2D plane (Fig. 18*A*). Across twelve animals, 154 different stimulation sites were used from 45 total shank placements for a total of 4109 ICD-ICC site pairs. Note that each shank placement could have three to four ICD sites along the shank, in which we slightly staggered those sites so they could be visualized and analyzed. Two parameters of spread are mapped for each ICD location (Fig. 18*A*). The first is the percent of ICC sites suppressed, represented by the color of the circles, with darker colors indicating larger spread. The second parameter is the

maximum number of ICC sites for a given ICD location in which larger circles indicate

more sites could have been suppressed in the ICC. Large-dark circles represent ICD sites

that elicited a large amount of spread in comparison to large-light circles that represent

more sites could have been suppressed in the ICC. Large-dark circles represent ICD sites
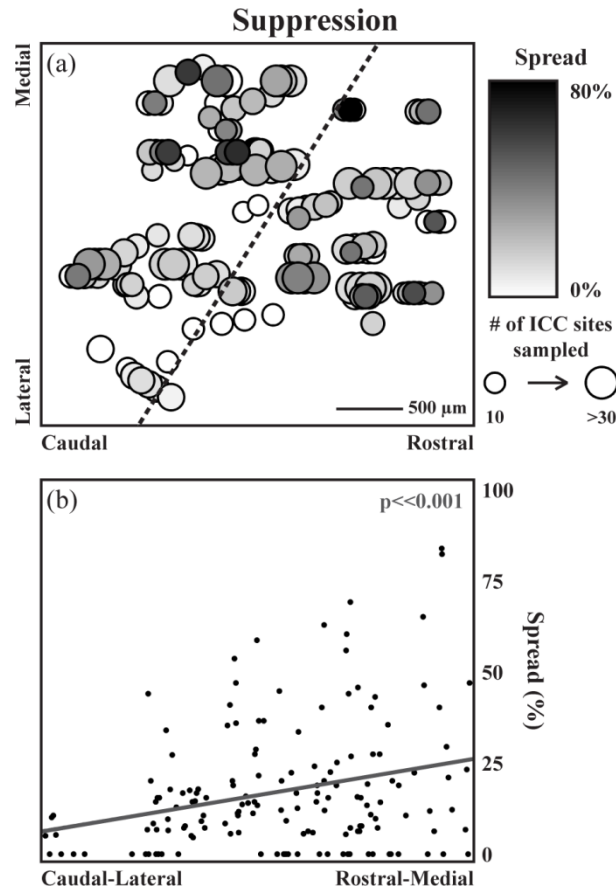
Figure 18. Residual suppression spread depends on ICD stimulation location. *A*, All stimulation sites (n=154) were mapped onto a horizontal plane through the ICD. Two parameters were mapped along the plane: spread and total number of sites that could be modulated. Large-dark circles indicate that maximal suppressive spread across the ICC can be elicited by stimulation of that ICD location. *B*, The suppression spread significantly increased (p<<0.001) as a function of location along the steepest gradient axis from the caudal-lateral to the rostral-medial regions in the ICD. The steepest gradient axis for suppression spread is shown on the map as a dotted line. A total of 740 out of 4109 ICD-ICC site pairs were suppressed by ICD stimulation.

that elicited a large amount of spread in comparison to large-light circles that represent ICD sites that had the potential to suppress a large number of ICC sites but failed to do so. Since we visually observed a location trend, we further analyzed the ICD map to define the steepest gradient axis for spread, which corresponds to a vector across ICD showing the direction of the greatest change in suppression spread. The steepest gradient axis was calculated by two-dimensional multiple linear regression analysis where the modulation response was predicted by the location of each stimulation site. Figure 18*B* shows that the spread of suppression significantly increases as a function of ICD location along that steepest gradient axis ($p \ll 0.001$; along the dotted black line in Fig. 18*A*). The weakest spread of suppression occurred from stimulation of sites in the caudal-lateral region of the ICD. Similar plots and analyses were performed for facilitation spread. No clear location trend was observed across the ICD (Fig. 19) and we did not identify any significant steepest gradient axis for facilitation spread (data not shown). Our findings indicate that the greater spread of suppression versus facilitation for PAES_18 is due to ICD stimulation location rather than ICC recording location. In particular, PAES_18 causes greater suppression in ICC when stimulating in more rostral and medial ICD locations, while eliciting facilitation in ICC when stimulating throughout the ICD.
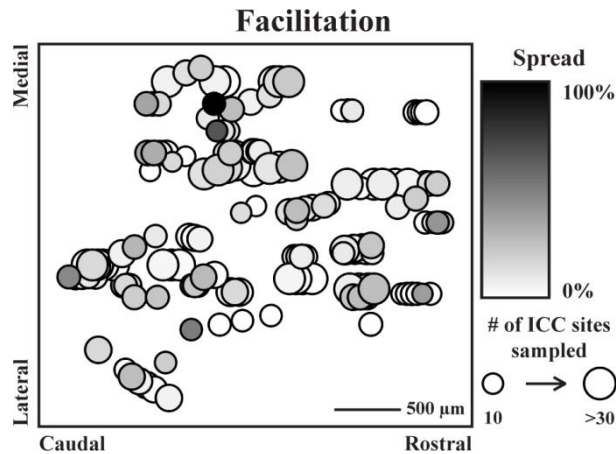
Figure 19. No trend for ICD stimulation location was observed for residual facilitation spread. All stimulation sites (n=154) were mapped onto a horizontal plane through the ICD. Two parameters were mapped along the plane: spread and total number of sites that could be modulated. Large-dark circles indicate that maximal facilitatory spread across the ICC can be elicited by stimulation of that ICD location. A total of 314 out of 4109 ICD-ICC site pairs were facilitated by ICD stimulation.

Differences in residual spread across stimulation paradigms

In contrast to PAES_18, we did not observe any location trends for ES-only and PAES_8. Figure 20 summarizes the differences in spread effects for these three stimulation paradigms, using only the data from experiments in which we mapped multiple shank locations across the ICC. The spread of suppression for PAES_18 is significantly larger than that of the other two paradigms (18.2 ± 9.7% compared to 12.9 ± 8.9% for ES-only, p<0.05, and 12.5 ± 12.1% for PAES_8, p<0.05). Conversely, the facilitation spread is significantly reduced for PAES_18 compared to the other two paradigms (6.1 ± 6.5% compared to 9.9 ± 6.9% for ES-only, p<0.05, and 9.6 ± 5.9% for PAES_8, p<0.05). In comparing suppression versus facilitation effects, Figure 20 indicates that paired stimulation with a specific delay (i.e., PAES_18; p<<0.001) can

79

cause different extents of suppressive versus facilitatory modulation that does not occur for another delay (i.e., PAES_8) or ES-only.
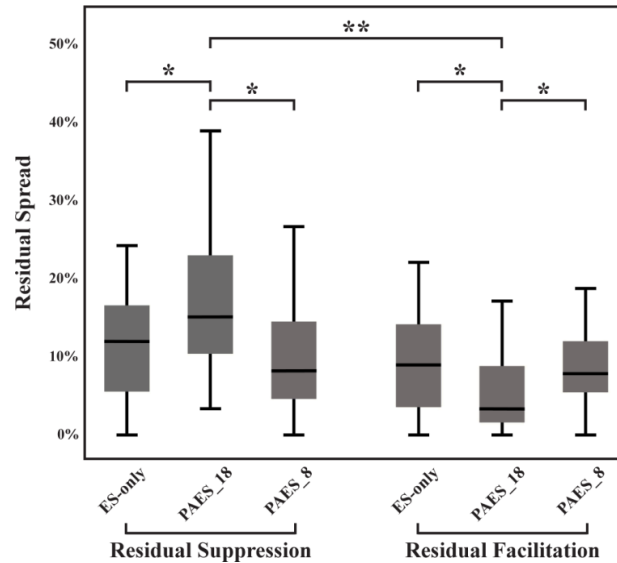
Figure 20. Comparison of residual spread induced by different stimulation paradigms. PAES_18 induced significantly more residual suppression and less residual facilitation than ES-only and PAES_8 (two-tailed, unequal variance, ranked t-test with Bonferroni correction; $p<0.05$ *). PAES_18 also induced significantly more suppression than facilitation ($p<<0.001$ **). This figure plots the median and distribution of suppression and facilitation spread values. The mean ± SD for each paradigm are as follows: ES-only - suppression spread = 12.9 ± 8.9% and facilitation spread = 9.9 ± 6.9%; PAES_18 - suppression spread = 18.2 ± 9.7% and facilitation spread = 6.1 ± 6.5%; PAES_8 - suppression spread = 12.5 ± 12.1% and facilitation spread = 9.6 ± 5.9%. The total number of ICC sites analyzed and the resulting number of sites suppressed and facilitated are as follows: ES-only 324 suppressed and 219 facilitated out of 2377 ICC sites; PAES_18 - 456 suppressed and 146 facilitated out of 2428 ICC sites; PAES_8 - 288 suppressed and 222 facilitated out of 2313 ICC sites.

Immediate modulation guides residual modulation

In addition to the residual analysis described above, we also analyzed and compared the immediate changes in the ICC caused by PAES_18 and by PAES_8. ICD-ICC site pairs could be modulated immediately and/or residually or show no change due

to paired stimulation, as shown in Table 2. From the pooled results of PAES-18 and PAES-8, a total of 705 ICD-ICC site pairs (8.70%) were both immediately and residually modulated significantly across all experiments. Of the total 8102 ICD-ICC site pairs that were analyzed for significant immediate and/or residual modulation (4109 ICD-ICC site pairs from PAES-18 and 3993 ICD-ICC site pairs from PAES-8), 14.46% were only immediately modulated and 15.84% were only residually modulated. Around 60% of the ICD-ICC site pairs sampled in these experiments showed no immediate or residual modulation consistent with the results shown in Figures 13 and 14, where a single ICD stimulation site generally modulated only a subset of ICC sites.

Table 2. Immediate and residual modulation resulting from paired paradigms.

Immediate Modulation	Residual Modulation	Number of ICD-ICC Site Pairs	Percentage
Suppression	Suppression	467	5.76
Facilitation	Facilitation	176	2.17
Suppression	Facilitation	35	0.43
Facilitation	Suppression	27	0.33
Suppression	No Change	690	8.52
Facilitation	No Change	481	5.94
No Change	Suppression	763	9.42
No Change	Facilitation	520	6.42
No Change	No Change	4943	61.01

ICD-ICC site pairs were pooled for this analysis from both PAES_18 and PAES_8 to determine if a correlation exists between immediate and residual modulation regardless of the paired paradigm used. A total of 8102 ICD-ICC site pairs were analyzed for significant immediate and/or residual modulation due to PAES_18 (4109 ICD-ICC site pairs) or PAES_8 (3993 ICD-ICC site pairs). Results show that 8.70% of all ICD-ICC site pairs are both immediately and residually modulated while 14.46% are only immediately modulated and 15.84% are only residually modulated due to paired paradigms.

However, all the ICD sites stimulated here were still able to activate ICC sites across all laminae (Fig. 17). It is possible that stimulating additional ICD sites not

sampled in this study would activate different subsets of ICC sites and thus would decrease the number of unmodulated sites. For each of the ICD-ICC site pairs that were immediately and residually modulated, the strength of the immediate modulation and of the residual modulation were compared (Fig. 21). Of all the site pairs modulated immediately and residually by a paired paradigm, 66.2% were immediately suppressed and also residually suppressed and 25.0% were immediately facilitated and also residually facilitated. These results suggest that the type of modulation (i.e., suppression or facilitation) that occurs during PAES-18 or PAES-8 drives the type of residual modulation for site pairs that are both immediately and residually modulated. Only 8.8% of site pairs switched modulation direction following stimulation.
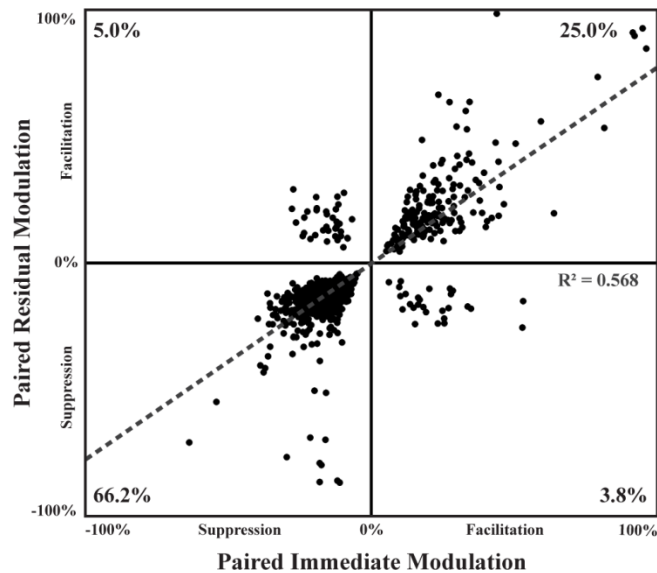
Figure 21. Type of immediate modulation generally directs the type of residual modulation. Sites that exhibited significant immediate and significant residual modulation due to a paired paradigm were plotted based on the strength of each of the modulations (n_{total}=705). Data was pooled from PAES_18 and PAES_8 to assess the relationship between immediate and residual modulation regardless of the paired paradigm used. Immediate and residual modulations were typically in the same direction (i.e., both suppressive or both facilitatory) in which 66.2% of the sites were suppressed and 25% were facilitated. Only 8.8% of the sites showed a switch in modulation type.

DISCUSSION

The goals of these experiments were to identify the types of ICC modulation possible through electrical stimulation of the ICD, to determine if any location trends existed in either the ICC or the ICD, and to compare the extent of suppression and facilitation elicited in ICC by different ICD stimulation paradigms. For all three electrical stimulation paradigms, we observed both immediate and residual suppression and facilitation across different ICC locations. We also observed that stimulation of every location in the ICD caused some amount of significant modulation in neural activity in the ICC. In particular, each ICD site could modulate a different subset of ICC neurons (<40% of the ICD-ICC sites pairs shown in Table 2 with varied patterns shown in Figure 13 and Figure 14). For PAES_18, more residual spread of suppression was elicited by stimulating rostral and medial regions of the ICD. Compared to PAES_8 and ES-only, PAES_18 also appeared to exhibit significantly more residual spread of suppression and less residual spread of facilitation, suggesting that paired stimulation with different inter-stimulus delays can alter the relative amount of suppression versus facilitation across the ICC. Furthermore, the type of residual modulation was predicted by the type of immediate modulation. In a majority of ICD-ICC site pairs that were both immediately and residually modulated, sites that were immediately suppressed (facilitated) were also residually suppressed (facilitated). In summary, our findings demonstrate that ICD stimulation can modulate the ICC and that targeting different ICD regions with paired acoustic-electrical stimulation may be a way to induce varying types of plasticity within

the ascending auditory pathway, which in turn could potentially modulate the tinnitus percept.

Functional connectivity between the ICD and the ICC

Our results show that stimulation of the ICD both increases and decreases spiking activity in the ICC, which is in contrast to the functional effects shown from the ICX to the ICC that were found to be inhibitory (Jen et al., 2001; Jen et al., 2002). Previous studies have shown that corticofugal activation and inactivation of the ICC can lead to excitatory and inhibitory changes within the ICC (Mitani et al., 1983; Syka and Popelar, 1984; Sun et al., 1989; Torterolo et al., 1998; Zhang and Suga, 2000; Zhou and Jen, 2000). Considering that projections from auditory cortex to the IC, including the ICC, are considered to be excitatory (i.e., glutamatergic; Rockel and Jones, 1973; Feliciano and Potashner, 1995; Saint Marie, 1996; Saldana et al., 1996), it is expected that inhibitory effects within the ICC are induced by the auditory cortex through a multi-synaptic pathway via the ICD and the ICX. Corticofugal excitatory effects, especially for frequency specific changes in the ICC, are expected to involve both direct projections to the ICC (Saldana et al., 1996; Yan and Suga, 1999; Bajo and Moore, 2005; Bajo et al., 2007; Lim and Anderson, 2007a; Xiong et al., 2009; Markovitz et al., 2013) and indirect multi-synaptic projections via the ICD. Our results support this type of functional organization, which is also consistent with the excitatory and inhibitory synapses from the ICD to the ICC shown in previous anatomical studies (González-Hernández et al., 1996; Saint Marie, 1996; Nakamoto et al., 2013).

Methodological considerations in interpreting location trends

There are several potential limitations to consider when interpreting our results. The first set of limitations relates to the ICD location trends observed in our study. Location trends could have been affected by the limited recovery time allowed by our chosen experimental protocol. The modulatory effects elicited by one stimulation site may have lasted for tens of minutes to several hours, and thus influenced or masked the modulatory effects of proceeding stimulation sites. However, we specifically designed our experimental protocol to minimize this issue, wherein the ICD stimulation locations were varied within an experiment and across all experiments by starting in different locations and moving to sites in different directions. Therefore, if a location trend was observed (i.e., for residual spread of suppression following PAES_18), then we know it truly exists. If a trend was not observed (i.e., for residual spread of facilitation following PAES_18 or other possible trends), then it may still exist but was somehow masked by our protocol.

ICD location trends may have also been missed due to the artificial way electrical stimulation activates central neurons. In using monopolar electrical stimulation, which can cause current spread out to hundreds of microns depending on the cell type and orientation (Ranck, 1975; McIntyre and Grill, 2000), we could have stimulated a complex network of neurons as well as overlapping populations across different ICD sites. Additionally, electrical stimulation may have activated axons passing by the stimulated sites that originate within or outside of ICD. One example of passing fibers includes commissural projections, which arise from every subregion in the IC and project to

homotopic regions of the contralateral IC (Aitkin and Phillips, 1984b; González Hernández et al., 1986; Coleman and Clerici, 1987; Saldaña and Merchán, 1992; Malmierca et al., 1995). These commissural projections are both glutamatergic and GABAergic (González-Hernández et al., 1996; Saint Marie, 1996; Hernández et al., 2006) and have induced both excitatory and inhibitory effects on neurons in the contralateral IC in functional electrical stimulation and pharmacology experiments (Smith, 1992; Moore et al., 1998; Malmierca et al., 2003; Malmierca et al., 2005), similar to the effect seen in the data presented here. Therefore, it is possible that the suppressive and facilitatory effects we observed in the ICC in response to ICD stimulation could be caused, in part, by activation of commissural neurons. Clinically, it is not an issue if we are activating a larger area of ICD including neurons within as well as passing fibers through ICD as long as electrical stimulation of the corresponding implant location in ICD in humans can sufficiently modulate the auditory brain to suppress tinnitus.

The second set of limitations relates to the ICC location trends observed in our study. Differences exist in the number of modulated sites per ICC lamina with maximum modulation occurring in the middle frequency layer. Based on previous anatomical studies, there does not seem to be a differential pattern of excitatory and inhibitory synapses across laminae that would suggest greater modulatory effects particularly for middle frequency regions (González-Hernández et al., 1996; Saint Marie, 1996; Nakamoto et al., 2013). The differential modulation seen across laminae may be due to the acoustic levels used in these experiments. In guinea pigs, auditory thresholds are lowest around 8 kHz (Heffner et al., 1971; Gourevitch et al., 2009), which coincides with

our middle frequency lamina (i.e., 6.0-9.1 kHz). Thus, the chosen acoustic levels elicited stronger activity within the middle frequency lamina compared to the lower and higher frequency laminae, which may have enabled stronger modulation.

In terms of spatial trends within a given ICC lamina, there appears to be a random distribution of modulated and unmodulated sites. It is possible that we missed a location trend across the ICC due to insufficient mapping across each lamina per animal or even the use of multi-unit recordings. Individual neurons recorded on the same electrode site may have exhibited different modulation effects but the summation of their neural activity in the multi-unit recordings could have canceled out or masked these individual effects.

Stimulus timing dependent plasticity

The results presented in Figure 20 suggest that the type and extent of modulation depends on the relative timing between paired acoustic-electrical stimulation. In particular, PAES_18 resulted in significantly more residual suppression and less residual facilitation than PAES_8. Both PAES_8 and ES-only exhibited similar amounts of residual spread for suppression and facilitation, whereas PAES_18 exhibited significantly greater residual spread of suppression than facilitation. This stimulus timing dependent plasticity can be likened to spike timing dependent plasticity; however, instead of looking at how pre- and post-synaptic cells potentiate or depress based on timing, we are looking at how electrical and acoustic stimulation facilitate or suppress a population of cells based on timing (Magee and Johnston, 1997; Markram et al., 1997; Bi and Poo, 1998;

Zhang et al., 1998; Abbott and Nelson, 2000; Yao and Dan, 2001; Dan and Poo, 2004; Caporale and Dan, 2008). Spike and stimulus timing dependent plasticity have been demonstrated in the auditory system at the brainstem level as well as the cortex (Tzounopoulos et al., 2004; Dahmen et al., 2008; Basura et al., 2013; Koehler and Shore, 2013b, a). Our results suggest that timing dependent plasticity induced by paired acoustic-electrical stimulation is also occurring at the auditory midbrain level. For PAES_18, the ICD-induced activity would have generally reached the ICC after the onset of acoustic-driven activity, which may have caused the stronger suppressive effect. A delay shorter than the 8 ms that was used for PAES_8 may have been needed for the ICD-induced activity to reach the ICC before the acoustic-driven activity to cause a stronger facilitatory effect. We did not observe any significant differences in facilitatory versus suppressive effects for PAES_8.

Two aspects of our protocol need to be considered when interpreting these results. First, we used a set ordering of the different stimulation paradigms with limited recovery time. We cannot rule out that the stronger suppressive effects caused by PAES_18 compared to PAES_8 or ES-only were partly attributed to the order and prolonged influence of the different stimulation paradigms. It may be possible that while ES-only did not result in large amounts of suppression, it did act as a primer allowing for larger suppression to occur in response to PAES_18. Thus, the greater suppression seen following PAES_18 may be due to an individual paradigm or to the sequence of paradigms. At the same time, it may be possible that because of the large suppression occurring due to PAES_18, further suppression in response to PAES_8 was not possible.

From our protocol and data, we can claim that it is possible to induce varying extents of suppressive versus facilitatory modulation, but whether it can be sufficiently achieved using a paired paradigm with a specific delay (e.g., PAES_18) or requires a sequence of stimulation paradigms (e.g., ES-only followed by PAES_18) warrants further investigation. For this initial study, we chose to focus on varying ICD and ICC electrode array placements with limited recovery time for several reasons explained in *Methods: Stimulation parameters*. This limited recovery makes it difficult to completely separate out the individual paradigm effects. Further studies are underway to parse out the modulatory effects that can be achieved by individual paradigms. For these studies, the ICC is probed with a repeated sequence of acoustic-only stimulation following each electrical stimulation paradigm in order to monitor the modulatory effects over time and to allow the effects to diminish before moving onto the next paradigm. Additionally, the stimulation site is held constant and each paradigm is presented in a random sequence throughout an experiment to further minimize any residual effects of one paradigm on another.

The second consideration in interpreting our plasticity results is that these experiments were performed under ketamine anesthesia, which may have influenced the types of modulatory effects observed in our study. Ketamine is known to influence auditory responses in the cortex (Zurita et al., 1994; Kisley and Gerstein, 1999; Gaese and Ostwald, 2001; Syka et al., 2005). In comparison, ketamine has been shown to have little or no effect on auditory coding within the ICC (Astl et al., 1996b; Ter-Mikaelian et al., 2007). Ketamine may also limit plasticity changes in the auditory brain by effecting

synaptic potentiation and depression (Salami et al., 2000; Leong et al., 2004). In this experiment, under ketamine anesthesia, we were still able to induce a significant amount of immediate and residual suppression and facilitation across the ICC with ICD stimulation. Therefore, we can conclude that the results are promising for eliciting differential modulation of neural activity across the ICC, but modulation by different paradigms needs to be verified in an awake preparation.

Clinical implications for tinnitus treatment

Tinnitus has commonly been associated with properties such as hyperactivity of neurons across the auditory system, including the ICC (Noreña and Eggermont, 2003; Kaltenbach et al., 2005; Ma et al., 2006; Bauer et al., 2008; Lanting et al., 2009; Melcher et al., 2009; Roberts et al., 2010; Møller, 2011b; Manzoor et al., 2013; Mulders et al., 2014; Vogler et al., 2014). Based on the findings from this study, targeted ICD stimulation combined with varying delays of broadband noise stimulation may suppress activity in the ICC associated with tinnitus. Specifically, we found that using paired acoustic-electrical stimulation with a specific delay (i.e., PAES_18, though it may require a sequence of stimulation where ES-only precedes PAES_18) and stimulation of more medial and rostral ICD regions resulted in greater suppressive versus facilitatory effects in the ICC. Tinnitus has also been linked with other neural properties, such as hypersynchrony, tonotopic reorganization, and changes in firing patterns, and within other auditory and non-auditory nuclei (Møller, 1984; Chen and Jastreboff, 1995; Lockwood et al., 1998; Muhlnickel et al., 1998; Komiya and Eggermont, 2000; Seki and

Eggermont, 2003; Zhang et al., 2003; Eggermont and Roberts, 2004; Wienbruch et al., 2006; Chen et al., 2012; Galazyuk et al., 2012). We will need to investigate these neural properties, especially in tinnitus animal models, to assess if ICD stimulation can suppress or fix the pathogenic activity directly driving the tinnitus percept. Additionally, this treatment may also be relevant for a hyperacusis, a condition resulting in increased sensitivity to certain frequencies. We will need to determine if ICD stimulation can suppress the increased acoustic-driven activity and gain experienced and reduce sensitivity (Gu et al., 2010; Aazh et al., 2014). As discussed above, ICD stimulation may be activating passing fibers, such as from the contralateral IC, in addition to neurons projecting to the ICC from the ICD. Regardless of what is being activated, the main clinical goal would be to identify appropriate locations for array implantation and stimulation strategies that can induce neural changes that translate into therapeutic results for the patient.

There is already an ongoing clinical trial funded by the National Institutes of Health in which deaf patients will be implanted with the AMI. Many of these patients will also have tinnitus and can be stimulated with different electrode sites to evaluate their modulatory effects on the tinnitus percept. Based on our animal findings, we have decided to incorporate some of the stimulation paradigms into the clinical trial for treating tinnitus with the AMI. Before implantation, the AMI array needs to be modified to enable ICD simulation. Each AMI shank has a Dacron mesh that prevents over-insertion of the neuroprosthetic array into the IC and positions the sites within the ICC. To allow some sites to be placed in the ICD, each AMI shank will be modified to add

91

dorsal sites closer to that mesh (Lim and Lenarz, 2015). With the initial AMI patient population, we will not be able to combine broadband noise stimulation with ICD stimulation since the patients will be deaf. However for these patients, we will investigate stimulation strategies that combine ICD stimulation with precisely timed stimulation across multiple ICC sites to attempt to mimic the paradigms used here as well as test the safety of this treatment. We will also not be able to access multiple locations throughout the ICD in human as was possible in our animal studies. As a results, electrodes may be implanted outside the optimal rostral and medial regions of ICD that appear to cause greater suppressive versus facilitatory effects. While our data shows that stimulation of different ICD locations generally modulates different subsets of ICC neurons, tinnitus treatment may then be limited if the electrode is not stimulating appropriate locations to target tinnitus-affected neurons. Since patients will already be implanted with the AMI for hearing restoration, we have the opportunity to investigate a wide range of stimulation patterns as best we can considering these limitations, which will hopefully reveal some parameters that can effectively suppress or at least modulate the tinnitus.

Demonstrating the ability to decrease the tinnitus percept in these initial AMI patients using paired ICD/ICC stimulation along with the suppression results from paired acoustic-electrical paradigms in animal studies could open up the possibility for implanting the AMI array in a larger population of patients with severe tinnitus. We would eventually seek a Phase I safety study for the treatment of tinnitus in patients with functional hearing in whom we can implement the paired acoustic-electrical stimulation paradigm. For patients who do not have sufficient hearing, cochlear implants will remain

an option that have been effective in reducing the tinnitus percept in some patient groups (Osaki et al., 2005; Baguley and Atlas, 2007; Quaranta et al., 2008; Van de Heyning et al., 2008; Kleinjung et al., 2009; Zeng et al., 2011). Another possible alternative for patients with severe tinnitus with or without sufficient hearing is round window stimulation. Reduction in tinnitus using round window stimulation has been promising in acute cases (Cazals et al., 1978; Portmann et al., 1979; Rubinstein et al., 2003), but repeatability of tinnitus suppression needs to be further explored (Møller, 2011b; Punte et al., 2013). More invasive approaches for treating tinnitus are being developed and increasingly used across different patient groups including stimulation of the auditory cortex or caudate nucleus as well as vagal nerve stimulation paired with acoustic stimulation (Cheung and Larson, 2010; De Ridder et al., 2011; Engineer et al., 2011; De Ridder et al., 2014). While cochlear implants, round window stimulation, and several invasive brain treatments remain an option for some tinnitus patients, new approaches including AMI stimulation need to continually be developed so a larger population of patients can achieve tinnitus suppression.

Chapter 4: Neuromodulation within the Midbrain Using Paired Acoustic and Electrical Stimulation to Treat Tinnitus

With the development of smaller DBS devices with more sites for stimulation, DBS can potentially be used to treat a wider range of neurological conditions, including tinnitus. Tinnitus typically manifests as hyperactivity and increased neural synchrony throughout the auditory system. We hypothesize that by using DBS in spatially specific regions, tinnitus-related neural activity can be suppressed leading to a reduction in the percept. Particularly, we hypothesize that stimulation in the IC using a new type of DBS device originally designed for hearing restoration, known as the AMI, will be able to suppress tinnitus. This hypothesis will be tested in an upcoming AMI clinical trial, but prior to the trial, we wanted to identify stimulation paradigms that provide lasting suppression of acoustic-driven activity and synchrony. Results revealed that overall stimulation of the ICD suppressed acoustic-driven activity, but not synchrony. Importantly, we identified two stimulation paradigms that provide lasting suppression. These optimal paradigms will be implemented directly in humans in the upcoming AMI clinical trial.

Introduction

DBS has been successfully used to treat a number of neurological disorders including Parkinson's, essential tremor, dystonia, and obsessive compulsive disorder, and is continuing to expand to other applications with clinical trials underway for depression, epilepsy, and Alzheimer's (Johnson et al., 2013). In all of these applications, it has been possible to implement the traditional DBS device; however further expansion to new applications may be reduced by limitations of the traditional DBS lead. Though current steering can be employed to increase targeting specificity, the size and number of contacts make the traditional DBS lead unusable for certain neuromodulation applications

(i.e., due to small target location, proximity to neighboring regions where activation results in unwanted side effects, need for small and discrete activation areas, etc.). For those applications, new DBS devices, including the ABI and the AMI with their decreased size and increased number of contacts may prove more valuable.

Tinnitus is one condition which may benefit from stimulation with the new DBS devices. Tinnitus is characterized by a phantom auditory percept and is often a result of hearing loss (Sindhusake et al., 2003; Hoffman and Reed, 2004). The hearing loss typically leads to hyperactivity and increased neural synchrony throughout the auditory system (Eggermont and Roberts, 2004; Henry et al., 2014). As such, restoration of normal neural activity through DBS may result in suppression of the tinnitus percept. The new DBS devices would prove advantageous in two regards. First, the new DBS devices can be used to target areas within the auditory nuclei that can modulate the tinnitus-affected neurons without stimulating the entire nuclei, which may cause additional auditory sensations. Second, as aberrant activity can manifest in limited regions dependent on hearing loss (Kaltenbach and Afman, 2000; Vogler et al., 2014), selective targeting can be employed to either directly stimulate tinnitus-affected neurons or to stimulate the surrounding regions as necessary to indirectly drive suppression of the tinnitus-related neural activity (De Ridder et al., 2006). Already, the ABI has been implemented for treating tinnitus with favorable results, in which the electrode array stimulates portion of the modulatory region of the auditory brainstem. Stimulation by the ABI has resulted in most patients reporting reduced or masked percepts (Soussi and Otto, 1994; Behr et al., 2007). Encouraged by these results, the use of the AMI for tinnitus will

be tested in an upcoming clinical trial, in which a couple sites of the AMI will be used to activate the modulatory region of the auditory midbrain and hopefully alter and interact with the tinnitus-affected neurons within the ascending auditory pathway leading to the phantom percept.

The AMI was originally designed for implantation into the IC for hearing restoration (Lenarz et al., 2006; Lim et al., 2009b), but previous results from animal experiments revealed the potential for using the AMI to treat patients who also have tinnitus (Offutt et al., 2014). The new generation AMI has two shanks, each with ten sites for hearing restoration and one site for tinnitus therapy (Lim and Lenarz, 2015). Each shank will be positioned into the IC such that the ten sites for hearing restoration will reside in the ICC where the primary processing of auditory information occurs (Aitkin, 1979). The one superficial site on each shank designated for tinnitus treatment will be placed in the outer cortices of the IC, which can modulate activity within the ICC (Jen et al., 2001; Jen et al., 2002; Offutt et al., 2014) and potentially interact with midbrain neurons driving or linked to the tinnitus percept (Ma et al., 2006; Bauer et al., 2008; Melcher et al., 2009; Vogler et al., 2014). It is important to note that five deaf patient will be implanted with the AMI for hearing restoration from 2015 to 2018. Most of these patients will also have tinnitus due to their deafness, and thus it will be possible to evaluate the effects of IC stimulation on their tinnitus percept with minimal additional risk to the patients.

If this AMI clinical trial demonstrates the ability to decrease the tinnitus percept, then we would next seek to expand treatment to two populations: patients with the most

96

debilitating tinnitus but with moderate to near-normal hearing, and hyperacusis patients. For tinnitus patients with residual hearing, we would be able to use sound stimulation in conjunction with AMI stimulation, opening up a greater parameter space to better address their needs, as will be further explained through the results of this chapter. For hyperacusis patients who have an increased sensitivity and painful sensation to particular frequencies or sound inputs, stimulation with the AMI could be used to suppress the increased acoustic-driven activity associated with hyperacusis (Gu et al., 2010; Aazh et al., 2014), as was possible in our animal experiments described in this chapter.

The aim of this study was to better understand the neuromodulation effects achievable by stimulation of the outer IC, particularly the ICD, in order to guide stimulation parameters in the upcoming AMI clinical trial. We wanted to expand upon our previous results that showed stimulation of the ICD can both suppress and facilitate ICC neural activity, by examining a larger stimulation parameter space to determine optimal paradigms for suppression and by evaluating the lasting effects. We stimulated a single ICD location with different electrical and acoustic paradigms and measured the changes in acoustic-driven activity and synchrony across sites in the ICC. Our results reveal that modulation of ICC neural activity can last at least up to thirty minutes following electrical and/or acoustic stimulation and the amount of suppression and facilitation is dependent on the stimulation paradigm used. We were able to identify two paradigms that produce maximum suppression, one that can be used in the upcoming AMI patients and one that can be used in future patients that still have hearing. Future studies are needed to further evaluate the effects of these stimulation paradigms in

humans and animals with tinnitus and on a longer time scale than was possible in our experiments.

METHODS

Surgery and Experimental Setup

Experiments were performed on eleven Hartley guinea pigs (mass: 440 ± 59; Elm Hill, Chelmsford, MA) following the University of Minnesota Institutional Animal Care and Use Committee standards. Basic surgical and electrophysiological protocols have been detailed in previous works (see Chapter 2, Lim and Anderson, 2007a; Offutt et al., 2014) and are only summarized here. Animals were initially anesthetized with an intramuscular dose of ketamine (40 mg/kg) and xylazine (10 mg/kg), and additional doses were administered to maintain an areflexive state. Animals were placed in a stereotaxic frame and a craniotomy was performed over the right hemisphere.

All experiments were completed in an electrically and acoustically isolated chamber. TDT hardware (Tucker-Davis Technologies, Alachua, FL) controlled by custom-written MATLAB software (MathWorks, Natick, MA) was used for stimulation delivery and data collection. Acoustic stimulation was delivered to the left ear at a sampling frequency of 195 kHz through a hollow ear bar coupled to the speaker. A 0.25-in condenser microphone (ACO Pacific, Belmont, CA) was used to calibrate the speaker and ear bar system. Monopolar electrical stimulation was delivered into the midbrain through an optically isolated stimulator with a return electrode placed in the parietal lobe. Multi-unit neural activity was recorded using a monopolar configuration with a return

electrode within the neck muscle. The neural signals were passed through an analog DC-blocking and anti-aliasing filter from 1.6-7.5 kHz, sampled at a rate of 25 kHz, and filtered from 0.3-3 kHz to identify spikes. Spikes were detected when voltages exceeded three times the standard deviation of the noise floor.

Electrode Placement

Bi-shank silicon substrate electrode arrays were used for both recording and stimulating (16 sites per shank, 403 μm^2 site size, 100 μm site spacing, 500 μm shank spacing; NeuroNexus, Ann Arbor, MI). The recording array was placed at a 45° angle to the sagittal plane and inserted along the tonotopic axis of the ICC. The stimulating array was placed perpendicular to the horizontal plane to enter the ICD. Both arrays were long enough to pass through the visual cortex to reach the IC. Broadband noise stimulation (50 ms duration, 0.5 ms rise/fall time, 6 octave bandwidth from 0.625 to 40 kHz, 70 dB-SPL) was used during insertion of the electrodes to confirm location in the IC. Location within the IC was determined by responses to pure tone stimulation at varying frequencies and levels (50 ms duration, 0.5 ms rise/fall time, 1.0-40 kHz, 8 steps/octave, 0-70 dB-SPL, 10 dB steps). Sites within the ICC showed strong frequency selectivity with a progression of sites that preferred low to high frequencies from shallower to deeper locations (Merzenich and Reid, 1974; Snyder et al., 2004; Malmierca et al., 2008). Sites within the ICD showed weak or no frequency selectivity and did not display an organized gradient of preferred frequencies (see Chapter 2, LeBeau et al., 2001; Palmer et al., 2013).

Paradigms and Protocol

Eight different electrical stimulation paradigms and two control paradigms were tested in each of the animals. Each paradigm was presented for 100 trials at 2 trials/s The electrical stimulation paradigms included ES-only (100 µA biphasic, charge balanced, cathodic leading pulse, 205 µS/phase) and paired stimulation consisting of acoustic (90 ms, 5 ms rise/fall time, 50 dB-SPL) and electrical stimulation at varying delays (**PAES_n_{delay}**; where n_{delay} = -7 ms to 23 ms, 5 ms steps relative to the onset of acoustic stimulation). The control paradigms included AS-only and no stimulation at all (**Control**). The Control paradigm was presented before any other stimulation paradigm and if time permitted, after all stimulation paradigms, allowing us to assess changes in spike activity inherent to the ICC and overall effects of stimulation, respectively. The remaining paradigms were presented in a randomized order across experiments. In a single experiment, all paradigms were presented once before any paradigms were repeated. Aside from Control, all stimulation paradigms were presented as the first stimulation paradigm in at least one experiment, to assess effects elicited without the possible influence of previous paradigms. The number of presentations for each stimulation paradigm is as follows: PAES_-7, n=12; PAES_-2, n=12; PAES_3, n=13; PAES_8, n=13; PAES_13, n=13; PAES_18, n=13; PAES_23, n=13; ES-only, n=12; AS-only, n=12; Control, n=16).

Data Analysis

In order to evaluate the modulation elicited by each paradigm, ICC neural activity in response to acoustic stimulation (90 ms, 5 ms rise/fall time, 50 dB-SPL, 100 trials) was collected before, immediately after (T_0), and thirty minutes after (T_{30}) each neuromodulation paradigm. Only ICC sites that demonstrated significant acoustic-driven activity were included in the analysis. Significant acoustic-driven activity was determined using signal detection theory as described in (Green and Swets, 1966; Lim and Anderson, 2007a), wherein ICC sites were included if the spike count distributions from 50 ms of acoustic-driven activity and from 50 ms of spontaneous activity were significantly different from each other (d'>1). Those ICC sites were next assessed to determine if significant modulation occurred following a paradigm. The window used for modulation analysis began 8 ms after the onset of acoustic stimulation and ended at the offset of acoustic stimulation. The spike count distribution from acoustic stimulation before was compared to the spike count distribution at T_0 and at T_{30} using a two-tailed, unequal variance, ranked t-test (Ruxton, 2006a). Significant suppression (facilitation) occurred if there was a decrease (increase) in spike count following the paradigm (p<0.01). Once significantly suppressed or facilitated ICC sites were identified, modulation was quantified for each paradigm using a metric called spread. Spread measures the percent of sites that were significantly suppressed (facilitated) by each paradigm and was calculated by dividing the number of suppressed (facilitated) ICC sites by the total number of ICC sites with significant acoustic-driven activity.

Modulation of synchrony was also evaluated on all sites with significant acoustic-driven activity by first determining significance of synchrony at each time point and then assessing changes in significance over time. To evaluate modulation of synchrony, ten seconds of spontaneous activity were recorded before, at T_0, and at T_{30}. At each time point, the maximum cross correlation value for each ICC site pair was calculated. For each site pair, bootstrapping was completed to find the mean and standard deviation of the maximum cross correlation values from 1000 inter-spike interval shuffled comparisons. ICC site pairs were considered significantly synchronous at a time point if the measured maximum cross correlation value was two standard deviations greater than the calculated mean cross correlation value. Only ICC site pairs that demonstrated significant synchrony at a given time point were included for further analysis. Next, modulation of synchrony occurred if an ICC site pair changed significantly from before to after a paradigm (e.g., if an ICC site pair was significantly synchronous before and was not at T_0 then suppression of synchrony immediately after the paradigm occurred, or if a pair was not significantly synchronous before and became synchronous at T_{30} then lasting facilitation of synchrony occurred). Finally, spread for synchrony modulation was calculated by dividing the number of suppressed (facilitated) ICC sites pairs by the total number of significantly synchronous ICC site pairs. In addition, analysis was completed to account for the site pairs that remained significantly synchronous before and after a paradigm by evaluating the change in maximum cross correlation values regardless if those changes were significant or not. For this additional analysis, if the maximum cross correlation value decreased (increased) between time points, the site pairs was deemed to

be suppressed (facilitated). Spread was then calculated for synchrony by dividing the number of suppressed (facilitated) ICC site pairs by the total number of site pairs. The second analysis yielded no significant differences and results are not further discussed in this chapter.

To determine overall effects of each paradigm, paradigm comparisons were completed separately for acoustic-driven modulation and synchrony modulation. Spread of acoustic-driven modulation and synchrony modulation per paradigm were pooled across all animals for these comparisons. Paradigms were compared using a two-tailed, unequal variance, ranked t-test with Bonferroni correction ($p<0.05$). The amount of suppression and facilitation spread elicited per paradigm (Bonferroni corrected $p<0.005$) as well as the amount of suppression spread elicited compared to Control (Bonferroni corrected $p<0.0056$) were assessed to determine optimal stimulation paradigms. For these comparisons, all Control paradigms have been pooled together as the results from Control paradigms presented at the start of the experiment and at the end of the experiment were not systematically different for acoustic-driven modulation (mean $\pm$ SEM, T_0 Sup – Start: 15.1 $\pm$ 4.5%, End: 15.1 $\pm$ 7.0%; T_0 Fac – Start: 12.9 $\pm$ 1.8%, End: 10.2 $\pm$ 3.2%; T_{30} Sup – Start: 16.4 $\pm$ 3.5%, End: 16.2 $\pm$ 3.7%; T_{30} Fac – Start: 15.7 $\pm$ 4.6%, End: 13.7 $\pm$ 7.8%) or for synchrony modulation (T_0 Sup – Start: 7.3 $\pm$ 4.7%, End: 15.9 $\pm$ 7.2%; T_0 Fac – Start: 12.9 $\pm$ 6.3%, End: 11.3 $\pm$ 6.1%; T_{30} Sup – Start: 4.7 $\pm$ 0.6%, End: 16.3 $\pm$ 6.2%; T_{30} Fac – Start: 13.8 $\pm$ 4.6%, End: 9.8 $\pm$ 3.2%). Spread from Control at the start and spread from Control at the end are plotted in *Results* for visual comparison.

Histology

A histological protocol was completed for each experiment to verify the location of the recording and stimulating arrays and sites in the IC (Fig. 22). This protocol has been detailed in previous works and will be summarized here (see Chapter 2, Markovitz et al., 2012; Offutt et al., 2014). Prior to placement in the IC, electrode arrays were dipped in Di-I (Sigma-Aldrich, St Louis, MO) that was absorbed into the tissue for later identification. Following an experiment, the heads were placed in 3.7% paraformaldehyde. Within 10 days, the full brain was extracted and the right midbrain was blocked out for further processing. The right midbrain was then cryo-sliced to 60 μm thick slices, the slices were imaged, and the images were imported into a 3D CAD software for reconstruction (Rhinoceros, Seattle, WA). Using anatomical landmarks, the slices were aligned to create the 3D reconstruction, and the 3D reconstructions were normalized across all animals. The reconstructed recording electrode array and the single stimulation site with its corresponding electrode array shank location from each experiment were imported into a single normalized brain for location comparison across all eleven animals (Fig. 22). The location of the stimulation site was determined relative to the anatomical border of the IC, appropriately adjusted for changes due to the fixation process (see Chapter 2, Markovitz et al., 2012).

By analyzing the histological reconstructions, we can determine the similarity of our placements to each other and to the regions we were targeting. As our previous study indicated that all areas in the ICC can be modulated by stimulation of the ICD and that the largest amount of suppression could be achieved by stimulation of the rostral-medial

area of the ICD (Offutt et al., 2014), we aimed for similar recording and stimulating locations across animals based on anatomical and vasculature landmarks on the surface of the occipital lobe. All recording locations can be seen in the ICC in Figure 22*A*. As expected, there was some variability in placement but electrode arrays were generally in the same location. Based on previous results, modulation is not noticeably dependent on ICC recording location and therefore there is minimal concern that ICC recording location will contribute to significant variance in the results (Offutt et al., 2014). The single stimulation site (black sphere) and corresponding electrode array shank from each experiment are shown in the three dimensional reconstruction in Figure 22*B*. The ICD stimulation sites across experiments were then projected onto the yellow plane to be visualized in two dimensions (Fig. 22*C*). This is the same plane as was used in the previous ICD stimulation study, thus sites can be compared to previous location results. Sites from this study were in more medial ICD locations (black circles), which was in our intended region and within the area of the ICD where the greatest suppression was found in our previous study (gray circles, suppression spread greater than 25%; Offutt et al., 2014). This map indicates that for each individual animal, we were targeting areas of the ICD that produced large amounts of suppression previously (Offutt et al., 2014).
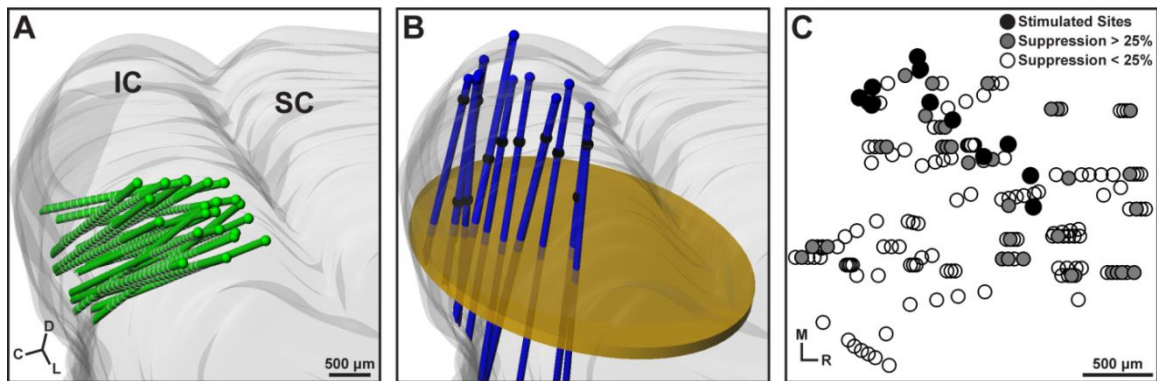
Figure 22. Locations of recording electrode arrays in the ICC and stimulation sites in the ICD. **A**, The ICC electrode array reconstructions from all eleven animal experiments are shown in a single midbrain reconstruction. **B**, The ICD stimulation site (black sphere) and its corresponding electrode array shank from each of the eleven animal experiments are shown in a single midbrain reconstruction. **C**, The ICD stimulation sites were projected onto a flat plane (yellow plane in **B**) and compared to ICD stimulation locations from a previous study (Offutt et al., 2014). The ICD stimulation locations from this experiment are concentrated in the medial area of the ICD (black circles). The previous study found that the largest suppression can be elicited from rostral-medial locations in the ICD (gray circles indicating suppression spread was greater than 25%). Thus, the ICD sites from this study are activating areas from the previous study that elicited a greater extent of suppression. The image from **C** was adapted from (Offutt et al., 2014).

RESULTS

We analyzed and compared the modulation effects from different ICD stimulation paradigms at two different time points to identify optimal paradigms and to examine lasting effects of modulation. As interference with the ongoing tinnitus-related neural activity is likely necessary to affect the tinnitus percept, we believe treatments need to decrease hyperactivity and disrupt neural synchrony associated with tinnitus. In these experiments we could not directly monitor the effects on these neural correlates of tinnitus, as we were not using animal models of tinnitus. Due to the ongoing controversy

in the field over a reliable animal model for tinnitus (Eggermont, 2013; Ropp et al., 2014) and to simplify the interpretation of our initial experiments in animals, we instead focused on the ability to suppress neural activity in normal hearing animals. Encouraging results from our study could then be further explored and confirmed in animal models of tinnitus and humans with tinnitus. Thus, in analyzing these results, we defined an optimal paradigm as one that elicited significantly more suppression than the Control paradigm ($p_{vControl}$ < 0.056) and significantly more overall suppression compared to facilitation (p_{vFac} < 0.005). We compared the spread elicited by each paradigm at each time point for both acoustic-driven activity and synchrony. Our results show that overall there is more suppression of acoustic-driven activity elicited by ICD stimulation than facilitation at both time points, and that there are optimal paradigms at each time point for suppressing acoustic-driven activity. Our results also reveal that certain paradigms can be effective for suppressing synchrony, though many other paradigms did not reach significance or instead enhanced synchrony.

Acoustic-Driven Modulation

Suppression and facilitation could be elicited by each electrical stimulation paradigm at each time point, but spread was highly dependent on the paradigm. On average, the number of sites modulated increased over time (T_0: 31.4% versus T_{30}: 51.3%), with more suppression (**Sup**) than facilitation (**Fac**) elicited at both T_0 (Fig. 23*A*, Sup: 22.3%, Fac: 9.1%) and T_{30} (Fig. 23*B*, Sup: 30.7%, Fac: 20.6%). Examining the effects of individual paradigms at both time points reveals three paradigms that meet the

107

criteria of providing more suppression spread than facilitation spread and more suppression spread than Control: PAES_8 at T_0, PAES_18 at T_{30}, and ES-only at T_{30}. For all three paradigms, significance was only achieved at a single time point. For PAES_8, suppression occurred immediately after the paradigm but did not last (Fig. 23*C*, Sup: 30.8 ± 4.6%, Fac: 5.0 ± 1.9%, p_{vFac}=1.4E-6, $p_{vControl}$=0.0037). By contrast, modulation achieved from PAES_18 and ES-only did not occur immediately after the paradigm but rather had a delayed onset leading to lasting suppression (Fig. 23*D*, PAES_18 − Sup: 47.2 ± 7.1%, Fac: 11.7 ± 3.8%, p_{vFac}=2.9E-5, $p_{vControl}$=6.5E-4; ES-only − Sup: 41.9 ± 5.9%, Fac: 11.3 ± 2.8%, p_{vFac}=5.8E-5, $p_{vControl}$=9.8E-4). There was one more paradigm, PAES_13 at T_0, which did provide significantly more suppression spread compared to facilitation spread (Sup: 30.0 ± 6.3%, Fac: 3.0 ± 1.1%, p_{vFac}=2.8E-5), but failed to meet our criteria for an optimal parameter as it was not significantly greater than Control ($p_{vControl}$=0.043). There were no differences found between suppression and facilitation spread elicited by Control at either T_0 (Sup: 15.1 ± 3.7%, Fac: 12.1 ± 1.6%, p_{vFac}=0.99) or T_{30} (Sup: 16.3 ± 2.6%, Fac: 15.1 ± 3.8%, p_{vFac} =0.49). Furthermore, as there were no significant differences found for spread between the two time points for Control for suppression (p=0.48) or facilitation (p=0.98), we can conclude that the effects over time were caused by the stimulation paradigms and not solely due to inherent changes in the brain state of the animals (e.g., due to anesthesia, health of the animal, or intrinsic oscillations in brain activity). Overall, these findings demonstrate that electrical stimulation or paired stimulation of the ICD induces modulation within the ICC that can

evolve over time and that the type of changes are highly dependent on the delay between acoustic and electrical stimulation.

In assessing these effects, it is possible that modulation remained longer than the allotted thirty minute window, perhaps affecting the results of the following paradigm. In general, there was more modulation at T_{30} compared to T_0 indicating that at least for some paradigms, greatest modulation appeared over time. Though we cannot directly assess the influence of one paradigm on the results of the following paradigm, certain recourse was taken to minimize the effects and address this concern. First, by randomizing the paradigm order, we were able to average out the effects one specific paradigm may have on the following. Thus, we cannot explicitly isolate a single paradigm as affecting or even priming the subsequent paradigm. Second, for each experiment a different stimulation paradigm was used after the initial Control paradigm, such that the effects from the first stimulation paradigm of each experiment would not be influenced by other stimulation paradigms. The results are not shown, but overall those first stimulation cases match what is shown in Figure 23. There was a general trend of more suppression than facilitation at both time points (T_0 – Sup: 22.0%, Fac: 8.4%; T_{30} – Sup: 41.5%, Fac: 13.6%). When analyzing just the first stimulation cases of the experiments, all paradigms identified as significant in the pooled data in Figure 23 also provided larger suppression spread compared to facilitation spread in these first stimulation cases. These results include PAES_8 (Sup: 29.0%, Fac: 3.2%) and PAES_13 (Sup: 41.6%, Fac: 0.0%) at T_0, and PAES_18 (Sup: 50.0%, Fac: 3.8%) and ES-only (Sup: 50.0%, Fac: 10.7%) at T_{30}. To that end, we can say that while there may be an influence

of one paradigm on another, paradigms elicited similar trends in modulation regardless of whether it was presented as the first stimulation paradigm of an experiment or following other stimulation paradigms.
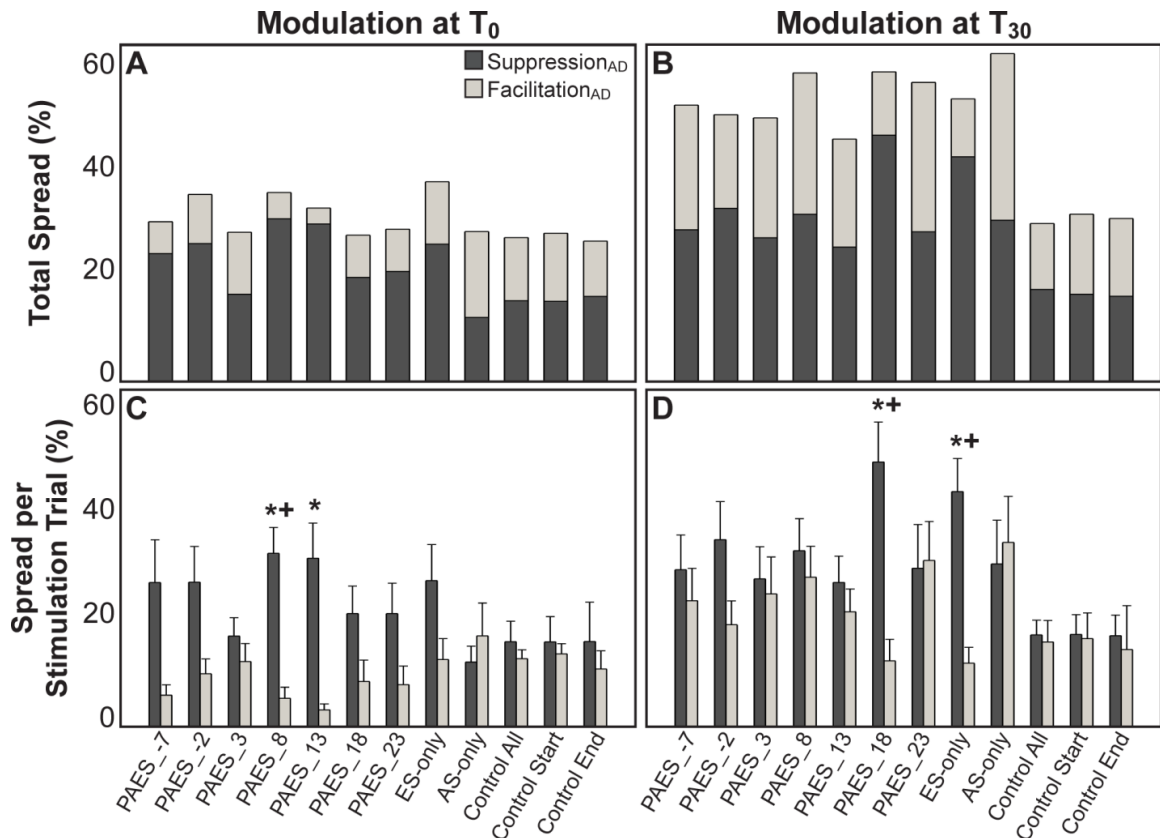
Figure 23. Acoustic driven modulation elicited by different paradigms. *A,B*, The total pooled spread across all stimulation trials of sites that were suppressed was greater than sites that were facilitated following the stimulation paradigm at T_0 (*A*, Sup: 22.3%, Fac: 9.1%) and at T_{30} (*B*, Sup: 30.7%, Fac: 20.6%). Overall there were a greater percentage of sites that were modulated at T_{30} compared to T_0 (T_0: 31.4%; T_{30}: 51.3%). Per animal there was an average of 30 ICC sites evaluated per paradigm and a total of 3240 ICC sites evaluated across all animals and all paradigms. *C,D*, The mean and SEM of spread elicited by each paradigm over 12-16 individual trials are presented (see *Methods: Paradigms and Protocol* for number of trials for each paradigm). *C*, At T_0, PAES_8 and PAES_13 elicited more suppression than facilitation (*, p_{vFac}=1.4E-6 and p_{vFac}=2.8E-5, respectively) and PAES_8 provided more suppression than the Control paradigm (+, $p_{vControl}$=0.0037). *D*, At T_{30}, PAES_18 and ES-only induced more

110

suppression than facilitation (p_{vFac}=2.9E-5 and p_{vFac}=5.8E-5, respectively) and more than the Control paradigm ($p_{vControl}$=6.5E-4 and $p_{vControl}$=9.8E-4, respectively). The amount of suppression compared to facilitation elicited by Control was unchanged between the two time points (T_0: p=0.99; T_{30}: p=0.49). The significant cases at T_0 include PAES_8 (Sup: 30.8 ± 4.6%, Fac: 5.0 ± 1.9%), and PAES_13 (Sup: 30.0 ± 6.3%, Fac: 3.0 ± 1.1%). The significant cases at T_{30} include PAES_18 (Sup: 47.2 ± 7.1%, Fac: 11.7 ± 3.8%) and ES-only (Sup: 41.9 ± 5.9%, Fac: 11.3 ± 2.8%). The spread for Control between T_0 (Sup: 15.1 ± 3.7%, Fac: 12.1 ± 1.6%) and T_{30} (Sup: 16.3 ± 2.6%, Fac: 15.1 ± 3.8%) were not significantly different for suppression (p=0.48) nor facilitation (p=0.98).

Modulation Specificity

We next assessed the specificity of each electrical stimulation paradigm by determining if ICC sites were suppressed or facilitated by a single paradigm or by multiple paradigms. ICC sites that are only able to be modulated by a single paradigm may provide information on synaptic dynamics between the ICC and the ICD, as well as indicate that we would be able to target particular ICC locations using different electrical stimulation paradigms. For this analysis, we only used the data from animals where all nine paradigms were presented (eight animals) and did not use any repetitions of paradigms in a single animal. There were a total of 241 ICC sites included in this analysis. For each ICC site, we counted the number of paradigms that elicited either significant suppression or significant facilitation for both time points. The ES-only, AS-only, and Control paradigms were not included in this analysis, as we were interested in how acoustic and electrical stimulation interacted in the ICC and if there were trends due to delays (i.e., a total of seven different delay paradigms). We only included sites where

modulation occurred, and thus all sites that showed no modulation over the seven paired paradigms were excluded from the total.

Both suppression and facilitation at T_0 showed specificity with 51.3% and 80.6% of the ICC sites only being suppressed and facilitated by a single paradigm, respectively (Fig. 24). By T_{30}, ICC sites could be suppressed or facilitated by more paradigms with a median of two paired stimulation paradigms per site. We further analyzed which paradigms provided modulation to determine if the delays were similar or if there were any timing dependencies in relation to the onset of spike activity in the ICC that led to facilitation versus suppression. In examining modulation at T_0, most facilitation was a result of paradigms where the electrical stimulation preceded the first spike in the ICC in response to acoustic stimulation (i.e., average first spike latency equal to 8.5 ± 3.1 ms). At T_0, a total of 72.5% of the ICC sites were facilitated by PAES_-7, PAES_-2, or PAES_3 and no other paradigms. Conversely, most suppression was a result of paradigms where electrical stimulation followed the first spike in the ICC, with 58.6% of the ICC sites suppressed by PAES_8, PAES_13, PAES_18, or PAES_23. In analyzing suppression and facilitation at T_{30}, no further stimulus-timing dependent relationships were observed. Overall, these results suggest that at least immediately, the type of modulation elicited (i.e., facilitation or suppression) is dependent on the timing of the electrical pulse in relation to transmission of sound information to the ICC.
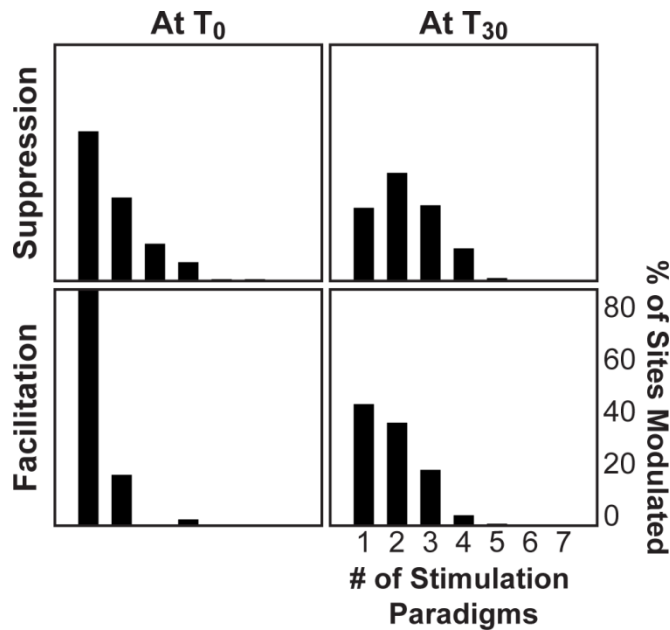
Figure 24. Specificity of the timing of paired stimulation. The number of electrical stimulation paradigms that elicited significant suppression or facilitation at each time point was analyzed for each ICC site to examine the specificity of modulation. Specificity was found for suppression and facilitation at T_0 in which ICC sites were mostly modulated by only one or two paradigms. This specificity was weaker at T_{30} in which ICC sites could be generally modulated by one to four different electrical stimulation paradigms. Suppression at T_0 was achieved mostly by one or two paired stimulation paradigm (51.3% or 28.6% of sites, respectively), which was typically due to a paradigm in which electrical stimulation followed the first spike in the ICC (i.e., PAES_8, PAES_13, PAES_18, PAES_23). Facilitation at T_0 was often achieved by only one electrical stimulation paradigm (80.6% of sites), which was typically due to a paradigm in which electrical stimulation preceded the first spike in the ICC (i.e., PAES_-7, PAES_-2, PAES_3).

Synchrony Modulation

Similar to acoustic-driven modulation, we assessed synchrony modulation to find paradigms that had greater suppression spread than facilitation spread and more suppression spread than Control. The average modulation of synchrony at T_0 and T_{30} was similar (T_0: 22.3%; T_{30}: 24.4%) and there was no overall trend between suppression and

113

facilitation within or across time points (Fig. 25*A,B*, T_0 – Sup: 11.9%, Fac: 10.4%; T_{30} – Sup: 11.6%, Fac: 12.8%). Unlike acoustic-driven modulation, analysis for synchrony yielded no paradigms at T_0 or at T_{30} (Fig. 25*C,D*) that met both criteria to be significant. However, PAES_-7 at T_{30} showed significantly more suppression of synchrony than facilitation (Sup: $17.1 \pm 4.7\%$, Fac: $4.1 \pm 1.0\%$, p_{vFac}=0.003), but not more suppression spread than Control ($p_{vControl}$=0.038). There were other paradigms that were not significant as they failed to meet our criteria, but did trend toward more suppression of synchrony compared to facilitation spread including PAES_-7 at T_0 (Sup: $18.6 \pm 6.1\%$, Fac: $5.2 \pm 1.1\%$, p_{vFac}=0.17), PAES_3 at T_0 (Sup: $16.0 \pm 5.5\%$, Fac: $7.4 \pm 1.8\%$, p_{vFac}=0.41), and PAES_3 at T_{30} (Sup: $20.3 \pm 5.8\%$, Fac: $5.5 \pm 1.1\%$, p_{vFac}=0.052). Interestingly, examination of the paradigms that successfully suppressed acoustic-driven activity in Figure 23 revealed a trend toward more facilitation of synchrony in Figure 25. These included PAES_8 at T_0 (Sup: $10.3 \pm 3.3\%$, Fac: $15.4 \pm 6.3\%$, p=0.64), PAES_18 at T_{30} (Sup: $5.8 \pm 1.7\%$, Fac: $21.3 \pm 6.6\%$, p=0.008), and ES-only at T_{30} (Sup: $7.5 \pm 1.7\%$, Fac: $19.3 \pm 7.1\%$, p=0.28). There was no significant difference between the two time points for the Control paradigm for suppression spread (p=0.51) or facilitation spread (p=0.71), indicating that these significant changes or trends in Figure 25 over time were driven by the stimulation paradigms and not solely due to inherent changes in neural activity. Overall, there appears to be specific paradigms that can suppress or enhance synchrony at different time points, as can be observed in Figure 25, but there were no optimal paradigms that achieved our strict criteria for significance. It may be possible that

cumulative effects, differences across animals, and anesthetic effects contribute to the variability in results and the lack of significance across paradigms.
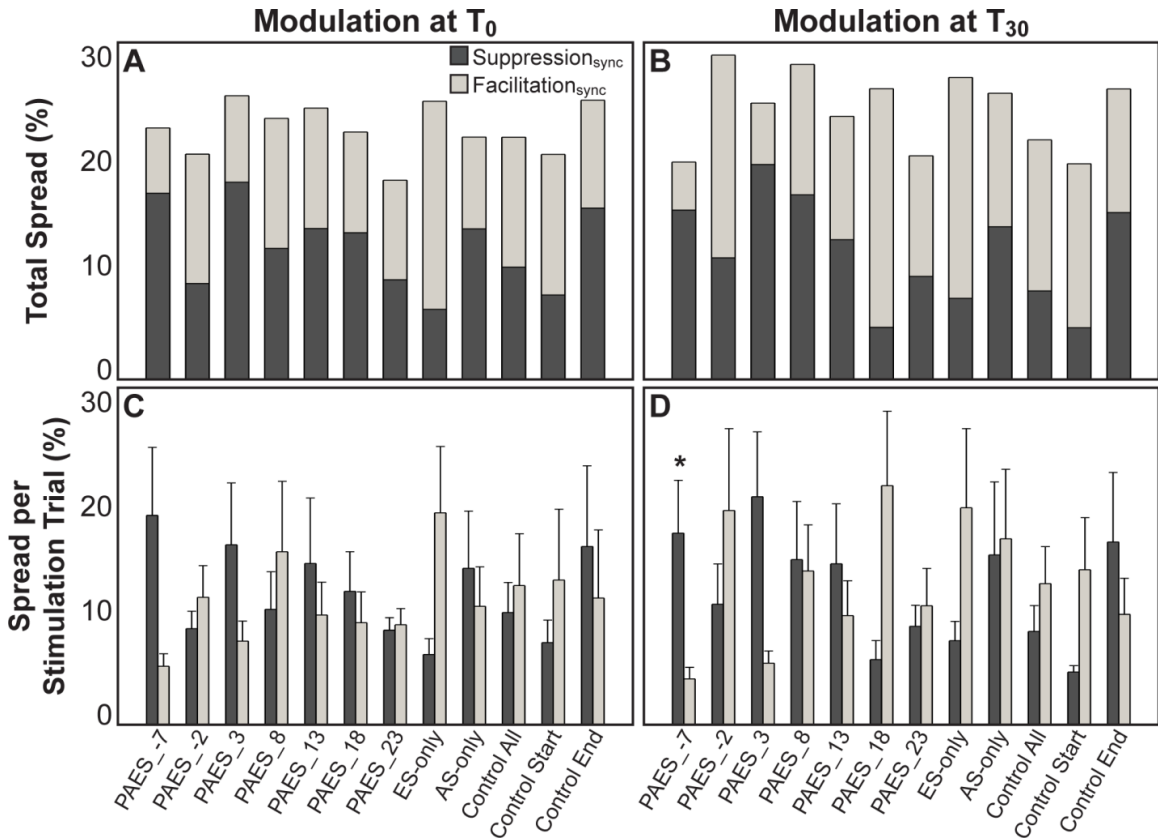
Figure 25. Synchrony modulation elicited by different paradigms. *A,B*, There was no difference in the total spread across all stimulation trials (pooled) at T_0 compared to T_{30} (T_0: 22.3%; T_{30}: 24.4%). The suppression and facilitation of synchrony at both time points was similar (T_0 – Sup: 11.9%, Fac: 10.4%; T_{30} – Sup: 11.6%, Fac: 12.8%). Per animal there was an average of 444 ICC site pairs evaluated for each paradigm and a total of 47,815 ICC site pairs evaluated across all animals and paradigms. *C,D*, The mean and SEM of spread of synchrony elicited by each paradigm over 12-16 individual trials are presented (see *Methods: Paradigms and Protocol* for number of trials for each paradigm). *C*, No significant modulation of synchrony was induced at T_0. *D*, At T_{30}, PAES_-7 induced more suppression of synchrony than facilitation (*****, Sup: 17.1 ± 4.7%, Fac: 4.1 ± 1.0%, p_{vFac}=0.003), but not more suppression of synchrony than the Control paradigm ($p_{vControl}$=0.038). There were no significant differences between suppression spread and

facilitation spread elicited by the Control paradigm at either time point (T_0 – Sup: 10.0 ± 2.7%, Fac: 12.4 ± 4.6%, p=0.67; T_{30} – Sup: 8.3 ± 2.3%, Fac: 12.5 ± 3.3%, p=0.16) nor was there a significant difference between time points for the Control paradigm for suppression spread (p=0.51) and facilitation spread (p=0.71).

DISCUSSION

The aims of this study were to expand upon our understanding of the functional connectivity between the ICD and the ICC and to identify optimal electrical stimulation paradigms that lead to suppression of activity within the auditory system that could be relevant for tinnitus treatment. The translational goal was to use these results to better inform the stimulation parameters that can be investigated in the first set of AMI patients who will also receive tinnitus treatment. We found two paradigms that provided lasting suppression of acoustic-driven activity, ES-only and PAES_18, but no paradigm that provided lasting suppression of synchrony. There were however electrical stimulation paradigms that exhibited trends toward suppressing synchrony. These results have implications for potentially modulating tinnitus-related neural activity such as hyperactivity and increased neural synchrony and suppressing the tinnitus percept.

Methodological considerations

There are certain limitations to consider when interpreting the results of this study including allotted recovery time, effects of anesthesia, and translation into tinnitus models. For this study we wanted to assess the lasting modulation effects of different paradigms by evaluating neural changes at a time point thirty minutes after presentation of a stimulation paradigm. We had opted to limit recovery time in our previous study by

116

only assessing modulation at T_0 and then presenting the subsequent stimulation paradigm in order to stimulate many different locations in the ICD (Offutt et al., 2014). Our concern from this initial study was that effects from individual paradigms were missed if they lasted beyond the initial time point and may have influenced or masked effects of other paradigms, particularly since paradigms were presented in a set order. The results from this previous study showed that PAES_18 provided the largest amount of suppression, with little effect from ES-only or PAES_8 (Offutt et al., 2014). In comparing those results with the findings from our current study, we see that PAES_18 continues to be a promising paradigm for suppression. However, ES-only and PAES_8 also met our criteria for optimal paradigms at T_{30} and T_0, respectively. These results validate our concerns that our previous study may have failed to capture ES-only modulation by only assessing at T_0 and modulation due to PAES_8 may have been masked by the lasting modulation effects of PAES_18. For this study we allowed for thirty minutes of recovery and used a randomized order to eliminate some of these cumulative and confounding effects. Still, this recovery period may not have been long enough to allow neural activity to return to baseline spiking. In order to investigate a sufficient number of paradigms, we were unable to allow for longer recovery periods. In future studies, we will focus on a few optimal parameters we identified in this study and allow for enough time for full recovery back to baseline activity.

These experiments were completed under ketamine anesthesia, which has been shown to have little effect on the acoustic-driven activity in the ICC, but may have increased the spontaneous firing rates (Astl et al., 1996b; Ter-Mikaelian et al., 2007).

117

Spontaneous activity was used to analyze synchrony and therefore it is possible that the lack of significant results could be attributed to anesthesia. Ketamine may have also affected synaptic potentiation and limited plasticity (Salami et al., 2000; Leong et al., 2004). However under ketamine anesthesia, we were still able to see significant modulation effects on acoustic-driven activity and differential modulation that was dependent on the paradigm used. Nevertheless, the effects of ICD modulation on ICC acoustic-driven activity and synchrony will need to be verified in an awake preparation.

Lastly, these results presented here were recorded from normal hearing animals. We hypothesized that reduction in acoustic-driven activity and synchrony in normal hearing animal models translates to reduction in hyperactivity and disruption in elevated neural synchrony in tinnitus animal models and that those modifications lead to suppression or elimination of the tinnitus percept. We will need to repeat our studies in tinnitus animal models to confirm our hypothesis. While we built this therapy on the belief that the neural correlates of tinnitus in the ICC are higher spontaneous firing rates and greater neural synchrony, (Ma et al., 2006; Bauer et al., 2008; Melcher et al., 2009; Manzoor et al., 2013; Vogler et al., 2014), we may find in the tinnitus animal models there are additional alterations to neural activity and plasticity due to tinnitus. Fortunately, we have the unique opportunity to explore our findings from normal hearing animals directly in human patients with tinnitus in the upcoming AMI clinical trial. Considering the controversy over current animal models of tinnitus (Eggermont, 2013; Ropp et al., 2014), we can compare the results we observe in these tinnitus patients with those in our animal models of tinnitus in future studies.

118

Functional Connectivity

One presumed role of the ICD in the central auditory system is to contribute to corticofugal modulation of the ICC. The projections from the auditory cortex to the ICC are sparse, mainly excitatory, and tonotopically organized (Bajo and Moore, 2005; Lim and Anderson, 2007b; Markovitz et al., 2013). Those direct projections alone cannot account for the excitatory and inhibitory plasticity found following cortical activation or inactivation (Mitani et al., 1983; Syka and Popelar, 1984; Sun et al., 1989; Torterolo et al., 1998; Zhang and Suga, 2000; Zhou and Jen, 2000). As such, it is believed that there is also indirect corticofugal modulation via the outer cortices that has a strong inhibitory component. This hypothesis is supported by anatomical studies that show extensive projections from the auditory cortex to both the ICD and the ICX (Winer et al., 1998; Bajo and Moore, 2005; Malmierca and Ryugo, 2011) and an extensive network of intrinsic IC connections (Coleman and Clerici, 1987; Saldaña and Merchán, 1992; Frisina et al., 1998). Studies have already demonstrated that stimulation of the A1 facilitated activity within the ICX and in turn ICX activation suppressed activity with the ICC (Jen et al., 2001; Jen et al., 2002). In conjunction with anatomical data showing projections from the auditory cortex to the ICD (Winer et al., 1998; Bajo and Moore, 2005; Malmierca and Ryugo, 2011), our study provides evidence for a second multi-synaptic pathway via the ICD which exhibits stronger suppressive than facilitatory modulation of the ICC.

Interestingly, greater modulation was achieved at T_{30} compared to T_0. Both the number of suppressed sites and the number of facilitated sites increased from T_0 to T_{30} for

all stimulation paradigms, but not the Control case (i.e., no stimulation paradigm). This result suggests that there is additional circuitry beyond just the ICD synapsing in the ICC that allows effects to appear over time. Perhaps there are local networks integrating the ICD input and driving a lasting plasticity. A better understanding of the distribution of projections from the ICD to the ICC would be necessary to confirm this option. A second circuit could involve the cortex and thalamus. Plasticity in the ICC driven by the ICC has been shown previously through a colliculo-thalamo-cortico-collicular loop (Zhang et al., 2005; Xiong et al., 2009). It may be that we are initially driving changes in the ICC in a limited area, but through this feedback loop further modulation is achieved in a larger area of the ICC, accounting for the increase spread over time. Further studies are needed to confirm this pathway.

Clinical Relevance

The results of this study are promising when considering implementation for tinnitus treatment in not only the current patient group with the AMI for hearing restoration, but also in possible future patients with residual hearing. Individuals receiving the AMI are all NF2 patients with acoustic neuromas growing on their auditory nerves (Lenarz et al., 2006; Schwartz et al., 2008; Colletti et al., 2009b; Lim et al., 2009b). The auditory nerve is typically severed during surgical resection of the tumors, leaving the patients deaf (Samii et al., 2007; Lim et al., 2009a). For this patient population we can employ the ES-only paradigm, which showed suppressive abilities in this study. Demonstrating a reduction in the tinnitus percept in this AMI patient

120

population may allow us to implant patients solely for tinnitus suppression, at least those with severe and debilitating tinnitus who still have residual hearing. These patients would be able to receive the PAES_18 paradigm in addition to ES-only paradigm, providing more treatment options. Looking beyond the application of tinnitus, this treatment may also be appropriate for hyperacusis. Hyperacusis is a central auditory condition that causes hypersensitivity to sounds, manifesting as increased acoustic-driven activity (Gu et al., 2010; Aazh et al., 2014). ICD stimulation with the AMI may help to suppress the acoustic-driven activity and reduce the elevated and painful loudness that the patients experience on a daily basis.

By having the opportunity to translate this treatment directly into tinnitus subjects, we will be able to more quickly discern paradigms that provide the best relief. The most effective paradigms may be outside of what were tested in this study. For these studies we minimized the stimulation parameters we investigated by using a single biphasic pulse at a rate of 2 Hz, however different pulse sequences may deliver better, longer lasting suppression. Moreover, we may find that our assumption of suppression being necessary to combat the tinnitus percept is incorrect, and that facilitation is necessary in some patients. As such, we can utilize other electrical stimulation paradigms that were evaluated. Regardless, in using the AMI we now have a platform that will allow us to continue to expand the clinical applications of DBS and continue to treat the needs of patients with other neurological conditions, such as debilitating tinnitus or hyperacusis.

CHAPTER 5: CONCLUSION

SUMMARY OF RESULTS

Given the ever present need for new tinnitus treatments and a deep brain stimulator that can target the inferior colliculus, we set out to assess the feasibility of using the IC to treat tinnitus. We wanted to look beyond the ICC as a stimulation target and examine the possibility of stimulating the outer cortices for better outcomes. We hypothesized that using the ICO as a target, we would be able to modulate more of the ICC through the extensive intrinsic network than ICC stimulation alone would achieve, and that in turn the ICC could modulate neural activity in the entire auditory system through the many ascending and descending projections originating from the ICC. We further hypothesized that this modulation would be able to achieve disruption of the hyperactivity and increased neural synchrony associated with tinnitus that is found in the ICC and throughout the auditory system, and that these changes in neural activity would result in reduction or completed suppression of the tinnitus percept. These hypotheses however encompass more work than could be completed in a single thesis. As so very little was known about the outer cortices and due to the controversy surrounding tinnitus-animal models (Eggermont, 2013; Ropp et al., 2014), we started with examining their functionality in normal hearing animals. The intention was that this body of work would set the stage for future studies assessing the effects of this tinnitus treatment in human patients and determining if this stimulation is actually modulating tinnitus-related neural activity within the ICC and throughout the auditory system. For this thesis we focused on assessing the functional properties and purposes of the subregions in the ICO in order to

122

narrow which regions to target for treatment. Based on those electrophysiological results in conjunction with the anatomical connectivity of the ICO with the rest of the auditory system, we next focused on investigating the modulation ability of just the ICD to determine if effects were suitable for tinnitus treatment. Finally we optimized stimulation parameters for what we believed would best treat tinnitus. These three separate projects comprise the thesis presented here.

In Chapter 2, we completed a comprehensive mapping of auditory responses across the entire IC. As previous studies had focused most attention toward the ICC, we wanted to expand to the outer cortices to provide a more complete picture of how auditory information is processed at the level of the IC. We assessed broadband noise and pure tone responses for both spectral and temporal properties and correlated those responses with location to determine if spatial trends existed. For spectral properties including threshold, Q-values at 10 dB about threshold, and Q-values at 60 dB-SPL, we found no spatial trend exist, but that trends could be found for ICC sites dependent on the BFs. In contrast, we found that there were clear spatial trends for spontaneous activity and temporal properties, including FSL, FSL jitter, and response duration, with no BF dependencies. Most interestingly, these spatial trends extended throughout the IC, with no distinction between the spatial trend in the ICC and in the ICO. Shorter latencies, increased precision, sustained responses compared to stimulation duration, and more spontaneous activity were recorded in the rostral-lateral IC compared to the caudal-medial IC, regardless of subregions. In assessing the responses in the outer cortices, we discovered that there were two populations that are likely linked to the two separate

123

subregions in the ICO: the ICD and the ICX. Across the whole IC, the ICD had the slowest, least precise responses and the ICX had the fastest, most precise responses. The responses were even faster than what was found in the ICC. We believe the different responses reflect the different functions of the subregions. The slow responses in the ICD allow for coordinated reception of ascending auditory information and descending control signals to be integrated to modulate the ICC perhaps for auditory attention and learning. The fast responses in the ICX allow for sound localization and head orientation to be coordinated with perception for timely interaction with the surrounding environment. Guided by the known incoming and outgoing projections of these regions and supported by the responses found, we concluded that the ICD would better serve in our treatment. Additionally, we could use the full, detailed three-dimensional reconstruction to aid in electrode placement in the ICC and the ICD in subsequent studies.

In Chapter 3 we delved into that proposed modulation function of the ICD by evaluating the effects of ICD stimulation on ICC neural activity. We were initially interested in location effects (i.e. locations in the ICC that could be modulated and locations in the ICD that induced the largest amount of modulation). We assessed ICC location effects by stimulating from a single ICD electrode array placement and recording from multiple ICC electrode array placements. Conversely, we assessed ICD location effects by stimulating from multiple ICD electrode array placements and recording from a single ICC electrode array placement. The secondary focus of these experiments was to evaluate a limited number of stimulation paradigms. We discovered that ICD stimulation induced both suppressive and facilitatory changes in the ICC, but that overall more

suppression can be elicited than facilitation. In evaluating the stimulation paradigms, we found that paired acoustic and electrical stimulation with an inter-stimulus delay of 18 ms provided the greatest suppression, and thus used those results to determine our location effects. Our location results revealed no trend in the ICC, but a clear trend in the ICD. Regardless of the location in the ICC, suppressive and facilitatory changes were found at each ICC electrode placement. For the ICD, the greatest amount of suppression was induced by stimulation of the rostral-medial portions of the ICD.

Armed with an optimal stimulation location, the aims of the study in Chapter 4 were to further investigate the effects of different stimulation paradigms, assess how long modulation lasts, and evaluate any effects on synchrony. For these studies we used eight stimulation paradigms, one electrical stimulation only, and seven paired acoustic and electrical stimulation with varying delays. As best possible we aimed for placement of the stimulation electrode array in the rostral-medial region of the ICD in each experiment. Later histological results confirmed we were more medial, but still within the optimal stimulation region of the ICD. For every stimulation paradigm tested, there was more suppression of acoustic-driven activity than facilitation, but little change in synchrony. We uncovered two paradigms that gave us significant suppression of acoustic-driven activity compared to facilitation and significant suppression of acoustic-driven activity compared to the control of no stimulation: paired acoustic and electrical stimulation with an inter-stimulus delay of 18 ms and electrical stimulation alone. The effects from these paradigms were not immediate but rather were significant thirty minutes after stimulation presentation.

125

Summarizing across all the studies, we identified the functional attributes of the ICD that suggest its purpose is for modulation and showed that indeed by activating the ICD we can suppressed and facilitate activity in the ICC. We determined optimal stimulation locations in the ICD for inducing suppression and stimulation paradigms to use that elicit suppression lasting up to thirty minutes. Guided by these results, we are able to move into translational human studies.

CLINICAL RELEVANCE AND FUTURE STUDIES

Overall our goal for this thesis was to show that modulation by the ICD was possible and provide substantial evidence for translating this tinnitus treatment into humans. The results of the initial ICD modulation study (see Chapter 3) were enough to enact a hardware change in the AMI. A single stimulation site was moved closer to the Dacron mesh to ensure stimulation in the outer cortices of the IC (Lim and Lenarz, 2015). The next step is to test this treatment in our human patients. By transitioning directly in patients, we have the ability to quickly assess the effectiveness of the treatment and make changes as necessary. In our animal studies we only tested a single biphasic pulse at a rate of 2 Hz, but in our patients we can quickly scan through different pulse sequences to determine the best fit for each patient. For each patient, we will need to evaluate the necessary frequency of treatment (i.e., once per day, continuous, etc.). Inherently hearing restoration and tinnitus treatment are at odds. Hearing restoration uses electrical stimulation to facilitate hearing and speech understanding, while tinnitus treatment uses electrical stimulation to decrease a sound percept. The difficulty will be increasing the

right sounds and decreasing the tinnitus sounds. The primary purpose of the AMI will continue to be hearing restoration with tinnitus treatment applied as necessary. In this initial phase, stimulation will be tested in the clinic and programmed into the stimulation algorithm dependent on the results. For the future, we envision a system that can operate in both modes with the ability to switch in the hands of the patients. As each patient has different requirements and tolerances for their tinnitus, each patient should have the power to control their treatment. As an example, a patient may prefer to operate in the tinnitus treatment mode during sleeping hours as a full night of rest may be a greater priority than attention to environmental cues.

Should this treatment prove effective, the next step will be to return to animal models and determine the mechanisms of action in the CAS that lead to good outcomes. We hypothesized that this treatment would modulate tinnitus-related neural activity such that hyperactivity was decreased and neural synchrony was disrupted. In a tinnitus animal model we can assess if these changes indeed occur or if there is other plasticity within the system that we did not anticipate. Second, we hypothesized that the success of this method is based on the ability of the ICD to not only alter ICC neural activity, but that effects would be seen throughout the auditory system due to the widespread projection network extending from the ICC. This hypothesis could be assessed in both normal hearing and tinnitus animal models to better understand connectivity and descending modulation and address effects on tinnitus-related neural activity in other auditory nuclei, respectively. Finally, a third step would be to move to chronic animals to address the

question of necessary treatment frequency and to study the effects of treatment over time to understand the plasticity that can be induced due to ICD stimulation.

REFERENCES

Aazh H, McFerran D, Salvi R, Prasher D, Jastreboff M, Jastreboff P (2014) Insights from the First International Conference on Hyperacusis: causes, evaluation, diagnosis and treatment. Noise & health 16:123-126.

Abbott LF, Nelson SB (2000) Synaptic plasticity: taming the beast. Nat Neurosci 3 Suppl:1178-1183.

Adams JC (1979) Ascending projections to the inferior colliculus. J Comp Neurol 183:519-538.

Adams JS, Hasenstab MS, Pippin GW, Sismanis A (2004) Telephone use and understanding in patients with cochlear implants. Ear Nose Throat J 83:96, 99-100, 102-103.

Aitkin L, Schuck D (1985) Low frequency neurons in the lateral central nucleus of the cat inferior colliculus receive their input predominantly from the medial superior olive. Hear Res 17:87-93.

Aitkin L, Tran L, Syka J (1994) The responses of neurons in subdivisions of the inferior colliculus of cats to tonal, noise and vocal stimuli. Exp Brain Res 98:53-64.

Aitkin LM (1979) The auditory midbrain. Trends in Neurosciences 2:308-310.

Aitkin LM, Boyd J (1978) Acoustic input to the lateral pontine nuclei. Hear Res 1:67-77.

Aitkin LM, Phillips SC (1984a) Is the inferior colliculus an obligatory relay in the cat auditory system? Neurosci Lett 44:259-264.

Aitkin LM, Phillips SC (1984b) The interconnections of the inferior colliculi through their commissure. J Comp Neurol 228:210-216.

Aitkin LM, Kenyon CE, Philpott P (1981) The representation of the auditory and somatosensory systems in the external nucleus of the cat inferior colliculus. J Comp Neurol 196:25-40.

Aitkin LM, Webster WR, Veale JL, Crosby DC (1975) Inferior colliculus. I. Comparison of response properties of neurons in central, pericentral, and external nuclei of adult cat. J Neurophysiol 38:1196-1207.

Aitkin LM, Dickhaus H, Schult W, Zimmermann M (1978) External nucleus of inferior colliculus: auditory and spinal somatosensory afferents and their interactions. J Neurophysiol 41:837-847.

Alibardi L (2000) Cytology of large neurons in the guinea pig dorsal cochlear nucleus contacting the inferior colliculus. Eur J Histochem 44:365-375.

Alkhatib A, Biebel UW, Smolders JW (2006) Inhibitory and excitatory response areas of neurons in the central nucleus of the inferior colliculus in unanesthetized chinchillas. Exp Brain Res 174:124-143.

Astl J, Popelár J, Kvasnák E, Syka J (1996a) Comparison of response properties of neurons in the inferior colliculus of guinea pigs under different anesthetics. Audiology 35:335-345.

Astl J, Popelar J, Kvasnak E, Syka J (1996b) Comparison of response properties of neurons in the inferior colliculus of guinea pigs under different anesthetics. Audiology 35:335-345.

ATA (2013) Understanding the Facts In: American Tinnitus Association

Axelsson A, Ringdahl A (1989) Tinnitus--a study of its prevalence and characteristics. Br J Audiol 23:53-62.

Baguley DM, Atlas MD (2007) Cochlear implants and tinnitus. Prog Brain Res 166:347-355.

Bajo VM, Moore DR (2005) Descending projections from the auditory cortex to the inferior colliculus in the gerbil, Meriones unguiculatus. J Comp Neurol 486:101-116.

Bajo VM, King AJ (2012) Cortical modulation of auditory processing in the midbrain. Front Neural Circuits 6:114.

Bajo VM, Nodal FR, Moore DR, King AJ (2010) The descending corticocollicular pathway mediates learning-induced auditory plasticity. Nat Neurosci 13:253-260.

Bajo VM, Nodal FR, Bizley JK, Moore DR, King AJ (2007) The ferret auditory cortex: descending projections to the inferior colliculus. Cereb Cortex 17:475-491.

Bakin JS, Weinberger NM (1990) Classical conditioning induces CS-specific receptive field plasticity in the auditory cortex of the guinea pig. Brain Res 536:271-286.

Basura GJ, Koehler SD, Wiler JA, Shore SE (2013) Multi-sensory integration in primary auditory cortex is stimulus timing dependent and alters neural synchrony. Assoc Res Otolaryng Abstr 36:462.

Bauer CA, Turner JG, Caspary DM, Myers KS, Brozoski TJ (2008) Tinnitus and inferior colliculus activity in chinchillas related to three distinct patterns of cochlear trauma. Journal of neuroscience research 86:2564-2578.

Behr R, Mueller J, Shehata-Dieler W, Schlake HP, Helms J, Roosen K, Klug N, Hoelper B, Lorens A (2007) The high rate CIS auditory brainstem implant for restoration of hearing in NF-2 patients. Skull Base 17:91-107.

Bi GQ, Poo MM (1998) Synaptic modifications in cultured hippocampal neurons: dependence on spike timing, synaptic strength, and postsynaptic cell type. J Neurosci 18:10464-10472.

Binns KE, Grant S, Withington DJ, Keating MJ (1992) A topographic representation of auditory space in the external nucleus of the inferior colliculus of the guinea-pig. Brain Res 589:231-242.

Bledsoe SC, Koehler S, Tucci DL, Zhou J, Le Prell C, Shore SE (2009) Ventral cochlear nucleus responses to contralateral sound are mediated by commissural and olivocochlear pathways. J Neurophysiol 102:886-900.

Brozoski TJ, Bauer CA (2005) The effect of dorsal cochlear nucleus ablation on tinnitus in rats. Hear Res 206:227-236.

Brozoski TJ, Bauer CA, Caspary DM (2002) Elevated fusiform cell activity in the dorsal cochlear nucleus of chinchillas with psychophysical evidence of tinnitus. J Neurosci 22:2383-2390.

Brunso-Bechtold JK, Thompson GC, Masterton RB (1981) HRP study of the organization of auditory afferents ascending to central nucleus of inferior colliculus in cat. J Comp Neurol 197:705-722.

Caicedo A, Herbert H (1993) Topography of descending projections from the inferior colliculus to auditory brainstem nuclei in the rat. J Comp Neurol 328:377-392.

Calford MB, Aitkin LM (1983) Ascending projections to the medial geniculate body of the cat: evidence for multiple, parallel auditory pathways through thalamus. J Neurosci 3:2365-2380.

Calixto R, Lenarz M, Neuheiser A, Scheper V, Lenarz T, Lim HH (2012) Co-activation of different neurons within an isofrequency lamina of the inferior colliculus elicits enhanced auditory cortical activation. J Neurophysiol.

Cant NB, Benson CG (2006) Organization of the inferior colliculus of the gerbil (Meriones unguiculatus): differences in distribution of projections from the cochlear nuclei and the superior olivary complex. J Comp Neurol 495:511-528.

Caporale N, Dan Y (2008) Spike timing-dependent plasticity: a Hebbian learning rule. Annu Rev Neurosci 31:25-46.

Carlile S, Pettigrew AG (1987) Distribution of frequency sensitivity in the superior colliculus of the guinea pig. Hear Res 31:123-136.

Casseday JH, Fremouw T, Covey E (2002) The inferior colliculus: A hub for the central auditory system. In: Springer Handbook of Auditory Research: Integrative Functions in the Mammalian Auditory Pathway (Vol. 15) (Oertel D, Fay RR, Popper AN, eds), pp 238-318. New York: Springer-Verlag.

Cazals Y, Negrevergne M, Aran JM (1978) Electrical stimulation of the cochlea in man: hearing induction and tinnitus suppression. J Am Audiol Soc 3:209-213.

Chen GD, Jastreboff PJ (1995) Salicylate-induced abnormal activity in the inferior colliculus of rats. Hear Res 82:158-178.

Chen GD, Manohar S, Salvi R (2012) Amygdala hyperactivity and tonotopic shift after salicylate exposure. Brain Res 1485:63-76.

Cheung SW, Larson PS (2010) Tinnitus modulation by deep brain stimulation in locus of caudate neurons (area LC). Neuroscience 169:1768-1778.

Chowdhury SA, Suga N (2000) Reorganization of the frequency map of the auditory cortex evoked by cortical electrical stimulation in the big brown bat. J Neurophysiol 83:1856-1863.

Cima RF, Andersson G, Schmidt CJ, Henry JA (2014) Cognitive-behavioral treatments for tinnitus: a review of the literature. J Am Acad Audiol 25:29-61.

Coleman JR, Clerici WJ (1987) Sources of projections to subdivisions of the inferior colliculus in the rat. J Comp Neurol 262:215-226.

Coles R (2000) Medicolegal Issues. In: Tinnitus Handbook (Tyler R, ed), pp 399-417. San Diego: Singular Publishing.

Colletti V, Shannon RV (2005) Open set speech perception with auditory brainstem implant? Laryngoscope 115:1974-1978.

Colletti V, Shannon R, Carner M, Veronese S, Colletti L (2009a) Outcomes in Nontumor Adults Fitted With the Auditory Brainstem Implant: 10 Years' Experience. Otol Neurotol 30:614-618.

Colletti V, Shannon RV, Carner M, Veronese S, Colletti L (2009b) Progress in restoration of hearing with the auditory brainstem implant. Prog Brain Res 175:333-345.

Dahmen JC, Hartley DE, King AJ (2008) Stimulus-timing-dependent plasticity of cortical frequency representation. J Neurosci 28:13629-13639.

Dan Y, Poo MM (2004) Spike timing-dependent plasticity of neural circuits. Neuron 44:23-30.

Davis PB, Paki B, Hanley PJ (2007) Neuromonics Tinnitus Treatment: third clinical trial. Ear Hear 28:242-259.

Davis PB, Wilde RA, Steed LG, Hanley PJ (2008) Treatment of tinnitus with a customized acoustic neural stimulus: a controlled clinical study. Ear Nose Throat J 87:330-339.

De Martino F, Moerel M, van de Moortele PF, Ugurbil K, Goebel R, Yacoub E, Formisano E (2013) Spatial organization of frequency preference and selectivity in the human inferior colliculus. Nat Commun 4:1386.

De Ridder D, Vanneste S, Engineer ND, Kilgard MP (2014) Safety and efficacy of vagus nerve stimulation paired with tones for the treatment of tinnitus: a case series. Neuromodulation 17:170-179.

De Ridder D, Vanneste S, Kovacs S, Sunaert S, Menovsky T, van de Heyning P, Moller A (2011) Transcranial magnetic stimulation and extradural electrodes implanted on secondary auditory cortex for tinnitus suppression. J Neurosurg 114:903-911.

De Ridder D, De Mulder G, Verstraeten E, Van der Kelen K, Sunaert S, Smits M, Kovacs S, Verlooy J, Van de Heyning P, Moller AR (2006) Primary and secondary auditory cortex stimulation for intractable tinnitus. ORL J Otorhinolaryngol Relat Spec 68:48-54; discussion 54-45.

DeBello WM, Feldman DE, Knudsen EI (2001) Adaptive axonal remodeling in the midbrain auditory space map. J Neurosci 21:3161-3174.

Dehmel S, Pradhan S, Koehler S, Bledsoe S, Shore S (2012) Noise overexposure alters long-term somatosensory-auditory processing in the dorsal cochlear nucleus--possible basis for tinnitus-related hyperactivity? J Neurosci 32:1660-1671.

Edeline JM, Pham P, Weinberger NM (1993) Rapid development of learning-induced receptive field plasticity in the auditory cortex. Behav Neurosci 107:539-551.

Edwards SB, Ginsburgh CL, Henkel CK, Stein BE (1979) Sources of subcortical projections to the superior colliculus in the cat. J Comp Neurol 184:309-329.

Eggermont JJ (2013) Hearing loss, hyperacusis, or tinnitus: what is modeled in animal research? Hear Res 295:140-149.

Eggermont JJ, Kenmochi M (1998) Salicylate and quinine selectively increase spontaneous firing rates in secondary auditory cortex. Hear Res 117:149-160.

Eggermont JJ, Komiya H (2000) Moderate noise trauma in juvenile cats results in profound cortical topographic map changes in adulthood. Hear Res 142:89-101.

Eggermont JJ, Roberts LE (2004) The neuroscience of tinnitus. Trends Neurosci 27:676-682.

Eggermont JJ, Tass PA (2015) Maladaptive neural synchrony in tinnitus: origin and restoration. Front Neurol 6:29.

Egorova M, Ehret G (2008) Tonotopy and inhibition in the midbrain inferior colliculus shape spectral resolution of sounds in neural critical bands. Eur J Neurosci 28:675-692.

Egorova M, Vartanyan I, Ehret G (2006) Frequency response areas of mouse inferior colliculus neurons: II. Critical bands. Neuroreport 17:1783-1786.

Egorova M, Ehret G, Vartanian I, Esser KH (2001) Frequency response areas of neurons in the mouse inferior colliculus. I. Threshold and tuning characteristics. Exp Brain Res 140:145-161.

Ehret G (1997) The auditory midbrain, a "shunting yard" of acoustical information processing. In: The Central Auditory System (Ehret G, Romand R, eds), pp 259-316. New York: Oxford University Press, Inc.

Ehret G, Egorova M, Hage SR, Muller BA (2003) Spatial map of frequency tuning-curve shapes in the mouse inferior colliculus. Neuroreport 14:1365-1369.

Engelhardt J, Dauman R, Arné P, Allard M, Dauman N, Branchard O, Perez P, Germain C, Caire F, Bonnard D, Cuny E (2014) Effect of chronic cortical stimulation on chronic severe tinnitus: a prospective randomized double-blind cross-over trial and long-term follow up. Brain Stimul 7:694-700.

Engineer ND, Percaccio CR, Pandya PK, Moucha R, Rathbun DL, Kilgard MP (2004) Environmental enrichment improves response strength, threshold, selectivity, and latency of auditory cortex neurons. J Neurophysiol 92:73-82.

Engineer ND, Riley JR, Seale JD, Vrana WA, Shetake JA, Sudanagunta SP, Borland MS, Kilgard MP (2011) Reversing pathological neural activity using targeted plasticity. Nature 470:101-104.

Fallon JB, Irvine DR, Shepherd RK (2008) Cochlear implants and brain plasticity. Hear Res 238:110-117.

Fallon JB, Irvine DR, Shepherd RK (2009) Neural prostheses and brain plasticity. J Neural Eng 6:065008.

Faye-Lund H (1985) The neocortical projection to the inferior colliculus in the albino rat. Anat Embryol (Berl) 173:53-70.

Faye-Lund H, Osen KK (1985) Anatomy of the inferior colliculus in rat. Anat Embryol (Berl) 171:1-20.

Feliciano M, Potashner SJ (1995) Evidence for a glutamatergic pathway from the guinea pig auditory cortex to the inferior colliculus. J Neurochem 65:1348-1357.

Friedland DR, Gaggl W, Runge-Samuelson C, Ulmer JL, Kopell BH (2007) Feasibility of auditory cortical stimulation for the treatment of tinnitus. Otol Neurotol 28:1005-1012.

Frisina RD, Walton JP, Lynch-Armour MA, Byrd JD (1998) Inputs to a physiologically characterized region of the inferior colliculus of the young adult CBA mouse. Hear Res 115:61-81.

Fritz J, Elhilali M, Shamma S (2005) Active listening: task-dependent plasticity of spectrotemporal receptive fields in primary auditory cortex. Hear Res 206:159-176.

Gaese BH, Ostwald J (2001) Anesthesia changes frequency tuning of neurons in the rat primary auditory cortex. J Neurophysiol 86:1062-1066.

Galazyuk AV, Wenstrup JJ, Hamid MA (2012) Tinnitus and underlying brain mechanisms. Curr Opin Otolaryngol Head Neck Surg 20:409-415.

Gao E, Suga N (1998) Experience-dependent corticofugal adjustment of midbrain frequency map in bat auditory system. Proc Natl Acad Sci U S A 95:12663-12670.

Gao E, Suga N (2000) Experience-dependent plasticity in the auditory cortex and the inferior colliculus of bats: role of the corticofugal system. Proc Natl Acad Sci U S A 97:8081-8086.

Geniec P, Morest DK (1971) The neuronal architecture of the human posterior colliculus. A study with the Golgi method. Acta Otolaryngol Suppl 295:1-33.

González Hernández TH, Meyer G, Ferres-Torres R (1986) The commissural interconnections of the inferior colliculus in the albino mouse. Brain Res 368:268-276.

González-Hernández T, Mantolán-Sarmiento B, González-González B, Pérez-González H (1996) Sources of GABAergic input to the inferior colliculus of the rat. J Comp Neurol 372:309-326.

Gourevitch B, Doisy T, Avillac M, Edeline JM (2009) Follow-up of latency and threshold shifts of auditory brainstem responses after single and interrupted acoustic trauma in guinea pig. Brain Res 1304:66-79.

Gourévitch B, Doisy T, Avillac M, Edeline JM (2009) Follow-up of latency and threshold shifts of auditory brainstem responses after single and interrupted acoustic trauma in guinea pig. Brain Res 1304:66-79.

Green D, Swets J (1966) Signal Detection Theory and Psychophysics. New York: Wiley.

Gruters KG, Groh JM (2012) Sounds and beyond: multisensory and other non-auditory signals in the inferior colliculus. Front Neural Circuits 6:96.

Gu JW, Halpin CF, Nam EC, Levine RA, Melcher JR (2010) Tinnitus, diminished sound-level tolerance, and elevated auditory activity in humans with clinically normal hearing sensitivity. J Neurophysiol 104:3361-3370.

Hackett TA, Barkat TR, O'Brien BM, Hensch TK, Polley DB (2011) Linking topography to tonotopy in the mouse auditory thalamocortical circuit. J Neurosci 31:2983-2995.

Hage SR, Ehret G (2003) Mapping responses to frequency sweeps and tones in the inferior colliculus of house mice. Eur J Neurosci 18:2301-2312.

Harper L (1976) Behavior. In: The Biology of the Guinea Pig (Wagner J, Manning P, eds), pp 31-51. New York: Academic Press.

Harrison RV (2001) Age-related tonotopic map plasticity in the central auditory pathways. Scand Audiol Suppl:8-14.

Hattori T, Suga N (1997) The inferior colliculus of the mustached bat has the frequency-vs-latency coordinates. J Comp Physiol A 180:271-284.

Heffner R, Heffner H, Masterton B (1971) Behavioral measurements of absolute and frequency-difference thresholds in guinea pig. J Acoust Soc Am 49:1888-1895.

Heller AJ (2003) Classification and epidemiology of tinnitus. Otolaryngol Clin North Am 36:239-248.

Henry JA, Roberts LE, Caspary DM, Theodoroff SM, Salvi RJ (2014) Underlying mechanisms of tinnitus: review and clinical implications. J Am Acad Audiol 25:5-22; quiz 126.

Herbert H, Aschoff A, Ostwald J (1991) Topography of projections from the auditory cortex to the inferior colliculus in the rat. J Comp Neurol 304:103-122.

Hernández O, Rees A, Malmierca MS (2006) A GABAergic component in the commissure of the inferior colliculus in rat. Neuroreport 17:1611-1614.

Hind JE, Goldberg JM, Greenwood DD, Rose JE (1963) Some discharge characteristics of single neurons in the inferior colliculus of the cat. II. Timing of the discharges and observations on binaural stimulation. J Neurophysiol 26:321-341.

Hirsch JA, Chan JC, Yin TC (1985) Responses of neurons in the cat's superior colliculus to acoustic stimuli. I. Monaural and binaural response properties. J Neurophysiol 53:726-745.

Hoddevik GH, Brodal A, Kawamura K, Hashikawa T (1977) The pontine projection to the cerebellar vermal visual area studied by means of the retrograde axonal transport of horseradish peroxidase. Brain Res 123:209-227.

Hoekstra CE, Versnel H, Neggers SF, Niesten ME, van Zanten GA (2013) Bilateral low-frequency repetitive transcranial magnetic stimulation of the auditory cortex in tinnitus patients is not effective: a randomised controlled trial. Audiol Neurootol 18:362-373.

Hoffman HJ, Reed GW (2004) Epidemiology of tinnitus. In: Tinnitus: Theory and management (Snow JB, ed), pp 16-41. Lewiston, NY: BC Decker Inc.

Hofman PM, Van Riswick JG, Van Opstal AJ (1998) Relearning sound localization with new ears. Nat Neurosci 1:417-421.

Huffman RF, Henson OW, Jr. (1990) The descending auditory pathway and acousticomotor systems: connections with the inferior colliculus. Brain Res Brain Res Rev 15:295-323.

Hyde PS, Knudsen EI (2000) Topographic projection from the optic tectum to the auditory space map in the inferior colliculus of the barn owl. J Comp Neurol 421:146-160.

Irvine DR, Rajan R, McDermott HJ (2000) Injury-induced reorganization in adult auditory cortex and its perceptual consequences. Hear Res 147:188-199.

Irvine DR, Rajan R, Smith S (2003) Effects of restricted cochlear lesions in adult cats on the frequency organization of the inferior colliculus. J Comp Neurol 467:354-374.

Irvine DRF (1992) Physiology of the Auditory Brainstem. In: The Mammalian Auditory Pathway: Neurophysiology (Popper AN, Fay RR, eds), pp 153-231. New York: Springer.

Irvine DRF (2010) Plasticity in the auditory pathway. In: The Oxford Handbook of Auditory Science: The Auditory Brain (Rees A, Plamer AR, eds), pp 387-416. New York: Oxford University Press, Inc.

Ito T, Hirose J, Murase K, Ikeda H (2014) Determining auditory-evoked activities from multiple cells in layer 1 of the dorsal cortex of the inferior colliculus of mice by in vivo calcium imaging. Brain Res 1590:45-55.

Izquierdo MA, Gutiérrez-Conde PM, Merchán MA, Malmierca MS (2008) Non-plastic reorganization of frequency coding in the inferior colliculus of the rat following noise-induced hearing loss. Neuroscience 154:355-369.

Jane JA, Masterton RB, Diamond IT (1965) The function of the tectum for attention to auditory stimuli in the cat. J Comp Neurol 125:165-191.

Jen PH, Sun X, Chen QC (2001) An electrophysiological study of neural pathways for corticofugally inhibited neurons in the central nucleus of the inferior colliculus of the big brown bat, Eptesicus fuscus. Exp Brain Res 137:292-302.

Jen PH, Zhou X, Zhang J, Chen QC, Sun X (2002) Brief and short-term corticofugal modulation of acoustic signal processing in the bat midbrain. Hear Res 168:196-207.

Ji W, Suga N (2009) Tone-specific and nonspecific plasticity of inferior colliculus elicited by pseudo-conditioning: role of acetylcholine and auditory and somatosensory cortices. J Neurophysiol 102:941-952.

Ji W, Gao E, Suga N (2001) Effects of acetylcholine and atropine on plasticity of central auditory neurons caused by conditioning in bats. J Neurophysiol 86:211-225.

Johnson MD, Lim HH, Netoff TI, Connolly AT, Johnson N, Roy A, Holt A, Lim KO, Carey JR, Vitek JL, He B (2013) Neuromodulation for brain disorders: challenges and opportunities. IEEE Trans Biomed Eng 60:610-624.

Kaltenbach JA (2006) Summary of evidence pointing to a role of the dorsal cochlear nucleus in the etiology of tinnitus. Acta Otolaryngol Suppl:20-26.

Kaltenbach JA (2011) Tinnitus: Models and mechanisms. Hear Res 276:52-60.

Kaltenbach JA, Afman CE (2000) Hyperactivity in the dorsal cochlear nucleus after intense sound exposure and its resemblance to tone-evoked activity: a physiological model for tinnitus. Hear Res 140:165-172.

Kaltenbach JA, Zhang J, Afman CE (2000) Plasticity of spontaneous neural activity in the dorsal cochlear nucleus after intense sound exposure. Hear Res 147:282-292.

Kaltenbach JA, Zhang J, Finlayson P (2005) Tinnitus as a plastic phenomenon and its possible neural underpinnings in the dorsal cochlear nucleus. Hear Res 206:200-226.

Kamke MR, Brown M, Irvine DR (2003) Plasticity in the tonotopic organization of the medial geniculate body in adult cats following restricted unilateral cochlear lesions. J Comp Neurol 459:355-367.

Kilgard MP, Merzenich MM (1998) Cortical map reorganization enabled by nucleus basalis activity. Science 279:1714-1718.

King AJ, Jiang ZD, Moore DR (1998) Auditory brainstem projections to the ferret superior colliculus: anatomical contribution to the neural coding of sound azimuth. J Comp Neurol 390:342-365.

Kisley MA, Gerstein GL (1999) Trial-to-trial variability and state-dependent modulation of auditory-evoked responses in cortex. J Neurosci 19:10451-10460.

Kleinjung T, Langguth B, Khedr E (2011) Transcranial Magnetic Stimulation. In: Textbook of Tinnitus (Møller AR, Langguth B, De Ridder D, Kleinjung T, eds), pp 697-709. New York: Springer.

Kleinjung T, Steffens T, Strutz J, Langguth B (2009) Curing tinnitus with a Cochlear Implant in a patient with unilateral sudden deafness: a case report. Cases journal 2:7462.

Knudsen EI (2002) Instructed learning in the auditory localization pathway of the barn owl. Nature 417:322-328.

Knudsen EI, Knudsen PF (1983) Space-mapped auditory projections from the inferior colliculus to the optic tectum in the barn owl (Tyto alba). J Comp Neurol 218:187-196.

Knudsen EI, Knudsen PF (1990) Sensitive and critical periods for visual calibration of sound localization by barn owls. J Neurosci 10:222-232.

Koehler SD, Shore SE (2013a) Stimulus timing-dependent plasticity in dorsal cochlear nucleus is altered in tinnitus. J Neurosci 33:19647-19656.

Koehler SD, Shore SE (2013b) Stimulus-timing dependent multisensory plasticity in the guinea pig dorsal cochlear nucleus. PloS one 8:e59828.

Komiya H, Eggermont JJ (2000) Spontaneous firing activity of cortical neurons in adult cats with reorganized tonotopic map following pure-tone trauma. Acta Otolaryngol 120:750-756.

Kraus N, Nicol T (2009) Auditory evoked potentials. In: Encyclopedia of Neuroscience (Binder MD, Hirokawa N, Windhorst U, eds), pp 214-218. Berlin: Springer.

Kumpik DP, Kacelnik O, King AJ (2010) Adaptive reweighting of auditory localization cues in response to chronic unilateral earplugging in humans. J Neurosci 30:4883-4894.

Kuwabara N, Zook JM (2000) Geniculo-collicular descending projections in the gerbil. Brain Res 878:79-87.

Langner G, Schreiner C, Merzenich MM (1987) Covariation of latency and temporal resolution in the inferior colliculus of the cat. Hear Res 31:197-201.

Langner G, Albert M, Briede T (2002) Temporal and spatial coding of periodicity information in the inferior colliculus of awake chinchilla (Chinchilla laniger). Hear Res 168:110-130.

Lanting CP, de Kleine E, van Dijk P (2009) Neural activity underlying tinnitus generation: results from PET and fMRI. Hear Res 255:1-13.

LeBeau FE, Malmierca MS, Rees A (2001) Iontophoresis in vivo demonstrates a key role for GABA(A) and glycinergic inhibition in shaping frequency response areas in the inferior colliculus of guinea pig. J Neurosci 21:7303-7312.

Lee CC, Sherman SM (2010) Drivers and modulators in the central auditory pathways. Front Neurosci 4:79.

Lenarz T, Lim HH, Reuter G, Patrick JF, Lenarz M (2006) The auditory midbrain implant: a new auditory prosthesis for neural deafness-concept and device description. Otol Neurotol 27:838-843.

Leong D, Puil E, Schwarz D (2004) Ketamine blocks non-N-methyl-D-aspartate receptor channels attenuating glutamatergic transmission in the auditory cortex. Acta Otolaryngol 124:454-458.

Lew HL, Jerger JF, Guillory SB, Henry JA (2007) Auditory dysfunction in traumatic brain injury. J Rehabil Res Dev 44:921-928.

Lim HH, Anderson DJ (2006) Auditory cortical responses to electrical stimulation of the inferior colliculus: implications for an auditory midbrain implant. J Neurophysiol 96:975-988.

Lim HH, Anderson DJ (2007a) Antidromic activation reveals tonotopically organized projections from primary auditory cortex to the central nucleus of the inferior colliculus in guinea pig. J Neurophysiol 97:1413-1427.

Lim HH, Anderson DJ (2007b) Spatially distinct functional output regions within the central nucleus of the inferior colliculus: Implications for an auditory midbrain implant. J Neurosci 27:8733-8743.

Lim HH, Shannon RV (2014) Two Laskers and Counting: Learning From the Past Enables Future Innovations With Central Neural Prostheses. Brain Stimul.

Lim HH, Lenarz T (2015) Auditory midbrain implant: research and development towards a second clinical trial. Hear Res 322:212-223.

Lim HH, Lenarz M, Lenarz T (2009a) A new auditory prosthesis using deep brain stimulation: Development and implementation. In: Implantable Neural Prostheses 1: Devices and Applications (Zhou D, Greenbaum E, eds), pp 117-154. New York: Springer Science+Business Media, LLC.

Lim HH, Lenarz M, Lenarz T (2009b) Auditory midbrain implant: a review. Trends Amplif 13:149-180.

Lim HH, Lenarz T, Anderson DJ, Lenarz M (2008a) The auditory midbrain implant: Effects of electrode location. Hear Res 242:74-85.

Lim HH, Lenarz M, Joseph G, Lenarz T (2013) Frequency representation within the human brain: stability versus plasticity. Sci Rep 3:1474.

Lim HH, Lenarz M, Joseph G, Pesch J, Lenarz T (2009c) Electrical stimulation of the human midbrain reveals tonotopy, plasticity, and novelty detection within the central auditory system. Assoc Res Otolaryng Abstr 32:221.

Lim HH, Lenarz T, Joseph G, Battmer RD, Patrick JF, Lenarz M (2008b) Effects of phase duration and pulse rate on loudness and pitch percepts in the first auditory midbrain implant patients: Comparison to cochlear implant and auditory brainstem implant results. Neuroscience 154:370-380.

Lim HH, Lenarz T, Joseph G, Battmer RD, Samii A, Samii M, Patrick JF, Lenarz M (2007) Electrical stimulation of the midbrain for hearing restoration: insight into the functional organization of the human central auditory system. J Neurosci 27:13541-13551.

Lockwood AH, Salvi RJ, Coad ML, Towsley ML, Wack DS, Murphy BW (1998) The functional neuroanatomy of tinnitus: evidence for limbic system links and neural plasticity. Neurology 50:114-120.

Loftus WC, Bishop DC, Oliver DL (2010) Differential patterns of inputs create functional zones in central nucleus of inferior colliculus. J Neurosci 30:13396-13408.

Lumani A, Zhang H (2010) Responses of neurons in the rat's dorsal cortex of the inferior colliculus to monaural tone bursts. Brain Res 1351:115-129.

Ma WL, Hidaka H, May BJ (2006) Spontaneous activity in the inferior colliculus of CBA/J mice after manipulations that induce tinnitus. Hear Res 212:9-21.

Ma X, Suga N (2001) Plasticity of bat's central auditory system evoked by focal electric stimulation of auditory and/or somatosensory cortices. J Neurophysiol 85:1078-1087.

Magee JC, Johnston D (1997) A synaptically controlled, associative signal for Hebbian plasticity in hippocampal neurons. Science 275:209-213.

Malmierca M, Ryugo D (2011) Descending Connections of Auditory Cortex to the Midbrain and Brain Stem. In: The Auditory Cortex (Winer JA, Schreiner CE, eds), pp 189-208: Springer US.

Malmierca MS, Le Beau FE, Rees A (1996) The topographical organization of descending projections from the central nucleus of the inferior colliculus in guinea pig. Hear Res 93:167-180.

Malmierca MS, Hernandez O, Rees A (2005) Intercollicular commissural projections modulate neuronal responses in the inferior colliculus. Eur J Neurosci 21:2701-2710.

Malmierca MS, Rees A, Le Beau FE, Bjaalie JG (1995) Laminar organization of frequency-defined local axons within and between the inferior colliculi of the guinea pig. J Comp Neurol 357:124-144.

Malmierca MS, Blackstad TW, Osen KK, Karagulle T, Molowny RL (1993) The central nucleus of the inferior colliculus in rat: a Golgi and computer reconstruction study of neuronal and laminar structure. J Comp Neurol 333:1-27.

Malmierca MS, Hernandez O, Falconi A, Lopez-Poveda EA, Merchan M, Rees A (2003) The commissure of the inferior colliculus shapes frequency response areas in rat: an in vivo study using reversible blockade with microinjection of kynurenic acid. Exp Brain Res 153:522-529.

Malmierca MS, Izquierdo MA, Cristaudo S, Hernandez O, Perez-Gonzalez D, Covey E, Oliver DL (2008) A discontinuous tonotopic organization in the inferior colliculus of the rat. J Neurosci 28:4767-4776.

Manzoor NF, Gao Y, Licari F, Kaltenbach JA (2013) Comparison and contrast of noise-induced hyperactivity in the dorsal cochlear nucleus and inferior colliculus. Hear Res 295:114-123.

Manzoor NF, Licari FG, Klapchar M, Elkin RL, Gao Y, Chen G, Kaltenbach JA (2012) Noise-induced hyperactivity in the inferior colliculus: its relationship with hyperactivity in the dorsal cochlear nucleus. J Neurophysiol 108:976-988.

Markovitz CD, Tang TT, Lim HH (2013) Tonotopic and localized pathways from primary auditory cortex to the central nucleus of the inferior colliculus. Front Neural Circuits 7:77.

Markovitz CD, Tang TT, Edge DP, Lim HH (2012) Three-dimensional brain reconstruction of in vivo electrode tracks for neuroscience and neural prosthetic applications. Frontiers in Neural Circuits 6.

Markovitz CD, Hogan PS, Wesen KA, Lim HH (2015) Pairing broadband noise with cortical stimulation induces extensive suppression of ascending sensory activity. J Neural Eng 12:026006.

Markram H, Lübke J, Frotscher M, Sakmann B (1997) Regulation of synaptic efficacy by coincidence of postsynaptic APs and EPSPs. Science 275:213-215.

Massopust LC, Ordy JM (1962) Auditory organization of the inferior colliculi in the cat. Exp Neurol 6:465-477.

McGee TJ, Ozdamar O, Kraus N (1983) Auditory middle latency responses in the guinea pig. Am J Otolaryngol 4:116-122.

McIntyre CC, Grill WM (2000) Selective microstimulation of central nervous system neurons. Ann Biomed Eng 28:219-233.

McKay CM, Lim HH, Lenarz T (2013) Temporal processing in the auditory system: insights from cochlear and auditory midbrain implantees. J Assoc Res Otolaryngol 14:103-124.

McLachlan N, Wilson S (2010) The central role of recognition in auditory perception: a neurobiological model. Psychol Rev 117:175-196.

Meininger V, Pol D, Derer P (1986) The inferior colliculus of the mouse. A Nissl and Golgi study. Neuroscience 17:1159-1179.

Melcher JR, Levine RA, Bergevin C, Norris B (2009) The auditory midbrain of people with tinnitus: abnormal sound-evoked activity revisited. Hear Res 257:63-74.

Merzenich MM, Reid MD (1974) Representation of the cochlea within the inferior colliculus of the cat. Brain Res 77:397-415.

Mitani A, Shimokouchi M, Nomura S (1983) Effects of stimulation of the primary auditory cortex upon colliculogeniculate neurons in the inferior colliculus of the cat. Neurosci Lett 42:185-189.

Moffat G, Adjout K, Gallego S, Thai-Van H, Collet L, Noreña AJ (2009) Effects of hearing aid fitting on the perceptual characteristics of tinnitus. Hear Res 254:82-91.

Moore DR, Kotak VC, Sanes DH (1998) Commissural and lemniscal synaptic input to the gerbil inferior colliculus. J Neurophysiol 80:2229-2236.

Morest DK, Oliver DL (1984) The neuronal architecture of the inferior colliculus in the cat: defining the functional anatomy of the auditory midbrain. J Comp Neurol 222:209-236.

Muhlnickel W, Elbert T, Taub E, Flor H (1998) Reorganization of auditory cortex in tinnitus. Proc Natl Acad Sci U S A 95:10340-10343.

Mulders WH, Barry KM, Robertson D (2014) Effects of furosemide on cochlear neural activity, central hyperactivity and behavioural tinnitus after cochlear trauma in guinea pig. PLoS One 9:e97948.

Møller AG (2011a) Pathology of the Auditory System that Can Cause Tinnitus. In: Textbook on Tinnitus (Møller A, Langguth B, De Ridder D, Kleinjung J, eds), pp 77-93. New York: Springer.

Møller AR (1984) Pathophysiology of tinnitus. Ann Otol Rhinol Laryngol 93:39-44.

Møller AR, Langguth, B., DeRidder, D., Kleinjung, T. (Eds.) (2011b) Textbook of tinnitus. In. New York: Springer Science+Business Media, LLC.

Nakamoto KT, Jones SJ, Palmer AR (2008) Descending projections from auditory cortex modulate sensitivity in the midbrain to cues for spatial position. J Neurophysiol 99:2347-2356.

Nakamoto KT, Mellott JG, Killius J, Storey-Workley ME, Sowick CS, Schofield BR (2013) Analysis of excitatory synapses in the guinea pig inferior colliculus: a study using electron microscopy and GABA immunocytochemistry. Neuroscience 237:170-183.

Nicolas-Puel C, Faulconbridge RL, Guitton M, Puel JL, Mondain M, Uziel A (2002) Characteristics of tinnitus and etiology of associated hearing loss: a study of 123 patients. Int Tinnitus J 8:37-44.

Nodal FR, Bajo VM, King AJ (2012) Plasticity of spatial hearing: behavioural effects of cortical inactivation. J Physiol 590:3965-3986.

Noreña AJ (2011) An integrative model of tinnitus based on a central gain controlling neural sensitivity. Neurosci Biobehav Rev 35:1089-1109.

Noreña AJ, Eggermont JJ (2003) Changes in spontaneous neural activity immediately after an acoustic trauma: implications for neural correlates of tinnitus. Hear Res 183:137-153.

.

Noreña AJ, Gourévitch B, Gourevich B, Aizawa N, Eggermont JJ (2006) Spectrally enhanced acoustic environment disrupts frequency representation in cat auditory cortex. Nat Neurosci 9:932-939.

O'Neill WE, Frisina RD, Gooler DM (1989) Functional organization of mustached bat inferior colliculus: I. Representation of FM frequency bands important for target ranging revealed by 14C-2-deoxyglucose autoradiography and single unit mapping. J Comp Neurol 284:60-84.

Offutt SJ, Ryan KJ, Konop AE, Lim HH (2014) Suppression and facilitation of auditory neurons through coordinated acoustic and midbrain stimulation: investigating a deep brain stimulator for tinnitus. J Neural Eng 11:066001.

Oliver DL (1984) Dorsal cochlear nucleus projections to the inferior colliculus in the cat: a light and electron microscopic study. J Comp Neurol 224:155-172.

Oliver DL (2005) Neuronal organization in the inferior colliculus. In: The Inferior Colliculus (Winer JA, Schreiner CE, eds), pp 69-114. New York: Springer Science+Business Media, Inc.

Oliver DL, Morest DK (1984) The central nucleus of the inferior colliculus in the cat. J Comp Neurol 222:237-264.

Oliver DL, Beckius GE, Shneiderman A (1995) Axonal projections from the lateral and medial superior olive to the inferior colliculus of the cat: a study using electron microscopic autoradiography. J Comp Neurol 360:17-32.

Oliver DL, Kuwada S, Yin TC, Haberly LB, Henkel CK (1991) Dendritic and axonal morphology of HRP-injected neurons in the inferior colliculus of the cat. J Comp Neurol 303:75-100.

Ortman JM, Velkott VA, Hogan H (2014) An aging nation: the older population in the United States. In: US Census Bureau, pp 25-1140. Washington DC.

Osaki Y, Nishimura H, Takasawa M, Imaizumi M, Kawashima T, Iwaki T, Oku N, Hashikawa K, Doi K, Nishimura T, Hatazawa J, Kubo T (2005) Neural mechanism of residual inhibition of tinnitus in cochlear implant users. Neuroreport 16:1625-1628.

Otto SR, Brackmann DE, Hitselberger WE, Shannon RV, Kuchta J (2002) Multichannel auditory brainstem implant: update on performance in 61 patients. J Neurosurg 96:1063-1071.

Ozdamar O, Kraus N (1983) Auditory middle-latency responses in humans. Audiology 22:34-49.

Palmer AR, Shackleton TM, Sumner CJ, Zobay O, Rees A (2013) Classification of frequency response areas in the inferior colliculus reveals continua not discrete classes. J Physiol 591:4003-4025.

Passchier-Vermeer W, Passchier WF (2000) Noise exposure and public health. Environ Health Perspect 108 Suppl 1:123-131.

Piccirillo JF, Kallogjeri D, Nicklaus J, Wineland A, Spitznagel EL, Vlassenko AG, Benzinger T, Mathews J, Garcia KS (2013) Low-frequency repetitive transcranial magnetic stimulation to the temporoparietal junction for tinnitus: four-week stimulation trial. JAMA Otolaryngol Head Neck Surg 139:388-395.

Pienkowski M, Eggermont JJ (2009) Long-term, partially-reversible reorganization of frequency tuning in mature cat primary auditory cortex can be induced by passive exposure to moderate-level sounds. Hear Res 257:24-40.

Pienkowski M, Eggermont JJ (2010a) Intermittent exposure with moderate-level sound impairs central auditory function of mature animals without concomitant hearing loss. Hear Res 261:30-35.

Pienkowski M, Eggermont JJ (2010b) Passive exposure of adult cats to moderate-level tone pip ensembles differentially decreases AI and AII responsiveness in the exposure frequency range. Hear Res 268:151-162.

Pienkowski M, Eggermont JJ (2011) Cortical tonotopic map plasticity and behavior. Neurosci Biobehav Rev 35:2117-2128.

Pienkowski M, Munguia R, Eggermont JJ (2011) Passive exposure of adult cats to bandlimited tone pip ensembles or noise leads to long-term response suppression in auditory cortex. Hear Res 277:117-126.

Popelár J, Syka J, Berndt H (1987) Effect of noise on auditory evoked responses in awake guinea pigs. Hear Res 26:239-247.

Portfors CV, Sinex DG (2005) Coding of Communication Sounds in the Inferior Colliculus. In: The Inferior Colliculus (Winer JA, Schreiner CE, eds), pp 411-425. New York: Springer Science+Business Media, Inc.

Portfors CV, Mayko ZM, Jonson K, Cha GF, Roberts PD (2011) Spatial organization of receptive fields in the auditory midbrain of awake mouse. Neuroscience 193:429-439.

Portmann M, Cazals Y, Negrevergne M, Aran JM (1979) Temporary tinnitus suppression in man through electrical stimulation of the cochlea. Acta Otolaryngol 87:294-299.

Prosen CA, Petersen MR, Moody DB, Stebbins WC (1978) Auditory thresholds and kanamycin-induced hearing loss in the guinea pig assessed by a positive reinforcement procedure. J Acoust Soc Am 63:559-566.

Punte AK, De Ridder D, Van de Heyning P (2013) On the necessity of full length electrical cochlear stimulation to suppress severe tinnitus in single-sided deafness. Hear Res 295:24-29.

Pérez-González D, Malmierca MS, Covey E (2005) Novelty detector neurons in the mammalian auditory midbrain. Eur J Neurosci 22:2879-2885.

Pérez-González D, Malmierca MS, Moore JM, Hernández O, Covey E (2006) Duration selective neurons in the inferior colliculus of the rat: topographic distribution and relation of duration sensitivity to other response properties. J Neurophysiol 95:823-836.

Qiu C, Salvi R, Ding D, Burkard R (2000) Inner hair cell loss leads to enhanced response amplitudes in auditory cortex of unanesthetized chinchillas: evidence for increased system gain. Hear Res 139:153-171.

Quaranta N, Fernandez-Vega S, D'elia C, Filipo R, Quaranta A (2008) The effect of unilateral multichannel cochlear implant on bilaterally perceived tinnitus. Acta Otolaryngol 128:159-163.

Rajan R, Irvine DR (1998) Absence of plasticity of the frequency map in dorsal cochlear nucleus of adult cats after unilateral partial cochlear lesions. J Comp Neurol 399:35-46.

Rajan R, Irvine DR, Wise LZ, Heil P (1993) Effect of unilateral partial cochlear lesions in adult cats on the representation of lesioned and unlesioned cochleas in primary auditory cortex. J Comp Neurol 338:17-49.

Ramachandran R, Davis KA, May BJ (1999) Single-unit responses in the inferior colliculus of decerebrate cats. I. Classification based on frequency response maps. J Neurophysiol 82:152-163.

Ranck JB, Jr. (1975) Which elements are excited in electrical stimulation of mammalian central nervous system: a review. Brain Res 98:417-440.

Rauschecker JP (1998) Cortical control of the thalamus: top-down processing and plasticity. Nat Neurosci 1:179-180.

Ress D, Chandrasekaran B (2013) Tonotopic organization in the depth of human inferior colliculus. Front Hum Neurosci 7:586.

Roberts LE, Bosnyak DJ (2011) Auditory Training in Tinnitus. In: Textbook of Tinnitus (Møller AR, B, De Ridder D, Kleinjung T, eds), pp 563-573. New York: Springer.

Roberts LE, Eggermont JJ, Caspary DM, Shore SE, Melcher JR, Kaltenbach JA (2010) Ringing ears: the neuroscience of tinnitus. J Neurosci 30:14972-14979.

Robertson D, Irvine DR (1989) Plasticity of frequency organization in auditory cortex of guinea pigs with partial unilateral deafness. J Comp Neurol 282:456-471.

Rockel AJ, Jones EG (1973) The neuronal organization of the inferior colliculus of the adult cat. I. The central nucleus. J Comp Neurol 147:11-60.

Rode T, Hartmann T, Hubka P, Scheper V, Lenarz M, Lenarz T, Kral A, Lim HH (2013) Neural representation in the auditory midbrain of the envelope of vocalizations based on a peripheral ear model. Front Neural Circuits 7:166.

Ropp TJ, Tiedemann KL, Young ED, May BJ (2014) Effects of unilateral acoustic trauma on tinnitus-related spontaneous activity in the inferior colliculus. J Assoc Res Otolaryngol 15:1007-1022.

Roth GL, Aitkin LM, Andersen RA, Merzenich MM (1978) Some features of the spatial organization of the central nucleus of the inferior colliculus of the cat. J Comp Neurol 182:661-680.

Rubinstein JT, Tyler RS, Johnson A, Brown CJ (2003) Electrical suppression of tinnitus with high-rate pulse trains. Otol Neurotol 24:478-485.

Ruxton GD (2006a) The unequal variance t-test is an underused alternative to the Student's t-test and the Mann-Whitney U test. Behav Ecol 17:688-690.

Ruxton GD (2006b) The unequal variance t-test is an underused alternative to Student's t-test and the Mann--Whitney U test. Behavioral Ecology 17:688-690.

Saint Marie RL (1996) Glutamatergic connections of the auditory midbrain: selective uptake and axonal transport of D-[3H]aspartate. J Comp Neurol 373:255-270.

Saint Marie RL, Baker RA (1990) Neurotransmitter-specific uptake and retrograde transport of [3H]glycine from the inferior colliculus by ipsilateral projections of the superior olivary complex and nuclei of the lateral lemniscus. Brain Res 524:244-253.

Sakai M, Suga N (2001) Plasticity of the cochleotopic (frequency) map in specialized and nonspecialized auditory cortices. Proc Natl Acad Sci U S A 98:3507-3512.

Sakai M, Suga N (2002) Centripetal and centrifugal reorganizations of frequency map of auditory cortex in gerbils. Proc Natl Acad Sci U S A 99:7108-7112.

Salami M, Fathollahi Y, Esteky H, Motamedi F, Atapour N (2000) Effects of ketamine on synaptic transmission and long-term potentiation in layer II/III of rat visual cortex in vitro. Eur J Pharmacol 390:287-293.

Saldana E, Merchan MA (2005) Intrinsic and commissural connections of the inferior colliculus. In: The Inferior Colliculus (Winer JA, Schreiner CE, eds), pp 155-181. New York: Springer Science+Business Media, Inc.

Saldana E, Feliciano M, Mugnaini E (1996) Distribution of descending projections from primary auditory neocortex to inferior colliculus mimics the topography of intracollicular projections. J Comp Neurol 371:15-40.

Saldaña E, Merchán MA (1992) Intrinsic and commissural connections of the rat inferior colliculus. J Comp Neurol 319:417-437.

Samii A, Lenarz M, Majdani O, Lim HH, Samii M, Lenarz T (2007) Auditory midbrain implant: a combined approach for vestibular schwannoma surgery and device implantation. Otol Neurotol 28:31-38.

Schaette R, Kempter R (2006) Development of tinnitus-related neuronal hyperactivity through homeostatic plasticity after hearing loss: a computational model. Eur J Neurosci 23:3124-3138.

Schofield BR (2001) Origins of projections from the inferior colliculus to the cochlear nucleus in guinea pigs. J Comp Neurol 429:206-220.

Schofield BR, Cant NB (1996) Projections from the ventral cochlear nucleus to the inferior colliculus and the contralateral cochlear nucleus in guinea pigs. Hear Res 102:1-14.

Schofield BR, Cant NB (1997) Ventral nucleus of the lateral lemniscus in guinea pigs: cytoarchitecture and inputs from the cochlear nucleus. J Comp Neurol 379:363-385.

Schofield BR, Cant NB (1999) Descending auditory pathways: projections from the inferior colliculus contact superior olivary cells that project bilaterally to the cochlear nuclei. J Comp Neurol 409:210-223.

Schreiner CE, Langner G (1988) Periodicity coding in the inferior colliculus of the cat. II. Topographical organization. J Neurophysiol 60:1823-1840.

Schreiner CE, Langner G (1997) Laminar fine structure of frequency organization in auditory midbrain. Nature 388:383-386.

Schwartz MS, Otto SR, Shannon RV, Hitselberger WE, Brackmann DE (2008) Auditory brainstem implants. Neurotherapeutics 5:128-136.

Seitz A, Watanabe T (2005) A unified model for perceptual learning. Trends Cogn Sci 9:329-334.

Seki S, Eggermont JJ (2003) Changes in spontaneous firing rate and neural synchrony in cat primary auditory cortex after localized tone-induced hearing loss. Hear Res 180:28-38.

Semple MN, Aitkin LM (1979) Representation of sound frequency and laterality by units in central nucleus of cat inferior colliculus. J Neurophysiol 42:1626-1639.

Shannon RV, Zeng FG, Kamath V, Wygonski J, Ekelid M (1995) Speech recognition with primarily temporal cues. Science 270:303-304.

Shekhawat GS, Stinear CM, Searchfield GD (2015) Modulation of Perception or Emotion? A Scoping Review of Tinnitus Neuromodulation Using Transcranial Direct Current Stimulation. Neurorehabil Neural Repair.

Shneiderman A, Oliver DL, Henkel CK (1988) Connections of the dorsal nucleus of the lateral lemniscus: an inhibitory parallel pathway in the ascending auditory system? J Comp Neurol 276:188-208.

Sindhusake D, Mitchell P, Newall P, Golding M, Rochtchina E, Rubin G (2003) Prevalence and characteristics of tinnitus in older adults: the Blue Mountains Hearing Study. Int J Audiol 42:289-294.

Sindhusake D, Golding M, Wigney D, Newall P, Jakobsen K, Mitchell P (2004) Factors predicting severity of tinnitus: a population-based assessment. J Am Acad Audiol 15:269-280.

Skinner P, Glattke TJ (1977) Electrophysiologic response audiometry: state of the art. J Speech Hear Disord 42:179-198.

Smith AL, Parsons CH, Lanyon RG, Bizley JK, Akerman CJ, Baker GE, Dempster AC, Thompson ID, King AJ (2004) An investigation of the role of auditory cortex in sound localization using muscimol-releasing Elvax. Eur J Neurosci 19:3059-3072.

Smith PH (1992) Anatomy and physiology of multipolar cells in the rat inferior collicular cortex using the in vitro brain slice technique. J Neurosci 12:3700-3715.

Snyder RL, Bierer JA, Middlebrooks JC (2004) Topographic spread of inferior colliculus activation in response to acoustic and intracochlear electric stimulation. J Assoc Res Otolaryngol 5:305-322.

Snyder RL, Bonham BH, Sinex DG (2008) Acute changes in frequency responses of inferior colliculus central nucleus (ICC) neurons following progressively enlarged restricted spiral ganglion lesions. Hear Res 246:59-78.

Snyder RL, Sinex DG, McGee JD, Walsh EW (2000) Acute spiral ganglion lesions change the tuning and tonotopic organization of cat inferior colliculus neurons. Hear Res 147:200-220.

Song JJ, Vanneste S, Van de Heyning P, De Ridder D (2012) Transcranial direct current stimulation in tinnitus patients: a systemic review and meta-analysis. TheScientificWorldJournal 2012:427941.

Soussi T, Otto SR (1994) Effects of electrical brainstem stimulation on tinnitus. Acta Otolaryngol 114:135-140.

Stanton SG, Harrison RV (1996) Abnormal cochleotopic organization in the auditory cortex of cats reared in a frequency augmented environment. Auditory Neuroscience 2:97-108.

Starr A, Hamilton AE (1976) Correlation between confirmed sites of neurological lesions and abnormalities of far-field auditory brainstem responses. Electroencephalogr Clin Neurophysiol 41:595-608.

Stiebler I (1986) Tone-threshold mapping in the inferior colliculus of the house mouse. Neurosci Lett 65:336-340.

Straka M, Schendel D, Lim HH (2013) Neural integration and enhancement from the inferior colliculus up to different layers of auditory cortex. J Neurophysiol.
.
Straka MM, McMahon M, Markovitz CD, Lim HH (2014) Effects of location and timing of co-activated neurons in the auditory midbrain on cortical activity: implications for a new central auditory prosthesis. J Neural Eng 11:046021.

Suga N (2008) Role of corticofugal feedback in hearing. J Comp Physiol A Neuroethol Sens Neural Behav Physiol 194:169-183.

Suga N (2012) Tuning shifts of the auditory system by corticocortical and corticofugal projections and conditioning. Neurosci Biobehav Rev 36:969-988.

Suga N, Ma X (2003) Multiparametric corticofugal modulation and plasticity in the auditory system. Nat Rev Neurosci 4:783-794.

Sun XD, Jen PH, Sun DX, Zhang SF (1989) Corticofugal influences on the responses of bat inferior collicular neurons to sound stimulation. Brain Res 495:1-8.

Syka J, Straschill M (1970) Activation of superior colliculus neurons and motor responses after electrical stimulation of the inferior colliculus. Exp Neurol 28:384-392.

Syka J, Popelar J (1984) Inferior colliculus in the rat: neuronal responses to stimulation of the auditory cortex. Neurosci Lett 51:235-240.

Syka J, Suta D, Popelar J (2005) Responses to species-specific vocalizations in the auditory cortex of awake and anesthetized guinea pigs. Hear Res 206:177-184.

Syka J, Popelar J, Kvasnak E, Astl J (2000) Response properties of neurons in the central nucleus and external and dorsal cortices of the inferior colliculus in guinea pig. Exp Brain Res 133:254-266.

Tan X, Wang X, Yang W, Xiao Z (2008) First spike latency and spike count as functions of tone amplitude and frequency in the inferior colliculus of mice. Hear Res 235:90-104.

Ter-Mikaelian M, Sanes DH, Semple MN (2007) Transformation of temporal properties between auditory midbrain and cortex in the awake Mongolian gerbil. J Neurosci 27:6091-6102.

Theodoroff SM, Lewis MS, Folmer RL, Henry JA, Carlson KF (2015) Hearing impairment and tinnitus: prevalence, risk factors, and outcomes in US service members and veterans deployed to the Iraq and Afghanistan wars. Epidemiol Rev 37:71-85.

Thompson AM (2005) Descending Connections of the Auditory Midbrain. In: The Inferior Colliculus (Winer JA, Schreiner CE, eds), pp 182-199. New York: Springer Science+Business Media, Inc.

Torterolo P, Zurita P, Pedemonte M, Velluti RA (1998) Auditory cortical efferent actions upon inferior colliculus unitary activity in the guinea pig. Neurosci Lett 249:172-176.

Trotter MI, Donaldson I (2008) Hearing aids and tinnitus therapy: a 25-year experience. J Laryngol Otol 122:1052-1056.

Tzounopoulos T, Kim Y, Oertel D, Trussell LO (2004) Cell-specific, spike timing-dependent plasticities in the dorsal cochlear nucleus. Nat Neurosci 7:719-725.

Van de Heyning P, Vermeire K, Diebl M, Nopp P, Anderson I, De Ridder D (2008) Incapacitating unilateral tinnitus in single-sided deafness treated by cochlear implantation. Ann Otol Rhinol Laryngol 117:645-652.

Vanneste S, De Ridder D (2012) Noninvasive and invasive neuromodulation for the treatment of tinnitus: an overview. Neuromodulation : journal of the International Neuromodulation Society 15:350-360.

Vogler DP, Robertson D, Mulders WH (2011) Hyperactivity in the ventral cochlear nucleus after cochlear trauma. J Neurosci 31:6639-6645.

Vogler DP, Robertson D, Mulders WH (2014) Hyperactivity following unilateral hearing loss in characterized cells in the inferior colliculus. Neuroscience.

Wada SI, Starr A (1983) Generation of auditory brain stem responses (ABRs). III. Effects of lesions of the superior olive, lateral lemniscus and inferior colliculus on the ABR in guinea pig. Electroencephalogr Clin Neurophysiol 56:352-366.

Wang H, Brozoski TJ, Caspary DM (2011) Inhibitory neurotransmission in animal models of tinnitus: maladaptive plasticity. Hear Res 279:111-117.

Wang J, Salvi RJ, Powers N (1996) Plasticity of response properties of inferior colliculus neurons following acute cochlear damage. J Neurophysiol 75:171-183.

Wang J, Ding D, Salvi RJ (2002) Functional reorganization in chinchilla inferior colliculus associated with chronic and acute cochlear damage. Hear Res 168:238-249.

Weinberger NM (2008) Cortical plasticity in associative learning and memory. In: Learning and Memory: A Comprehensive Reference (Eichenbaum H, Byrne J, eds), pp 187-218. New York: Academic Press.

Weinberger NM, Javid R, Lepan B (1993) Long-term retention of learning-induced receptive-field plasticity in the auditory cortex. Proc Natl Acad Sci U S A 90:2394-2398.

Wenstrup JJ, Ross LS, Pollak GD (1985) A functional organization of binaural responses in the inferior colliculus. Hear Res 17:191-195.

Wienbruch C, Paul I, Weisz N, Elbert T, Roberts LE (2006) Frequency organization of the 40-Hz auditory steady-state response in normal hearing and in tinnitus. Neuroimage 33:180-194.

Willard FH, Martin GF (1983) The auditory brainstem nuclei and some of their projections to the inferior colliculus in the North American opossum. Neuroscience 10:1203-1232.

Willott JF, Urban GP (1978) Response properties of neurons in nuclei of the mouse inferior colliculus. Journal of Comparative Physiology A 127:175-184.

Willott JF, Lu SM (1982) Noise-induced hearing loss can alter neural coding and increase excitability in the central nervous system. Science 216:1331-1334.

Willott JF, Aitkin LM, McFadden SL (1993) Plasticity of auditory cortex associated with sensorineural hearing loss in adult C57BL/6J mice. J Comp Neurol 329:402-411.

Winer JA (2005) Three systems of descending projections to the inferior colliculus. In: The Inferior Colliculus (Winer JA, Schreiner CE, eds), pp 231-247. New York: Springer Science+Business Media, Inc.

Winer JA, Schreiner CE, eds (2005) The Inferior Colliculus. New York: Springer Science+Business Media, Inc.

Winer JA, Larue DT, Diehl JJ, Hefti BJ (1998) Auditory cortical projections to the cat inferior colliculus. J Comp Neurol 400:147-174.

Winer JA, Chernock ML, Larue DT, Cheung SW (2002) Descending projections to the inferior colliculus from the posterior thalamus and the auditory cortex in rat, cat, and monkey. Hear Res 168:181-195.

Wise LZ, Irvine DR (1983) Auditory response properties of neurons in deep layers of cat superior colliculus. J Neurophysiol 49:674-685.

Wu Y, Yan J (2007) Modulation of the receptive fields of midbrain neurons elicited by thalamic electrical stimulation through corticofugal feedback. J Neurosci 27:10651-10658.

Xiong Y, Zhang Y, Yan J (2009) The neurobiology of sound-specific auditory plasticity: a core neural circuit. Neuroscience and biobehavioral reviews 33:1178-1184.

Yan J, Suga N (1999) Corticofugal amplification of facilitative auditory responses of subcortical combination-sensitive neurons in the mustached bat. J Neurophysiol 81:817-824.

Yan J, Ehret G (2002) Corticofugal modulation of midbrain sound processing in the house mouse. Eur J Neurosci 16:119-128.

Yan J, Zhang Y, Ehret G (2005) Corticofugal shaping of frequency tuning curves in the central nucleus of the inferior colliculus of mice. J Neurophysiol 93:71-83.

Yan W, Suga N (1998) Corticofugal modulation of the midbrain frequency map in the bat auditory system. Nat Neurosci 1:54-58.

Yao H, Dan Y (2001) Stimulus timing-dependent plasticity in cortical processing of orientation. Neuron 32:315-323.

Zeng FG, Tang Q, Dimitrijevic A, Starr A, Larky J, Blevins NH (2011) Tinnitus suppression by low-rate electric stimulation and its electrophysiological mechanisms. Hear Res 277:61-66.

Zhang JS, Kaltenbach JA (1998) Increases in spontaneous activity in the dorsal cochlear nucleus of the rat following exposure to high-intensity sound. Neurosci Lett 250:197-200.

Zhang JS, Kaltenbach JA, Wang J, Kim SA (2003) Fos-like immunoreactivity in auditory and nonauditory brain structures of hamsters previously exposed to intense sound. Exp Brain Res 153:655-660.

Zhang LI, Bao S, Merzenich MM (2001) Persistent and specific influences of early acoustic environments on primary auditory cortex. Nat Neurosci 4:1123-1130.

Zhang LI, Tao HW, Holt CE, Harris WA, Poo M (1998) A critical window for cooperation and competition among developing retinotectal synapses. Nature 395:37-44.

Zhang Y, Suga N (1997) Corticofugal amplification of subcortical responses to single tone stimuli in the mustached bat. J Neurophysiol 78:3489-3492.

Zhang Y, Suga N (2000) Modulation of responses and frequency tuning of thalamic and collicular neurons by cortical activation in mustached bats. J Neurophysiol 84:325-333.

Zhang Y, Suga N (2005) Corticofugal feedback for collicular plasticity evoked by electric stimulation of the inferior colliculus. J Neurophysiol 94:2676-2682.

Zhang Y, Suga N, Yan J (1997) Corticofugal modulation of frequency processing in bat auditory system. Nature 387:900-903.

Zhang Y, Hakes JJ, Bonfield SP, Yan J (2005) Corticofugal feedback for auditory midbrain plasticity elicited by tones and electrical stimulation of basal forebrain in mice. Eur J Neurosci 22:871-879.

Zhou X, Jen PH (2000) Brief and short-term corticofugal modulation of subcortical auditory responses in the big brown bat, Eptesicus fuscus. J Neurophysiol 84:3083-3087.

Zurita P, Villa AE, de Ribaupierre Y, de Ribaupierre F, Rouiller EM (1994) Changes of single unit activity in the cat's auditory thalamus and cortex associated to different anesthetic conditions. Neurosci Res 19:303-316.

APPENDIX I: CHRONIC PROTOCOL AND EAR PLUG INDUCED AUDITORY PLASTICITY

Tonotopic plasticity exists throughout the adult auditory system as a result of cochlear trauma, behavioral conditioning, passive exposure, and direct electrical stimulation. Long lasting reorganization has been seen in the A1, but tonotopic shifting has also been documented in the ICC and MGB. Interestingly, dependent on the plasticity paradigm used, this reorganization is reversible. Restoration of normal tonotopic reorganization following AMI is an illustrative example of reversible auditory plasticity.. Questions remain about the control signals driving tonotopic plasticity that ultimately allow for restoration. Based on the results of the AMI patient, we propose there is a fixed representation for tonotopy that is maintained in the ICC, with tonotopic changes found in higher auditory centers. To test this hypothesis, we wanted to induce a reversible hearing loss using ear plugs that may lead to a reversible auditory plasticity and monitored noninvasively. Preliminary results from a pilot study indicated that reversible plasticity is possible and can be monitored noninvasively. However, no final conclusions about the mechanism can be made, as further studies were suspended due to numerous shortcomings including unreliable frequency attenuation. Ultimately, this appendix can serve as a guide for continued tonotopic plasticity studies aimed at addressing fixed plasticity and for chronic animal implantation.

INTRODUCTION

Tonotopic Plasticity

In the past couple decades, extensive evidence has emerged showing that auditory plasticity is not confined to sensitive or critical periods in the developing brain but rather the adult brain is capable of modification due to environmental influences or salient events. Numerous experimental paradigms including cochlear trauma, behavioral conditioning, passive exposure, and direct electrical stimulation, have been used to alter the frequency selectivity of auditory neurons to alter tonotopic maps in the A1, the MGB,

and to a lesser extent the ICC (*reviewed in* Suga and Ma, 2003; Fritz et al., 2005; Weinberger, 2008; Xiong et al., 2009; Irvine, 2010; Pienkowski and Eggermont, 2011). In each experimental paradigm, frequencies of interest were targeted by various means and spatial modifications in the tonotopic maps for the selected frequency region and the immediate surrounding regions were monitored. The studies demonstrate adaptive plasticity was possible in tonotopic maps of the developed brain and probed the mechanism of action and necessary circuitry.

Cochlear trauma paradigms, which include cochlear lesions, ototoxic drugs, and noise exposure, have resulted in hearing loss of the frequencies of interest (i.e., frequencies in region of damage or exposure range), leading to tonotopic reorganization throughout the auditory system (Robertson and Irvine, 1989; Rajan et al., 1993; Willott et al., 1993; Rajan and Irvine, 1998; Eggermont and Komiya, 2000; Irvine et al., 2003; Kamke et al., 2003). The tonotopic reorganization induced by these paradigms has been characterized by a reduction in the representation of the lost frequencies and an expansion of the surrounding frequencies (*reviewed in* Irvine, 2010). The greatest changes have been found within the A1, which showed that not only did expansion occur, but that the neurons in the expanded area had thresholds near normal values (Robertson and Irvine, 1989; Rajan et al., 1993). Similar expansion and threshold changes were found in the MGBv (Kamke et al., 2003), but not in ICC (Irvine et al., 2003). Results of ICC tonotopic expansion have been inconsistent, showing long term effects with varying thresholds, rapidly appearing but not lasting effects, or no effects at all, and warrant further study (Willott and Lu, 1982; Wang et al., 1996; Snyder et al., 2000; Harrison,

148

2001; Wang et al., 2002; Izquierdo et al., 2008; Snyder et al., 2008; Fallon et al., 2009). Cochlear trauma experiments suggested that robust, lasting adaptive plasticity may be limited to the thalamus and cortex.

Similar to cochlear trauma, passive exposure to frequencies of interest also resulted in reduction in the representation of those frequencies. An initial result indicated that passive exposure would cause overrepresentation and increased selectivity in the auditory cortex for the exposed tones; similar to what was shown in the developing brain (Stanton and Harrison, 1996; Zhang et al., 2001; Engineer et al., 2004). However, a larger body of work has indicated that the opposite is true in adults, with suppression of activity and reduction of the representation of the exposed frequencies and overrepresentation of the surrounding frequencies (Noreña et al., 2006; Pienkowski and Eggermont, 2009, 2010a, b; Pienkowski et al., 2011). Interestingly, the changes seen in the auditory cortex likely also occurred within the thalamus according to recorded LFPs, but not in the ICC indicated by auditory brainstem responses (Noreña et al., 2006; Pienkowski and Eggermont, 2009, 2010a, b; Pienkowski et al., 2011). Plasticity resulting from passive exposure also suggested that reorganization is restricted to the thalamus and cortex.

Where the cochlear trauma and passive exposure paradigms resulted in a contraction in A1 of the frequency representation for frequencies of interest, the behavioral conditioning paradigm resulted in expansion for the frequencies of interest. For example, tones paired with foot shock have caused over representation of the conditioned tone and reduction of the surrounding frequencies in cortical and collicular maps (Bakin and Weinberger, 1990; Edeline et al., 1993; Gao and Suga, 1998; Ji et al.,

149

2001). A comparison of the adaptive plasticity in these two regions elicited by conditioning revealed that reorganization persists in A1 far longer than in the ICC, with tonotopic maps being restored in the ICC after three hours of recovery time whereas A1 took twenty six hours to fully recover (Gao and Suga, 2000). This study suggested that the shift in the ICC served to enhance the cortical shifting as part of a feedback loop, but promptly returned to the original state.

Lastly, the direct electrical stimulation paradigm elicited reorganization similar to what was seen in behavioral conditioning with expansion of the stimulated frequencies of interest. A majority of the direct electrical stimulation studies have activated the A1 and induced frequency expansion in the A1 through local circuitry (Chowdhury and Suga, 2000; Ma and Suga, 2001; Sakai and Suga, 2001, 2002) as well as in the ICC and MGB through corticofugal projections (Zhang and Suga, 1997; Rauschecker, 1998; Yan and Suga, 1998; Zhang and Suga, 2000; Ma and Suga, 2001; Yan and Ehret, 2002; Yan et al., 2005). Similarly, stimulation in the ICC and MGB shifted the ICC, through a cortical feedback loop (Zhang and Suga, 2005; Wu and Yan, 2007). However, corticofugal shifting was extinguished when the cortex was inactivated (Zhang and Suga, 1997; Zhang et al., 1997; Zhang and Suga, 2000). From these studies it is apparent that cortex is necessary to drive alterations in subcortical nuclei.

From these different experimental paradigms, it is apparent that the topographic representation of the frequencies of interest can expand and contract dependent on the paradigm used. With this overwhelming evidence in support of plasticity in the adult brain, a 'stability-plasticity' dilemma is introduced. How can the brain be plastic while

150

maintaining the stability required to perform necessary functions (Seitz and Watanabe, 2005). The results from these experiments present a solution. Overall, these results showed the changes experienced by the cortex were more robust that those witnessed in the IC. It appeared that early reorganization or at least altered sensitivity manifested in the ICC and was transmitted to the thalamus and cortex where lasting modifications remained. The lasting modifications in the A1 can then gate subcortical reorganization through descending projections. Therefore, the stability of the ICC and the plasticity of the cortex and thalamus may allow for proper auditory processing while also adapting. The stability and plasticity that the auditory system can achieve is well illustrated by the reorganization and restoration of tonotopic maps experience by an AMI patient.

Auditory Midbrain Implant Plasticity

In 2006, the first clinical trial for the AMI was completed in five patients at the Hannover Medical University in Germany. The AMI was only approved for use in NF2 patients, as insertion of the AMI during the tumor removal procedure added only minimal surgical risk (Samii et al., 2007; Lim et al., 2009a). Of the five patients, three were implanted within the IC with only one of the patients being correctly implanted in ICC (Samii et al., 2007; Lim et al., 2008b; Lim et al., 2009b; Lim et al., 2013). As such, this patient received the greatest benefits from the implant, achieving open set speech (i.e., speech understanding with lip reading cues) and environmental awareness (Lim et al., 2007; Lim et al., 2009c; Lim et al., 2013). However, what is most interesting about this

patient is the auditory plasticity measured due to hearing loss and then due to electrical stimulation of the ICC.

Following surgery and 1.5 month recovery, the patient was brought in for the first implant fitting to determine the optimal stimulation strategy. The AMI was designed such that each electrode contact resided in a different frequency layer, thus the first step was to map the implant to establish what perceived pitch was elicited by stimulation of each electrode contact. The pitch ordering was done with a qualitative scale, where the patient rated the perceived pitch either from zero to five with zero correlating to low frequencies sounds such as a boat horn and five correlating to high frequencies sounds like a bird chirping, and with a two-alternative forced choice (**2-AFC**) pitch ranking test (Lim et al., 2007; Lim et al., 2013). In the 2-AFC pitch ranking method, the subject selected which of two sequentially stimulated sites elicited a higher pitch. The order was determined based on how frequently a site was the considered higher pitch. The initial pitch ordering revealed an altered tonotopic map (Fig. 26). Unlike a typical tonotopic map which would show a gradient of low to high frequencies in the dorsal-lateral to ventral-medial direction, the patient's map showed low to medium back to low frequencies along the same direction. The non-tonotopic ordering and presumed non-tonotopic ICC map was surprising, but based on the patient's history, not wholly unexplained. The alterations were likely attributed to the high frequency hearing loss the patient experienced six years prior to the implant, as a result of the tumor (Lim et al., 2013). Since the central auditory system was no longer receiving high frequency auditory information from the periphery, it was likely that the tonotopic map reorganized to represent only the frequencies

unaffected by the tumor. Given the resulting non-tonotopic pitch ordering, a non-tonotopic stimulation strategy was employed. The highest frequency information detected by the external microphone generated stimulation of the electrode that elicited the highest pitch perceived by patient (i.e., the middle layers). The rest of the implant was similarly mapped, with the remainder of the site ordering dependent on the qualitative pitch ordering (Lim et al., 2013).
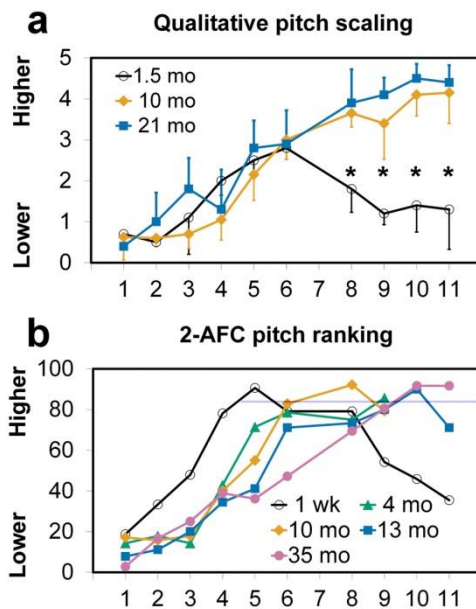
Figure 26. Pitch ordering measured in AMI patient over three years showed restoration of original tonotopy, including return of high pitches. Results were measured using A, a qualitative pitch scaling test and B, 2-AFC pitch ranking test. Results from both tests at the initial time point indicate that there was a non-tonotopic ordering that lacked higher pitches. Results from both tests at the final time point indicate a tonotopic order returned, including higher pitches. The asterisks indicate significantly higher values at 10- and 21-month follow-up compared to the 1.5-month values (p<0.006, two-tailed ranked, unequal variance t-test). This figure has been adapted from (Lim et al., 2013) with permission from the Nature Publishing Group.

This stimulation strategy was used until the patient's four month follow up, where pitch ordering was retested. Unexpectedly, instead of the non-tonotopic pitch ordering found in the first visit, a new ordering appeared that was now organized from low to medium perceived pitches from electrodes stimulated in the dorsal-lateral to ventral-medial direction. Using a non-tonotopic stimulation strategy, a tonotopic organization had emerged, though with limited frequency range (Lim et al., 2013). The stimulation strategy was adjusted to account for the new, tonotopic ordering. Perhaps the most astonishing result came during the ten month follow up. Retesting of the pitch ordering during this visit showed that not only was the tonotopic ordering still intact, but new pitches were perceived that were higher than what had previously been measured (Lim et al., 2013). Stimulation of the ICC by the AMI was able to restore a tonotopic pitch ordering similar to what would be expected in a normal hearing listener per animal and human studies (Geniec and Morest, 1971; Schreiner and Langner, 1997; Oliver, 2005; Malmierca et al., 2008; De Martino et al., 2013; Ress and Chandrasekaran, 2013).

The auditory plasticity experienced by this patient is somewhat puzzling; as non-tonotopic stimulation was able to restore a tonotopic pitch ordering and we believe restore the tonotopic map in the ICC. It seems unlikely that remapping of the circuitry could have happened as described in previous plasticity studies, where frequency representations can expand or contract but not completely reorganize. As such, it was expected that the non-tonotopic stimulation would only reinforce the non-tonotopic map and that tonotopic stimulation would have been needed to possibly restore a tonotopic map. Therefore we propose a different form of auditory plasticity that can explain what

154

was witnessed in the patient. Instead of plasticity that is constantly adapting based on the input, we propose that the IC is capable of maintaining multiple states (i.e., multiple frequency maps). Dependent on the input, the IC can switch between necessary states. In this patient, we propose that electrical stimulation by the AMI allowed the IC to switch from a non-tonotopic to a tonotopic state.

The idea of multiple plastic states has been well documented in sound localization (Hofman et al., 1998; Knudsen, 2002; Bajo et al., 2010; Kumpik et al., 2010). For example, owls with vision obscured by prisms were able to learn to correctly localize sound with a new map and then quickly return to the original map following prism removal (Knudsen and Knudsen, 1990; Knudsen, 2002). Anatomical tracer studies showed that both learned and original maps were maintained concurrently as projections within the sound localization circuitry of the IC. It was determined that an instructive signal from the visual system designated which state (i.e., projections) was necessary, mediating the switch by NMDA and GABA receptors (Hyde and Knudsen, 2000; DeBello et al., 2001; Knudsen, 2002). In ferrets, the role of the auditory cortex was established in the sound localization circuit, showing that projections from layer V of A1 were necessary to enable learning-induced plasticity within the IC (Bajo et al., 2007; Bajo et al., 2010). Thus, we propose that similar to the multiple states that can be maintained for sound localization, fixed and learned plastic states also exist for tonotopic maps that would allow for the tonotopic reorganization and restoration seen in the AMI patients.

Fixed Representation Hypothesis

Based on the changes seen in our AMI patient and guided by fixed topographic maps for sound localization, we hypothesize that there is a fixed representation for tonotopy that exists within the ICC, with plastic reorganization predominately occurring in higher auditory centers (i.e., MGB and A1). This hypothesis is supported by previous work that showed peripheral damage results in limited frequency reorganization of the ICC though changes were seen in higher auditory centers (Irvine et al., 2000; Irvine et al., 2003; Kamke et al., 2003; Fallon et al., 2008; Izquierdo et al., 2008). We further hypothesize that projections from the ICC to the thalamus also remain fixed but are either active or dormant, with new axonal projections arising dependent on available auditory information to form the plastic map. The ability to switch between the plastic and original map and thus activate necessary collicular projections may be dependent on both ascending and descending inputs to the ICC. Auditory information transmitted through ascending projections to the ICC may instruct which collicular projections are necessary, while descending projections from A1 may serve to activate or deactivate those collicular projections to enable plasticity and map switching. In this way, both a fixed map in the ICC and plastic map in the thalamus or A1 can exist simultaneously and be used as necessary.

This hypothesis is consistent with the AMI patient. Initial stimulation of the patient resulted in perception of only low frequencies. Due to the high frequency hearing loss, only low frequency auditory information was reaching the ICC and being passed to the thalamus and onward, likely resulting in a plastic map of only low frequencies. The

AMI was then used to stimulate all frequency regions of the ICC and thus reactivating dormant, fixed high frequency pathways leading to the return of the original tonotopic map in the thalamus and perception of the high frequencies.

PROPOSED METHODS AND PILOT STUDIES

Study Overview

In order to confirm that multiple maps can coexist in the auditory system, we wanted to induce a temporary, reversible high frequency hearing loss that would result in an altered tonotopic map similar to that found in the AMI patient. Measuring the time course for creation of the plastic map and return to the original map may determine if fixed maps exist. We postulated that if the time required to reacquire the original map was faster than learning a new, plastic map, fixed maps were present. However, if the time to reacquire the original map was comparable to learning, then likely relearning occurred, thereby eliminating the need for a fixed map. Additionally with these studies, we wanted to probe the role of descending projections in gating tonotopic plasticity through lesion studies to see if map switching ceased following removal of descending control.

Table 3. Proposed experimental groups for monitoring tonotopic plasticity within subcortical auditory nuclei.

Group	Ear Plugs	A1 Lesion	Terminal Steps	Reason	Number of GPs
1	No	No	After initial shift (2) or after return (2)	Control Group. Determine if shift is functional or due to aging	4
2	Yes	No	After initial shift	Verify that shifting occurred and quantify amount to correlate to ABR data	4
3	Yes	No	After return	Verify that return occurred and quantify amount to correlate to ABR data	4
4	Yes	Yes, Before ear plug insertion	After initial shift	Verify that no shifting occurred without descending projections	4
5	Yes	Yes, Before ear plug removal	After return	Verify that no return occurs without descending projections	4

Group 1 was a control to monitor changes due to age related hearing loss, all changes were to be compared to the tonotopic maps found within the control GPs. Groups 2 and 3 verified and quantified tonotopic reorganization and restoration, respectively. Additionally, the neural changes can be correlated to ABR changes. Groups 4 and 5 verified that corticofugal projections are necessary to gate subcortical plastic change. If changes occurred with an inactive cortex, additional gating signals would need to be explored.

To carry out these studies, we designed an experimental protocol that used molded, silicone ear plugs and monitored the changes using Auditory Brainstem Responses (**ABRs**) and Middle Latency Responses (**MLRs**). Terminal studies were to be carried out at different time points to assess tonotopic changes by recording throughout the ICC, the A1, and possibly the MGB. The study was designed to contain five trial groups shown in Table 3, each serving a different purpose in testing our hypothesis. The

following sections detail the design steps and decisions made preparing for this study, including expected outcomes, and the chronic surgical protocol.

Ear Plug Attenuation

To achieve frequency reorganization similar to that of the AMI patient, we chose to attenuate frequencies above 4 kHz, which is approximately in the middle of hearing range we have measured in guinea pigs (0.6 to 25 kHz). Thus the number of octaves that would be attenuated and unattenuated are relatively equal with 2.64 octaves and 2.73 octaves, respectively. We opted to attenuate a larger range of frequencies than was seen in the patient, since we wanted to target frequency regions that are highly active in guinea pig (4 to 10 kHz). The next step was to design ear plugs that fit the desired attenuation.

In designing these ear plugs, there were tradeoffs that needed to be considered between selective attenuation and cost and ease of use. The optimal attenuation profile would have been attained with the use of active ear plugs which have microphones and electronics that can detect the frequencies present and low pass filter only those of interest. However, in the scope of our animal experiments, active ear plugs would have been time intensive to design and fit to the guinea pig ear as well as cost prohibitive. The other option was to use passive ear plugs which provide a flat attenuation across a frequency spectrum. Though passive ear plugs did not have the desired attenuation profile, they allowed us to custom fit each guinea pig at each time point. We deemed ease of use to be the most important design constraint, because the size of the guinea pig's ear canal made it challenging to reuse ear plugs. As such we selected three silicone ear

impression products that we could mold into the ear and had curing time under five minutes. These included Insta-mold II (Insta-mold Products Inc, Oaks, PA), Otoform KC (Dreve Otoplastik GmbH, Unna, Germany), and Otoform AK (Dreve Otoplastik GmbH, Unna Germany).

Of the three selected ear impression products, we finalized our material choice based on three selection criteria: attenuation profile, ease of use, and overall cost of producing numerous, one-time-use molds. Attenuation profiles were characterized by coupling the speaker (Tucker-Davis Technologies, Alachua, FL) and microphone (ACO Pacific Inc, Belmont, CA) through a custom-made silicone cylinder. For each mold, there was one centimeter of solid silicone separating the speaker and the microphone. Frequencies from 0.1 to 50 kHz at 0.5 kHz steps were presented and the resulting level (dB-SPL) per frequency was recording (Fig. 27*A*) from which the attenuation profile was calculated (Fig. 27*B*). The measured values showed approximately the same attenuation profile past 20 kHz for all silicones. The only advantage was that Insta-mold II had slightly less attenuation at frequencies below 4 kHz. It was apparent from the plots that none of these attenuation profiles completely met our requirements, which was expected and will be considered in future directions. The second selection criterion was ease of use. The Insta-mold II and Otoform KC were made with by mixing a silicone with a hardening paste, whereas the Otoform AK required mixing two silicones. The curing rate and rigidity of the Insta-mold II and Otoform KC was the easiest to control by altering the amount of catalyst solution added. Finally in comparing cost, Otoform KC had the lowest cost and fastest delivery time. Considering all these factors, Otoform KC was

selected as the material for all the pilot studies. Otoform KC was the easiest to use and most cost effective for mass production. In the end, the attenuation profiles were too similar to influence the decision.
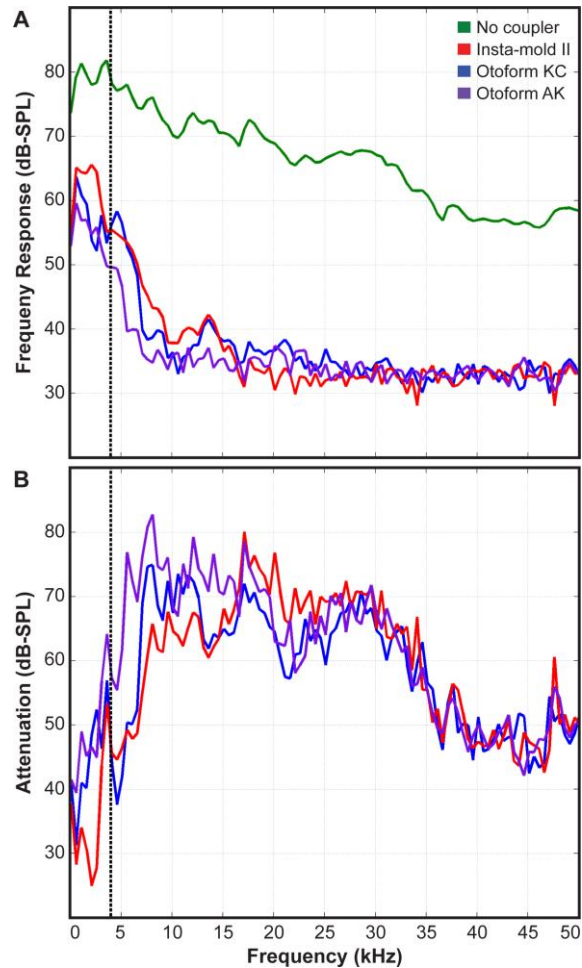
Figure 27. The different frequency response and attenuation measured from each silicone showed no obvious advantages for achieving the desired attenuation profile. *A*, Sound pressure levels (dB-SPL) were recorded by the microphone to frequencies from 0.1 to 50 kHz presented by the speaker without a coupler (green), with an Insta-mold II coupler (red), with a Otoform KC coupler (blue), and an Otoform AK coupler (purple). *B*, Attenuation was calculated by subtracting the coupled frequency response from the uncoupled frequency response. The dotted line marks the intended division between attenuated and unattenuated frequencies at 4 kHz. Attenuation was similar for frequencies above 20 kHz and only Insta-mold II had slightly less attenuation below 4 kHz.

161

Speed and efficiency were crucial when making each custom ear plug to avoid the ear plug material curing outside the ear canal and pinna and ensure complete coverage. Ears were first cleaned of ear wax. Next, the Otoform silicon was mixed with three drops of the hardening paste and placed in a curved tipped syringe, which allowed for better insertion into the ear canal. The pinna part of the ear was swabbed with a thin layer of cyanoacrylate for better fixation and then the ear canal and 90% of the pinna was filled with the silicone mixture. This process was repeated starting with mixing silicon for the other ear. Using the animal's body heat, the ear plugs cured within five minute.

ABRs and MLRs Recording Protocol and Analysis

ABRs and MLRs are a noninvasive measurement of auditory evoked potentials. ABRs are able detect the synchronized response of neurons in multiple auditory centers in the brain stem up to the thalamus and MLRs detect synchronized activity from the thalamus and the auditory cortex (Starr and Hamilton, 1976; McGee et al., 1983; Ozdamar and Kraus, 1983; Wada and Starr, 1983). Typical ABRs can be seen within the first 10 ms and typical MLRs can be found 8-50 ms following acoustic onset (Ozdamar and Kraus, 1983; Wada and Starr, 1983). Each peak in the waves represents the activity of a different auditory center (Fig. 28). In the ABRs, Wave I through VII indicate activity in vestibulocochlear cranial nerve, cochlear nucleus, superior olivary complex, lateral lemniscus, inferior colliculus, and thalamus, respectively (Starr and Hamilton, 1976; Skinner and Glattke, 1977; Wada and Starr, 1983). MLRs consist of two negative peaks (N_a and N_b) and two positive peaks (P_a and P_b) that correspond to activity in the thalamus

and cortex, respectively (McGee et al., 1983; Kraus and Nicol, 2009). The amplitude, absolute latency, and inter-peak latency of the ABR and MLR waves can be used as a measurement of auditory threshold and any change in those parameters can be attributed to alterations in frequency representation. As such, we would expect larger changes in the MLRs compared to the ABRs.
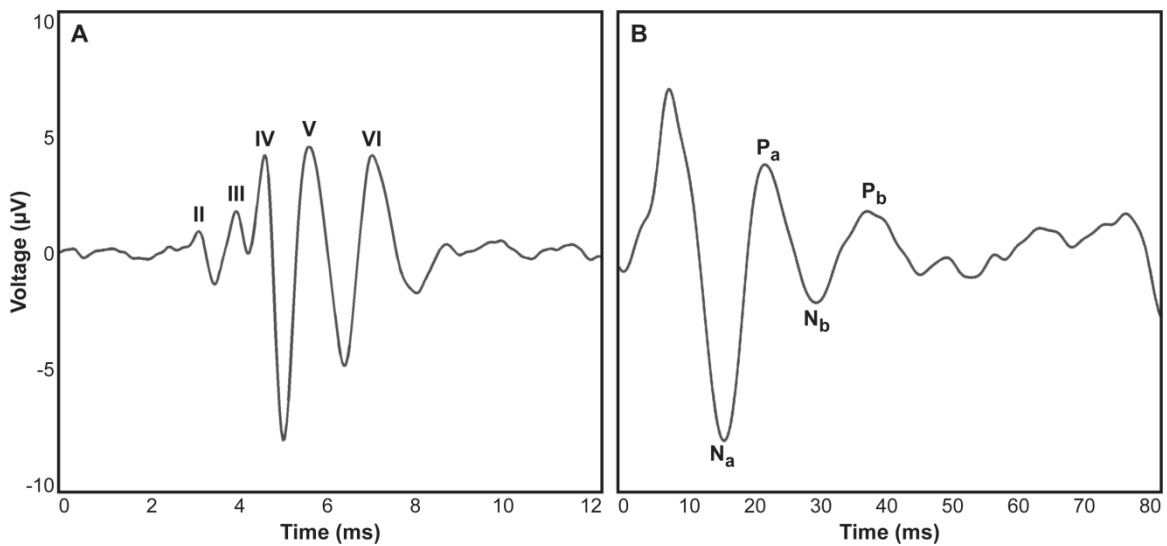
Figure 28. Positive peaks in ABRs represent synchronized neural activity in subcortical auditory nuclei and positive and negative peaks in MLRs represent synchronized thalamic and cortical activity. *A*, Our recording set up fails to capture Wave I of the ABRs which represent activity in the vestibulocochlear cranial nerve. Waves II and III represent neural activity in the cochlear nucleus, trapezoid body, and superior olivary complex. Waves IV and V reflect activity in the lateral lemniscus and inferior colliculus (Starr and Hamilton, 1976; Wada and Starr, 1983). Waves VI and VII reflect neural activity in thalamus and possible cortex cell neural activity (Skinner and Glattke, 1977) . *B*, The first positive and negative peaks correspond to activity in the thalamus and the second positive and negative peaks correspond to activity in the cortex.

For these experiments, we chose to minimize variance associated with the recording location by implanting screws into the skull and to reduce likelihood of

infection by using a two electrode configuration. Instead of three electrodes that would typically be used for common mode rejection, we opted to use the same electrode for the ground and reference. Initial test indicated no difference in noise floor when using two electrodes. The final electrode placements were made ipsilateral to the free field speaker, caudal to lambda and contralateral to the free field speaker, caudal to bregma. Experiments were performed in an acoustically and electrically isolated sound booth. Recordings were made from TDT hardware interfaced with custom written MATLAB software. The acoustic stimulation was delivered at a sampling rate of 195 kHz. The recorded signals were digitally sampled at 25 kHz and passed through analog and DC-blocking and anti-aliasing filters from 1.6 Hz to 7.5 kHz. The ABR/MLR acoustic stimulation protocol included eight pure tones (1 kHz, 4 kHz, 8 kHz, 14 kHz, 20 kHz) that were presented at varying levels (10-80 dB-SPL in 10 dB). The final results were calculated by averaging evoked response from 200-300 trials, though future work should average more than 500 trials per recording.

The ABR and MLR data was analyzed offline using a custom written MATLAB script to select the threshold of each frequency and calculated the amplitude and latency of each wave. ABR data was filtered from 100-3000 Hz with the signal recorded from the ipsilateral electrode, referenced to the contralateral electrode. MLR data was filtered from 10-300 Hz with a reverse electrode polarity compared to ABR data (i.e., signal recorded from the contralateral electrode referenced to the ipsilateral electrode). Thresholds were determined by visual inspection. Absolute latency was calculated as the time between

acoustic onset and maximum peak and inter-peak latency was calculated as the time between subsequent peaks.

Chronic Protocol

In order to monitor changes over time, we developed a chronic, aseptic surgical procedure that would minimize the likelihood of infection compared to our acute experimental protocol. An outline of the chronic procedure steps and workflow are shown in Figure 29 with details necessary to replicate the procedure provided in the text. For all steps of the procedure, personal protective equipment was required including hair net, closed cuff lab coats, and sterile gloves. One day prior to experimentation, all tools and equipment that may make contact with the animal were autoclaved in separate bags at 135°C for three minutes. Autoclave bags were not opened until necessary during the surgery.

The first step once acquiring the experimental animal (GPs) was to administer enrofloxacin (10mg/kg, Baytril) and ketoprofen (5 mg/kg, Ketofen) subcutaneously. No incision or anesthesia should be made before the initial dose of antibiotics and anti-inflammatory drugs. Next, an intramuscular injection of ketamine (40 mg/kg, Ketaject) and xylazine (10 mg/kg, AnaSed Injection) was given. Additional doses of ketamine mixed with two parts saline was administered as needed during the surgery. In order to minimize damage to the ear canal, the following surgical steps were performed out of the ear bars, though this also reduced stability during the surgical procedure. Heart rate, blood oxygenation, and temperature were monitored with a pulse oximeter and rectal

probe. The incision location was shaved, washed three times with Betadine then isopropyl alcohol, and then injected subcutaneously with lidocaine. An incision was made down the midline from bregma to lambda, exposing enough of the skull for the two electrode ABR/MLR recording configuration. The skull was cleaned of any muscle tissue and dried of any blood.

The dental cement was allowed to cure for ten minutes and then the ABRs/MLRs were recorded. The free field speaker was placed 1.2 cm from the left ear of the GP and alligator clips were used to connect the recording electrodes with the TDT hardware. A box was placed around the whole setup to ensure animal safety during the long recordings. A baseline recording was made before custom ear plugs were fit for each ear and then a second recording was made to test ear plug attenuation.

Following surgery and initial testing, GPS were placed in their cages and monitored under a heat lamp until they were able to support their own weight and move freely around the cage. For three and six days after the experiment, GPs are given daily injections of enrofloxacin and ketaprofen to prevent infection and reduce pain. For this initial study, no lesioning was done in the cortex. Details for the lesion protocol would need to be established for later studies.
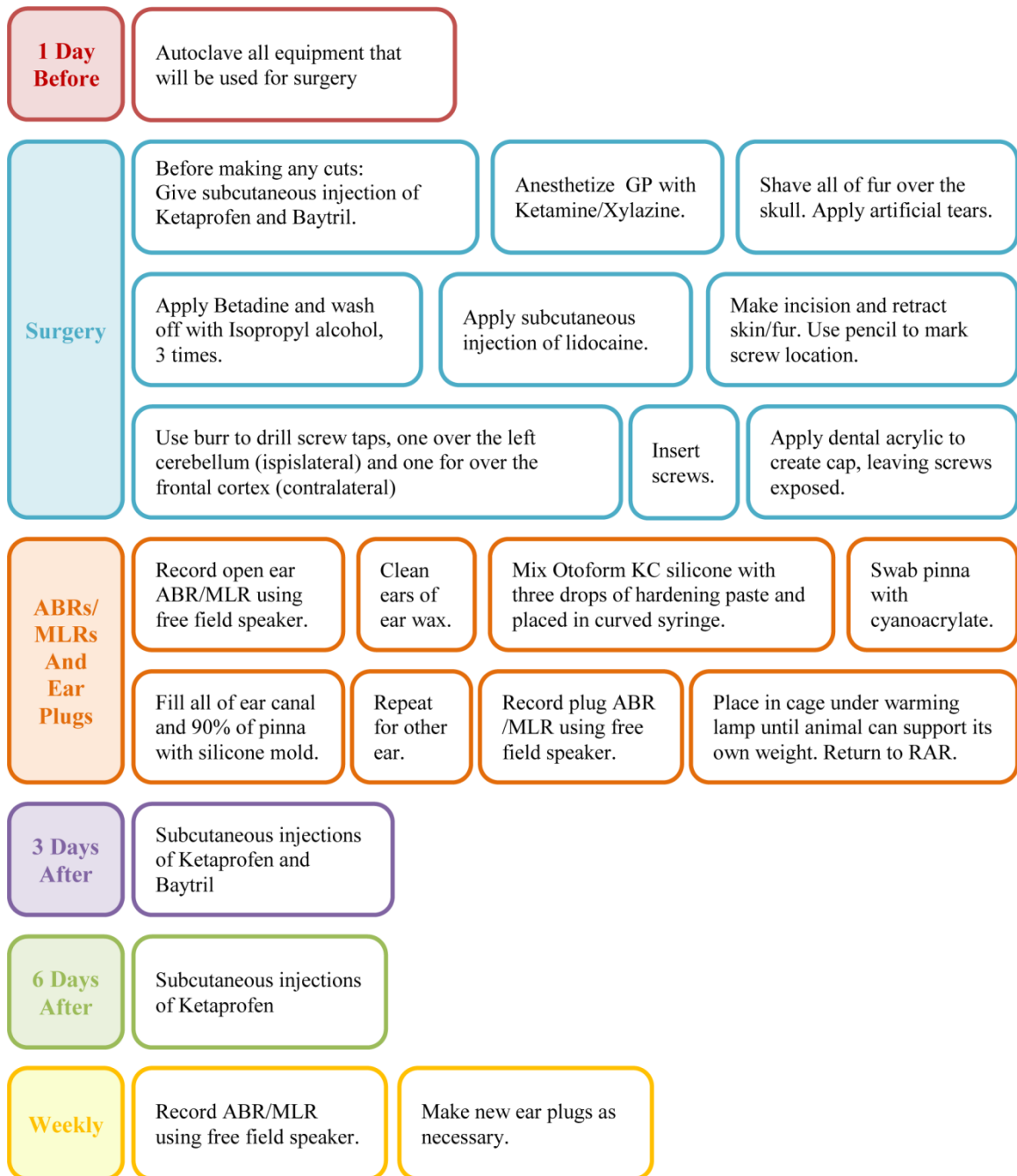
1 Day Before	Autoclave all equipment that will be used for surgery

Surgery	Before making any cuts: Give subcutaneous injection of Ketaprofen and Baytril.	Anesthetize GP with Ketamine/Xylazine.	Shave all of fur over the skull. Apply artificial tears.
	Apply Betadine and wash off with Isopropyl alcohol, 3 times.	Apply subcutaneous injection of lidocaine.	Make incision and retract skin/fur. Use pencil to mark screw location.
	Use burr to drill screw taps, one over the left cerebellum (ispislateral) and one for over the frontal cortex (contralateral)	Insert screws.	Apply dental acrylic to create cap, leaving screws exposed.

ABRs/ MLRs And Ear Plugs	Record open ear ABR/MLR using free field speaker.	Clean ears of ear wax.	Mix Otoform KC silicone with three drops of hardening paste and placed in curved syringe.	Swab pinna with cyanoacrylate.
	Fill all of ear canal and 90% of pinna with silicone mold.	Repeat for other ear.	Record plug ABR /MLR using free field speaker.	Place in cage under warming lamp until animal can support its own weight. Return to RAR.

3 Days After	Subcutaneous injections of Ketaprofen and Baytril

6 Days After	Subcutaneous injections of Ketaprofen

Weekly	Record ABR/MLR using free field speaker.	Make new ear plugs as necessary.

Figure 29. Chronic protocol steps and workflow for ear plug induced plasticity. Steps from preparing for the chronic protocol through the surgery to post-operative care are highlighted here, including steps that are necessary compared to the acute protocol. Further details for each step can be found in *Proposed Methods and Pilot Studies.*

PRELIMINARY RESULTS

We only completed two test animals with this protocol before the project was put on indefinite hold for reasons highlighted in *Discussion*. These first two animals served as a pilot study in order to determine the amount of time necessary to see changes in the auditory evoked protocols indicated possible ear plug induced changes and restoration. Thus, ABRs/MLRs were recorded weekly. An initial ABR/MLR was recorded on the day of surgery with and without placement of the ear plug (Fig. 30). For each subsequent recording, GPs were lightly anesthetized with an intramuscular injection of ketamine mixed with two parts saline. Typically this dosage was adequate to keep the GP anesthetized during transport and throughout the whole recording; however additional doses of ketamine and saline can be administered as necessary. The recording protocol was completed in the absence of ear plugs and then each ear was fit with a new ear plug.
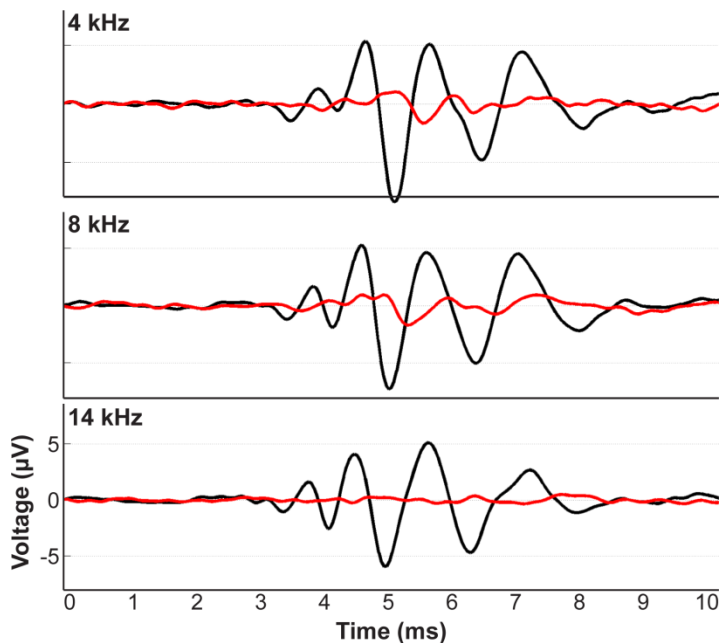

Figure 30. Ear plugs differentially attenuated frequencies indicated by differences in recorded ABRs. Baseline ABRs were recorded at 80 dB-SPL without ear plugs (black) with clear peaks for Waves III – VI. Following the placement of ear plugs (red), no peaks can be seen for 14 kHz, and shifted peaks are present for 4 kHz and 8 kHz.

Unfortunately, we were only able to monitor GP2 to the final time point as the bone screw and dental cement cap made for GP1 did not adhere, causing complications that ultimately led to termination. When changes in latency and threshold presumed to indicate tonotopic plasticity appeared, ear plugs were removed until normal or near-normal latencies and thresholds returned. Initial indications of tonotopic reorganization appeared after Week 4 (Fig. 31*A,B*) with return occurring one week after ear plug removal. Following weeks with ear plugs, the ABR peaks were reduced compared to the ABRs recorded in the previous and subsequent weeks. The ABRs from GP2 were averaged over only 200 traces which accounts for the added noise in the signal. Future studies should use longer recordings to reduce noise unrelated to synchronized activity. Following the initial reorganization, switches between the original and plastic map only took one week, shown first in Weeks 5-7 and Weeks 11-13 (Fig. 31*B*). Ear plugs were placed for the final weeks leading up to the terminal surgery. The tonotopic maps found within the ICC only showed frequencies between 2 and 9 kHz, which is a decreased range compared to normal hearing GPs (0.6 to 25 kHz, results not shown). These results revealed that we were able to elicit different ABRs that we attributed to ear plug induce plasticity. It was possible that the plasticity found could be ascribed to ear plug induce damage, however that seems highly unlikely as the results were reversible.
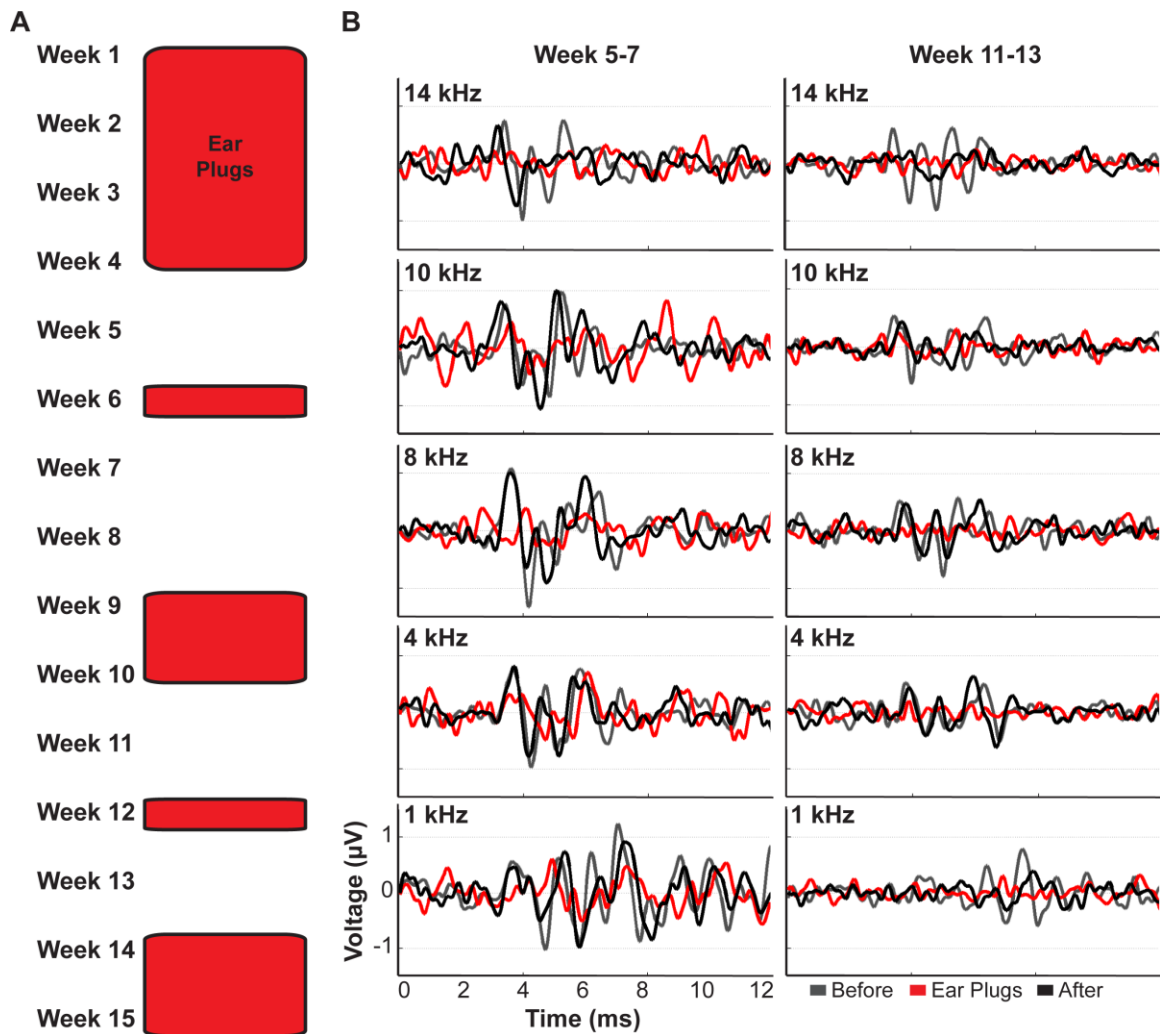
Figure 31. Ear plugs were able to induce reversible plasticity changes as monitored by ABRs. The initial reorganization resulted after four weeks of ear plug wear and restoration resulted after one week of recovery. *A*, The timeline for the pilot studied was completed to verify multiple switches between the original and chronic map was possible. *B*, Recordings were made at the end of the week (i.e., no ear plugs were present during Week 5 and Week 7, but were present during week 6). Weeks without ear plugs resulted in larger ABR peaks compared to the week with ear plugs (red). To visible difference is apparent in the recording from the week before (gray) and the week after (black). During ear plugs weeks, small peaks were present for 1 kHz and 4 kHz, though it was not clear which wave. In comparing Weeks 5-7 and Weeks 11-13, there was a loss in Wave amplitude that may denote damage to the peripheral ear.

DISCUSSION

There were several issues encountered during this pilot study that need to be remedied before piloting a second study. These issues include the dental cement cap and ear plug adherence, animal health, and the attenuation profile. With better methods in place, the second pilot study can be used to better determine shifting timelines and statistical methods. The section will introduce each issue and provide a possible solution.

The terminal times points for the pilot study were not selected by the experimenters but rather because the animals managed to remove their dental cement caps (GP1) or suffered injuries consistent with nerve damage (GP2). We believe that the first issue can be remedied by using more head screws to provide greater surface area for the dental cement adherence. Additionally, before applying dental cement, compressed air should be used to completely dry the skull which will ensure better fixation. The second issue is likely linked to sciatic nerve damage inflicted by anesthesia administration and can be avoided by changing the angle and approach of the injection.

Ultimately, these experiments ceased because the ear plugs were not reliable nor provided the desired attenuation profile. GPs are sensitive to environmental changes and do not respond well to irritation. Thus, the GPs displayed a head shaking behavior when ear plugs were present. Though they were not monitored 24 hours a day, we suspect that the animals continued this behavior until the ear plugs were expelled. Most weeks, either one or none of the ear plugs remained intact. One option would be to monitor the animals daily; however this would not eliminate the need for more secure ear plugs. A second option would be to use a more permanent solution to secure the ear plugs as the

171

cyanoacrylate was not strong enough to combat the head shaking behavior. In regard to the attenuation profile, though more attenuation occurs at higher frequencies, there was still a substantial amount of attenuation on the frequencies of interest. One option to enhance these frequencies would be to supplement the ear plugs with tones greater than 4 kHz, since previous studies have indicated contraction of tonotopic representation for passive tone frequencies. Using ear plugs in conjunction with tones would create a greater likelihood that we would achieve the tonotopic shifts we desire than either paradigm alone.

Finally with the discussed issues addressed, a timeline of chronic and acute time points would need to be established in the second pilot study before to beginning the final studies. The results of this study as well as the results of previous passive exposure and ear plugs studies indicated a timeline that would likely be one month to initial reorganization and one week to restoration. This second pilot study would also better inform where in the CAS recordings should be made during the terminal step. The study was originally designed to record throughout the ICC. However, in reconsidering the hypothesis, it may be beneficial to record in both the ICC and the thalamus. If we believe that the ICC remains fixed and the changes happen in higher auditory centers, the thalamus may likely show the altered and original map we desire whereas the ICC may show only the original map. Recordings in the auditory cortex could also be considered, but due to the lesion portion of our study, we could not get data from all animals.

In summary, we would need a more robust protocol to ensure that we are establishing an altered map through ear plug induced plasticity. This would allow us to

172

more confidently test our fixed plasticity hypothesis. In reviewing our pilot studies, there are many issues that need to be amended prior to addressing the aim of the study. However, the results of this pilot show promise for continuation and have enabled us to establish the first chronic protocol in GPs for our labs.